EXPERIMENTAL EVALUATION OF “BALL RUBBER BEARINGS” AT DIFFERENT TEMPERATURES

A THESIS SUBMITTED TO
THE GRADUATE SCHOOL OF NATURAL AND APPLIED SCIENCES
OF
MIDDLE EAST TECHNICAL UNIVERSITY

BY

SERKAN ERDAL

IN PARTIAL FULFILLMENT OF THE REQUIREMENTS
FOR
THE DEGREE OF MASTER OF SCIENCE
IN
CIVIL ENGINEERING

DECEMBER 2010

Approval of the thesis:

EXPERIMENTAL EVALUATION OF "BALL RUBBER BEARINGS" AT DIFFERENT TEMPERATURES

submitted by **SERKAN ERDAL** in partial fulfillment of the requirements for the degree of **Master of Science in Civil Engineering Department, Middle East Technical University** by,

Prof. Dr. Canan Özgen ______________________
Dean, Graduate School of **Natural and Applied Sciences**

Prof. Dr. Güney Özcebe ______________________
Head of Department, **Civil Engineering**

Assist. Prof. Dr. Alp Caner ______________________
Supervisor, **Civil Engineering Dept., METU**

Examining Committee Members:

Prof. Dr. M. Semih Yücemen ______________________
Civil Engineering Dept., METU

Assist. Prof. Dr. Alp Caner ______________________
Civil Engineering Dept., METU

Prof. Dr. Ahmet Yakut ______________________
Civil Engineering Dept., METU

Prof. Dr. Uğurhan Akyüz ______________________
Civil Engineering Dept., METU

M.Sc. Syed Ateeq Ahmad ______________________
General Manager, PROYA

Date: ______________________

I hereby declare that all information in this document has been obtained and presented in accordance with academic rules and ethical conduct. I also declare that, as required by these rules and conduct, I have fully cited and referenced all material and results that are not original to this work.

Name, Last name: SERKAN ERDAL

Signature :

ABSTRACT

EXPERIMENTAL EVALUATION OF
"BALL RUBBER BEARINGS"
AT DIFFERENT TEMPERATURES

Erdal, Serkan

M.Sc., Department of Civil Engineering

Supervisor: Assist. Prof. Dr. Alp Caner

December 2010, 115 pages

Rubber material used in seismic isolation systems has a tendency to stiffen in cold climate conditions. Structural responses of rubber based seismic isolation bearings are known to be temperature dependent. The main focus of this research is to investigate the temperature related behavior shifts at a certain type of a rubber based seismic isolation system.

This research is a complementary study to a recent experimental study on a newly developed seismic isolator called "Ball Rubber Bearing" (BRB). BRBs can be easily manufactured as in the case of a standard rubber based bridge bearing and can provide adequate energy dissipation during an earthquake. However, structural response of BRBs at low temperatures has not been examined yet.

In this research, behavior of BRBs exposed to different temperatures is examined under combined axial and cyclic lateral load. The performance of the specimens used in this study, "Elastomeric Bearing" (EB) and "Ball Rubber Bearing" (BRB) are compared with each other and also with previous researches conducted in this topic.

The results indicated that BRBs show better performance at low temperatures in terms of energy dissipation compared to room temperature performance. Big size bearings have higher energy dissipation per cycle compared to small size bearings by reason of size effect. The higher damping percentage is observed at the small size bearings compared to big size bearings due to better confinement of the inner core. As a result of temperature records heat exchange is not detected in the rubber during cyclic loading.

Keywords: seismic isolator, rubber, bearing, temperature

ÖZ

BİLYELİ KAUÇUK MESNETLERİN FARKLI SICAKLIKLARDA
DENEYSEL DEĞERLENDİRİLMESİ

Erdal, Serkan
Yüksek Lisans, İnşaat Mühendisliği Bölümü
Tez Yöneticisi: Yrd. Doç. Dr. Alp Caner

Aralık 2010, 115 sayfa

Sismik yalıtım sistemlerinde kullanılan kauçuk malzemenin soğuk iklim koşullarında sertleşme eğilimi vardır. Kauçuk tabanlı sismik yalıtım mesnetlerinin yapısal tepkilerinin sıcaklığa bağlı olduğu bilinmektedir. Bu araştırmanın ana odak noktası, belirli bir kauçuk tabanlı sismik yalıtım sistemindeki sıcaklıkla ilgili davranış değişikliklerini incelemektir.

Bu araştırma, yeni geliştirilen Bilyeli Kauçuk Mesnet (BKM) diye adlandırılan sismik izolatör üzerine yeni bir deneysel çalışmanın tamamlayıcı çalışmasıdır. Bilyeli Kauçuk Mesnetler (BKM) standart bir kauçuk tabanlı köprü mesnedi durumunda kolaylıkla imal edilebilir ve bir deprem sırasında yeterli enerji dağıtımı sağlayabilirler. Ancak, Bilyeli Kauçuk Mesnetlerin (BKM) düşük sıcaklıklardaki yapısal tepkisi henüz incelenmiş değildir.

Bu araştırmada, farklı sıcaklıklara maruz kalan Bilyeli Kauçuk Mesnetlerin (BKM) birleşik eksenel ve döngüsel yatay yükler altındaki davranışı incelenmiştir. Bu çalışmada kullanılan numunelerin, Elastomerik Mesnet (EM) ve Bilyeli Kauçuk Mesnet (BKM), performansları birbirleriyle ve bu konuda daha önce yapılmış araştırmalarla karşılaştırılmıştır.

Sonuçlar Bilyeli Kauçuk Mesnetlerin (BKM) düşük sıcaklıklardaki enerji dağıtım performansının oda sıcaklığındaki performansıyla karşılaştırıldığında daha iyi olduğunu göstermiştir. Büyük boyutlu mesnetler küçük boyutlu mesnetlere kıyasla boyut etkisi nedeniyle daha yüksek döngü başına enerji dağıtımına sahiptir. Küçük boyutlu mesnetlerin büyük boyutlu mesnetlerle kıyaslandığında iç çekirdek daha iyi sarıldığı için daha yüksek sönümleme yüzdesine sahip oldukları gözlemlenmiştir. Sıcaklık ölçümleri sonucunda döngüsel yükler altında kauçuğun içerisinde ısı değişimi tespit edilmemiştir.

Anahtar Kelimeler: sismik yalıtıcı, kauçuk, mesnet, sıcaklık

To My Parents

ACKNOWLEDGEMENTS

Assist. Prof. Dr. Alp Caner contributed a lot to reach to the current situation. I would like to thank for his guidance, advice, criticism, encouragements and insight throughout the research. I would like to present my sincere gratitude for his efforts.

I would like to thank to Prof. Dr. Ahmet Yakut for his suggestions and comments.

I also would like to thank to my former supervisor Prof. Dr. M. Semih Yücemen for his advices, encouragements and personal attention.

The support of Salim Azak both as a specialist, as a brother and a friend is beyond expression. He also contributed formatting the thesis and help about overcoming the problems related with test machine.

The technical assistance of METU Structure Mechanics Laboratory staff is gratefully acknowledged.

I present my special thanks to TÜBİTAK for financially supporting the research Project 109M323.

Last but not the least, I would like thank to my family. They always supported me. I appreciate their efforts.

TABLE OF CONTENTS

LIST OF TABLES

TABLES

LIST OF FIGURES

FIGURES

LIST OF SYMBOLS

A	Acceleration coefficient from section 3 [2]
$A_{bearing}$	Plan area of bearing
A_r	Area of the overlap between top and bottom bonded areas of the deformed bearing
A_{rubber}	Plan area of an elastomeric bearing excluding the central hole
B	Numerical coefficient related to the effective damping of the isolation system as set forth in table 2 (section 7) [2]
BRB_A	Ball rubber bearing type A
BRB_B	Ball rubber bearing type B
C_s	Elastic seismic response coefficient [2]
c_c	Thickness of the rubber cover at the sides
D	Diameter of bearing
D_b	Bonded diameter of the bearing
D0	Temperature reading at surface
D1	Temperature reading at first depth
D2	Temperature reading at second depth
D3	Temperature reading at third depth
d	Diameter of central hole or total deck displacement relative to ground ($d_i + d_{sub}$) [2]
d_s	Displacement due to daily temperature changes, wind loading etc.
d_{max}	Maximum displacement
d_y	Yield displacement
EB_A	Elastomeric bearing type A
EB_B	Elastomeric bearing type B
E_c	Instantaneous compression modulus of the rubber-steel composite under the specified level of vertical load

f_L | A correction factor accounting for the contribution of lead-core to secondary stiffness
F_{max} | Maximum horizontal force
F_y | Yield strength of the bearing
$F_{\gamma=50\%}$ | Horizontal force corresponding to 50% shear strain
G | Shear modulus of elastomeric bearing
G_C | Shear modulus at cold temperatures
G^*_{eq} | Equivalent shear modulus of ball rubber bearing
G_R | Shear modulus at room temperature
H_{max} | Maximum horizontal force
h_{ri} | Thickness of the inner rubber layer
h_{riA} | Inner rubber layer thickness of bearing type A
h_{riB} | Inner rubber layer thickness of bearing type B
h_{ro} | Thickness of the outer rubber layer
h_{rt} | Thickness of the total rubber
h_s | Thickness of steel shims
ID0 | Temperature reading at surface for insulated bearing
ID1 | Temperature reading at first depth for insulated bearing
ID2 | Temperature reading at second depth for insulated bearing
ID3 | Temperature reading at third depth for insulated bearing
K | Bulk modulus
K_d | Secondary stiffness
K_{dC} | Secondary stiffness at cold temperatures
K_{dR} | Secondary stiffness at room temperature
K_{eff} | Effective stiffness of the bearing or the sum of the effective linear stiffnesses of all bearings and substructures supporting the superstructure segment as calculated [2]
K_h | Horizontal stiffness of an EB
K_u | Elastic unloading stiffness
K_v | Vertical stiffness of an EB
L | Length of a rectangular EB (parallel to longitudinal bridge axis)
M | Magnitude of earthquake
n | Number of interior layer of elastomer, where interior layers are defined as those layers which are bonded on each face. Exterior layers are

	defined as those layers which are bonded only on one face. When the thickness of the exterior layer of the elastomer is more than one-half the thickness of an interior layer, the parameter, n, may be increased by one-half for each such exterior layer
P_{ver}	Vertical compressive load
$P_{ver,3.4MPa}$	Vertical compressive load corresponding to 3.4 MPa average compressive stresses
Q_d	Characteristic strength
$Q_{d,BRB}$	Characteristic strength of ball rubber bearing
Q_{dC}	Characteristic strength at cold temperatures
Q_{dR}	Characteristic strength at room temperature
S	Shape factor
S_i	Numerical coefficient for site soil profile as set forth in table 5-1 for seismically isolated structures [2]
T_{eff}	Period of seismically isolated structure, in seconds, in the direction under consideration [2]
T_1	First temperature level
T_2	Second temperature level
T_3	Third temperature level
W	Width of the bearing in the transverse direction or total vertical load of the isolation system ($DL+LL_S$) [2]
α_r	An empirical coefficient determined from test data
α_t	Temperature factor
β_{eq}	Equivalent viscous damping ratio
γ_c	Shear strain due to vertical compressive load
γ_{max}	Maximum shear strain
γ_r	Shear strain due to rotation
$\gamma_{s,eq}$	Shear strain due to seismic design displacement
$\gamma_{s,s}$	Shear strain due to service load displacement
Δ_{BA}	Bulge distance of bearing type A
Δ_{BB}	Bulge distance of bearing type B
Δ_s	Maximum shear deformation of the elastomer at the service limit state
δ	Aspect ratio
ε_c	Axial strain due to compression

ε_{1A}	First axial compressive strain level for bearing type A
ε_{2A}	Second axial compressive strain level for bearing type A
ε_{3A}	Third axial compressive strain level for bearing type A
ε_{4A}	Fourth axial compressive strain level for bearing type A
ε_{5A}	Fifth axial compressive strain level for bearing type A
ε_{1B}	First axial compressive strain level for bearing type B
ε_{2B}	Second axial compressive strain level for bearing type B
ε_{3B}	Third axial compressive strain level for bearing type B
ε_{4B}	Fourth axial compressive strain level for bearing type B
ε_{5B}	Fifth axial compressive strain level for bearing type B
θ	Rotation
θ_s	Maximum service rotation due to the total load
μ	Coefficient of friction
σ	Axial compressive stress
σ_s	Service average compressive stress due to the total load
σ_1	First axial compressive stress level
σ_2	Second axial compressive stress level
σ_3	Third axial compressive stress

ABBREVIATIONS

AASHTO	American Association of State Highway and Transportation Officials
ADRI	Added Damping Rubber Isolator
BRB	Ball Rubber Bearing
EB	Elastomeric Bearing
EDC	Energy Dissipated per Cycle
FPS	Friction Pendulum System
HDRB	High-Damping Rubber Bearing
LDRB	Low-Damping Rubber Bearing
LRB	Lead Rubber Bearing
LVDT	Linear Variable Differential Transformer
NCHRP	National Cooperative Highway Research Program

CHAPTER 1

INTRODUCTION

1.1. General

Seismic isolation systems have been used in different structures at different zones of the world such as America, Europe, China, Japan and New Zealand for the last century. Major manufacturers of seismic isolation systems consider India, Iran and Turkey as new markets due to their high risk earthquake zone classification. Nearly half of Turkey in terms of area and population is located in earthquake zone I being the most critical one as depicted in Figure 1.1. Most of these countries have extreme cold climates during winter time.

Designing earthquake-resistant buildings can be achieved by providing high ductility and strength in the structural load carrying mechanism. Increase in ductility of the structure may lead excessive floor displacements. Excessive relative deflections and accelerations with respect to ground at upper floors may result in damaging the structure. The relative deflections can be minimized by increasing rigidity of structure and the relative floor accelerations can be minimized by increasing ductility of structure. Alternatively, reducing relative floor displacements and floor accelerations at the same time is possible with seismic isolation method.

Seismic isolation system provides a separation between structure and ground in a feasible way and in this manner protects the structure from damaging effects of ground motion. The main principle of seismic isolation system is to increase the fundamental period of structure and reduce the floor accelerations relatively to the ground motion.

The earthquake forces transmitted to the structure is reduced by shifting the fundamental period of structure. On the other hand, seismic displacements may increase at the seismic isolation location due to the provided flexibility. For a typical multi-storey frame structure with base isolation, the relative story drift may decrease significantly since the structure may move almost rigidly over the base isolation.

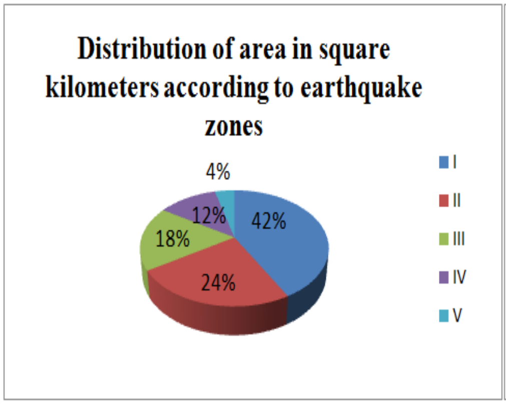

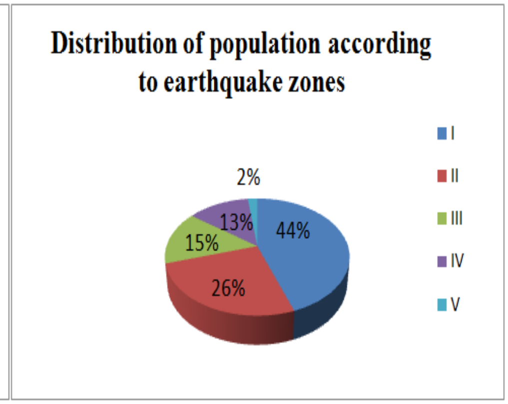

Figure 1.1. Population Density and Area in Square Kilometers According to Earthquake Zones of Turkey [16]

Three fundamental principles that need to be satisfied by a seismic isolation system are identified in American Association of State Highway and Transportation Officials (AASHTO) [2].

- The system shall permit lateral movement capacity without causing instability at vertical-load carrying device. The lateral movement will shift natural period of the structure and reduce the forces transmitted to the structure.

- The system shall limit deflections to a practical design level by using adequate damper or energy distributor.

- The system shall provide adequate rigidity under service load levels, such as wind and braking forces. Service load levels are typically much lower than the seismic loads at high seismic regions.

Fixed-base structures attract more seismic force than structures with flexible bases. Increased flexibility induced by the seismic isolation system lead to period shift can result in base shear reductions and increase in displacements. Effect of period shift of the structure on acceleration and displacement response is presented in Figure 1.2.

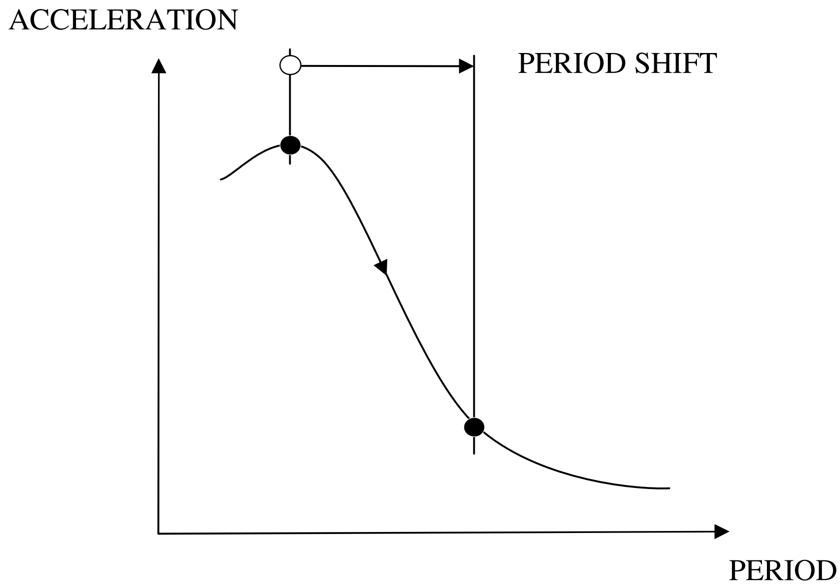

ACCELERATION RESPONSE SPECTRUM

(a)

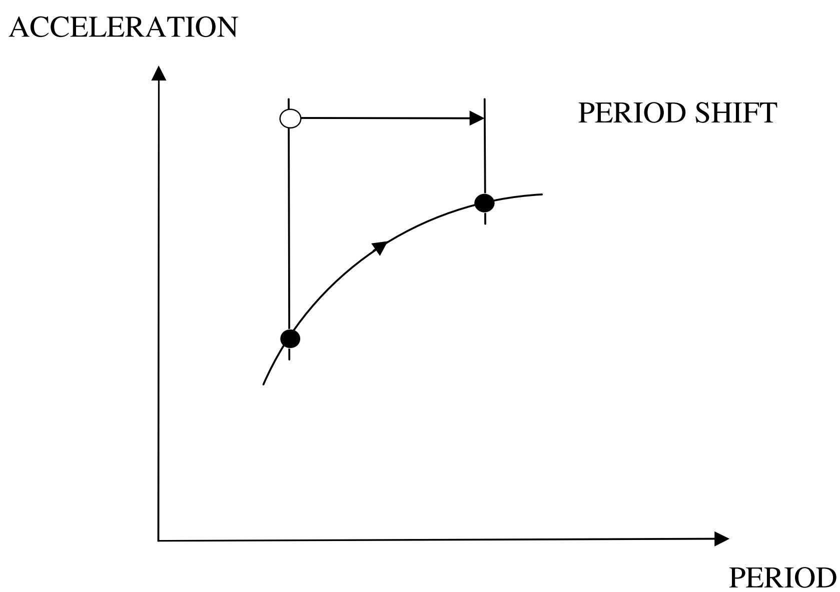

DISPLACEMENT RESPONSE SPECTRUM

(b)

Figure.1.2. Effect of Period on Acceleration and Displacement

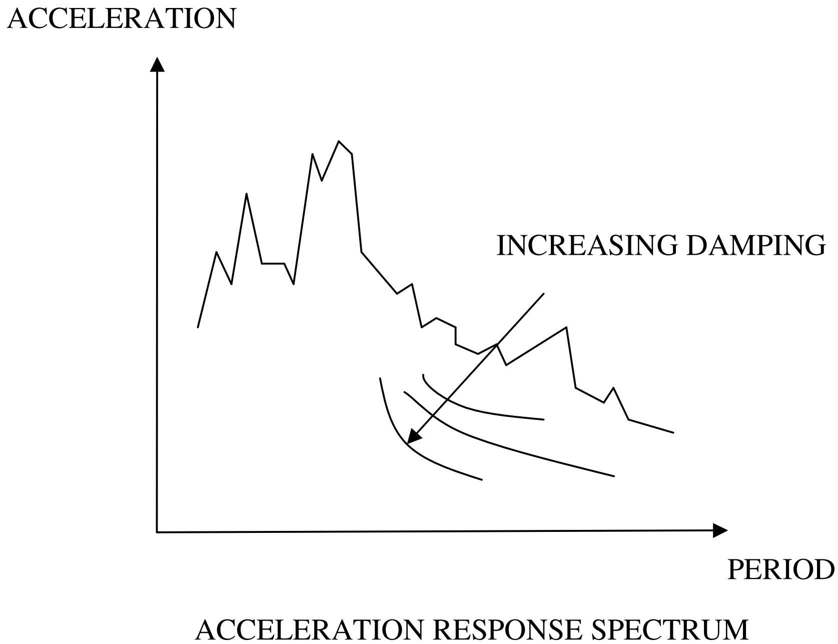

(a)

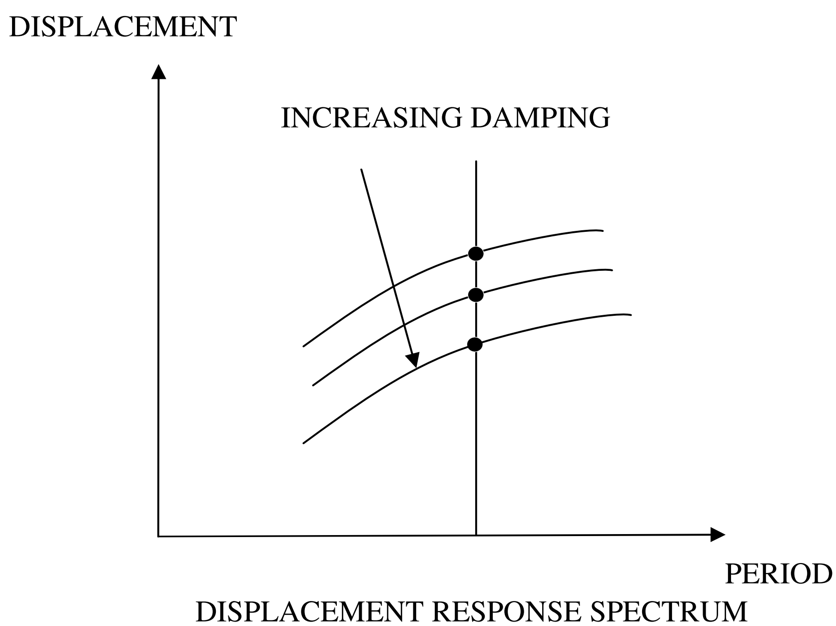

(b)

Figure 1.3. Effect of Damping on Acceleration and Displacement

Effect of damping on acceleration and displacement is presented in Figure 1.3. Energy dissipating mechanism provided by increased damping can help to reduce seismic accelerations and displacements.

Seismic isolators can be grouped in two major groups as rubber isolators and sliding isolators. Rubber isolators are; elastomeric bearings (EB), lead rubber bearings (LRB) and high damping rubber bearings (HDRB). Sliding isolators are; friction pendulum systems (FPS) and sliding isolators.

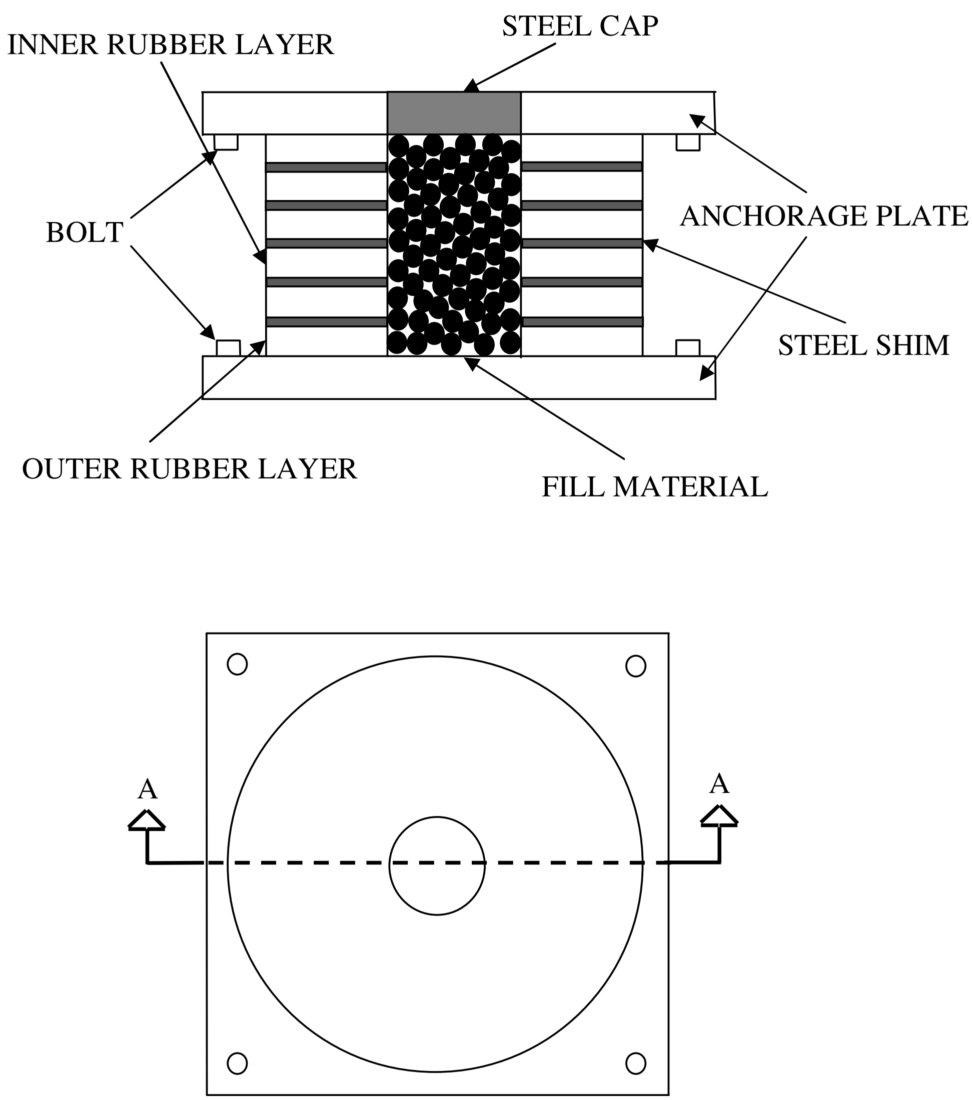

Figure 1.4. Plan and A-A cross section View of BRB

In this study, the inner hole of steel reinforced Elastomeric Bearing (EB) is filled with an average diameter of 1.65mm steel balls. The new type of bearing is called as

Ball Rubber Bearing (BRB). Plan and A-A cross section view of BRB is presented in Figure 1.4. Steel balls provide significant contribution to damping compared to other granular materials. The air pockets between steel balls serve as heat sinks which also do not allow higher heat releases during lateral movements. Manufacturing process of BRBs is easier and has lesser steps compared to other systems. Their cost is expected to be lower or same with the other systems.

1.2. Objective

Low temperature performance of seismic isolation systems has not been studied in details in the known literature. The BRB, a new seismic isolation system has never been tested under different thermal effects. Therefore, the objective of this research is to investigate the behavior of BRBs subjected to different temperature effects.

1.3. Scope

In this scope, the seasonal temperature changes around the major fault lines in Turkey were studied. A test program was developed to investigate the structural response of the BRBs under combined cyclic lateral loads and axial compression loads at different temperature levels. These temperature levels were selected based on the investigation of the seasonal temperature changes. In the test program, two different bearings having a similar shape factor but different size were tested. The results of the tests were evaluated to develop a design recommendation to structural engineers and any end user.

1.4. Literature Review

Seismic isolation is a collection of structural elements which should substantially decouple a superstructure from its substructure resting on a shaking ground thus protecting structure's integrity. There are various structural elements such as EBs, sliding plates, high damping rubber bearings (HDRB) and etc. to fulfill this purpose. Among these, EBs have been widely used in various field applications. A number of researches have studied about the behavior of EBs. The behaviors of EBs at low temperatures should be well understood since it is sensitive to temperature. This section reviews the literature on seismic isolation systems and emphasizes on EBs. It then proceeds to review the test methods of seismic isolation systems in order to assess the performance of EBs at low temperatures. The studies on response of isolated structures and finally economical impact of seismic isolations systems are given.

1.4.1. Studies on Seismic Isolation

One of the most difficult dilemmas in structural engineering is limiting the relative floor displacements and accelerations at the same time [17]. This problem has been overcome by seismic isolation method which is applied by inserting flexible and dissipative instruments between ground and structure so that the period of the structure is lengthened enough to reduce the forces transmitted to the structure. The fundamental theory of seismic isolation is uncoupling the structure from ground by using different techniques and materials [4]. Earlier versions of this method used practically by Romans. They succeeded to isolate the structures by using clay layers at foundation levels. History of modern seismic isolation concept goes back to almost hundred years ago. Prior to 1960's there were very few isolated buildings constructed with isolation systems despite the fact that there were lots of patent applications or examples of proposals for isolation systems in that period of time. By advancing in computer programming, constructing large scale shaking tables and generation of site specific ground motions allowed engineers to utilize seismic isolation system in new design or retrofit cases. Seismic isolation system found a wide range of application at different countries e.g. United States, New Zealand, Japan, Europe and China. There are some widely used solutions and equipment for seismic isolation systems such as lead rubber and/or EBs. Besides these widely used solutions, each earthquake vulnerable country developed almost authentic equipment or techniques for mitigating damaging effects of earthquakes.

Özden and Türer [14] performed analytical and experimental researches on using scrap automobile tires as an alternative low cost seismic base isolation. Automobile tires have been produced by steel mesh with rubber in different forms since 1950's. Therefore, it was expected to see similar effects of steel mesh in rubber and steel plates in EBs. The authors used different brands of tires and produced scrap tire bearing by placing one tire layer on another one. Experimental results revealed that scrap tire bearings had high shear modulus changing between 0.95 MPa-1.85MPa. Axial compressive load capacity of system is increased by putting extra layers to the system. Sufficient axial compressive load is another necessity of system for holding layers together. Moreover, the study of Özkaya [15] includes replacement of the lead core with a granular material with steel balls. According to his research 1.65mm steel balls are the most efficient granular size for core of the bearing and almost %50 of the axial compressive load is supported by steel balls. Energy dissipation took place in the core by the friction of steel balls.

In conclusion, seismic isolation systems have some advantageous and drawbacks. For instance, the drawback of the system developed by Özden and Türer [14] does not let retrofitting applications due to its practical difficulties during placing process. Whereas, BRBs can be used in almost all common applications and have easy manufacturing process plus their low cost price and maintenance practicality. For that reason, authors recommend to use them as bridge bearings in rural areas where have low traffic density and in new constructed heavy and massive structures. As a matter of fact, all seismic isolation systems shall provide sufficiently low horizontal stiffness, relatively high horizontal rigidity, high vertical rigidity, sufficient damping, self centering effect, anti failure system and sufficient strength against tensile loads in order to protect structure against earthquake [17].

1.4.2. Studies on Elastomeric Bearings (EBs)

There are two common types of elastomeric compounds either neoprene or natural rubber. Their disadvantages or advantages compared to each other by Roeder and Stanton [18]. The researchers [17,18,19] found out that crystallization stiffness of neoprene is higher than natural rubber which has second order transition only at approximately -40^{o}C (-40^{o}F) while neoprene displays second-order transition between -40^{o}C (-40^{o}F) and -50^{o}C (-58^{o}F). Furthermore, natural rubber is considered having better resistance to ozone cracking than neoprene.

After an extensive experimental program, Yakut and Yura [22a] concluded that parameters such as temperature, time, and amplitude of shear strain, coefficient of friction and rate of loading considered as important parameters. On the other hand, they emphasized that dynamic loading due to traffic and cyclic straining caused by daily temperature fluctuations does not have important effects on the shear modulus. They noted that creep rate has more significant effects at low temperatures and related mostly with initial deformation; but, it's overall effect is insignificant compared to creep at room temperature. Kulak and Hughes [11] underlined the shear stiffness and the energy dissipation as important characteristics of bearings. The fundamental horizontal frequency of a base isolated structure is governed by shear stiffness and amplitude of the system at fundamental system frequency which is controlled by energy dissipation [11].

Elastomers are generally operable at temperatures between -20^{o}C (-4^{o}F) to 40^{o}C (104^{o}F) and provide system frequencies between 0.4Hz and 0.8Hz [11]. The behaviors of EBs change significantly at low temperatures. Low temperatures and dynamic loading can cause increase in the stiffness of the rubber. Thus, bring large expansion forces which can cause damage in bridge and its substructure. According to Yakut and Yura [22] increase of shear stiffness of rubber bearings at low temperatures consist of two parts as instantaneous stiffening and crystallization stiffening respectively. Increase of shear stiffness caused by temperature change is called instantaneous stiffening and measured after the bearing temperature reaches environmental temperature. However, increase of stiffness with time is called as crystallization and that leads to molecular phase change in the material. In the study of Roeder, Stanton and Feller [19], low-temperature crystallization stiffness increase were 15 times more than the room temperature stiffness and greatest increases were observed at temperatures on the order of -30^{o}C to -35^{o}C (-22^{o}F to -31^{o}F). The initiation of crystallization stiffness takes longer time; however, larger stiffness increases were observed after crystallization started [12,19]. On the other hand, the increase in thermal instantaneous stiffness takes place more than 50 times the room temperature stiffness at temperatures below the second-order transition. When temperatures below the -35^{o}C (-31^{o}F) crystallization stiffness do not have significant increase. Therefore, instantaneous stiffness takes more important role in this case. Murray and Detenber [12] concluded that the stiffness increase directly related to this temperature and the duration of accumulated of crystallization. Reason for change of the behavior at low temperatures depends mostly on temperature of the elastomer exposure, duration of exposure to that temperature, loading rate, applied stress and present temperature of the elastomer [17,19]. Therefore, it is concluded that the behavior of the results gathered from experiments of EBs should be directly determined by tests performed to that bearing [17]. Tests longer than 28 were not considered necessary due to stiffness plateau occurs at the test longer than this duration. It is recommended performing crystallization tests at the anticipated low temperatures for a geographical region or at subfreezing temperatures might prolong in the region if the expected temperatures lower than -35 ^{o}C (-31^{o}F) [19]. It is observed that recovering the room temperature stiffness after specimen is warmed up more than 15^{o}C (27^{o}F) above the crystallization temperature and it takes 1-8hr [12,19].

Failure of the EBs is significant factor as design criteria. Therefore, structural engineers should analyze and understand all possible failure causes. Short bearings are more likely to encounter stability failure due to having low shear stiffness of rubber. Internal rupture and tension cracking of the elastomers are also serious problems that controlled by limiting the magnitude of loadings or deformations which might cause tensile stress or strain. Furthermore, excessive flexibility or creep can cause extreme deflections at bearings which lead serviceability failures. Roeder and Stanton [18] emphasized importance of edge cover for improving fatigue life of the bearing due to stress concentrations took place at the edges. The experiments reveal that ozone or mechanical cracking are common cause to these concentrations [18]. Moreover, the test results reveal that fatigue cracks in bearings under compression are another reason of the tensile stress concentrations at the edges of the bond between rubber and reinforcement. Failures of the reinforcement of the bearing as a result of rupture or yield under monotonic load or fatigue under cyclic loading cause significant problems such as reducing the ultimate load capacity. Last but not least, holes and discontinuities at reinforcement reduces net sections and cause stress concentrations.

Roeder and Stanton [18] came to conclusion that bearings having higher shape factors and harder elastomers are stiffer and flexible rubbers bulge more than stiff ones same as thick layers bulge more than thin layer. They also noted that providing increase at stiffness by a harder rubber decreases the shear strains. On the other hand, it makes bearing less effective while accommodating structural movements. It is observed that steel reinforced bearings have substantial reserve strength under monotonic loading which shows the significance of reinforcement strength to the capacity of the bearing [18]. Similarly in the study of Pınarbaşı and Akyüz [17] steel plates were observed to fail at about three times the yield force at the axial compression tests up to the failure. However, the steel plates support loads even after yielding. The authors [18] recommend having a safety factor of at least 4.0 since yielding of reinforcement took place on the order of 25% of the ultimate load.

1.4.3. Studies on Test Methods of Elastomeric Bearings (EBs) at Low Temperatures

There are various test methods for evaluating the performance of EBs at low temperatures. Standard specification for plain and laminated elastomeric bridge bearings AASHTO M-251 has test procedures such as shear modulus, compression stiffness, creep and shear bond in EBs. The drawback of AASHTO M251-97 related with applicability of only elastomers having hardness of 50 durometer has been overcome in AASHTO M251-06 by defining elastomers having hardnesses ranging between 50 to 70 durometer defined according to ASTM D 2240. One of the most disadvantage sides of test method is performing test in an open air instead of an enclosed environmental chamber [22b]. Reaching required strain level takes not less than 15 minutes which is effecting the temperature of bearing so shear modulus of bearing substantially. Yakut and Yura [22b] consider that it should not be expected to get realistic results related with shear modulus at defined temperature by using AASHTO M251. The ASTM D1043 test for instantaneous stiffening assumes linear relationship between applied torque and twisting angle which might be true for plastics but not for rubbers especially at room temperature. Another shortcoming of approach is limiting twisting angle between 10^{o} and 100^{o} which leads to accept relatively stiff materials in the elastic range. Therefore the limit does not provide us to compare stiffness's of nonlinear materials at two different twisting angles. Yakut and Yura [22b] recommend using shear force and expected daily shear strain at low temperature as performance criteria instead of shear modulus for crystallization tests. The current AASHTO test procedure assumes that thermally induced shear strain is independent from ambient temperature, that is, bearings always reach 25% shear strain at the ambient temperatures of -18, -26 and -37^{o}C (-0.4, -14.8 and -34.6^{o}F), which is not realistic in real case. The researchers concluded that maximum shear force depends on the daily temperature fluctuations, the average ambient temperature and duration of average ambient temperature after performing tests according to real data gathered from four different locations of United States [22b]. They elucidated shortcoming of current testing criteria such as applicability of same criteria for both instantaneous and crystallization stiffening. Furthermore, current performance criteria considered overly conservative which is $G_C/G_R<4$.

1.4.4. Studies on Response of Seismically Isolated Structures

The isolated structures have experienced lots of earthquakes and survived with little or no damage compared to fixed-base structures [4]. Assessing this performance in terms of engineering parameters, it is expected to measure reduction of accelerations through from ground to roof level and compare results with adjacent fixed-based structures. For this purpose, accelerographs were installed at different floors of structures. The accelerations recorded at ground and roof levels of these structures showed that significant reductions occurred at isolated structures compared to response of adjacent buildings. Table 1.1 summarizes the results of the performance of five isolated structures performance after the earthquakes. Most of these structures were constructed in Japan and experienced moderate earthquakes. It is obviously seen that the isolated structures have significant success in reducing accelerations so that the forces transmitted to supporting structure is less than compared to conventional structures.

Table 1.1. Observed Seismic Response of Isolated Structures [4]

Structure	Location	Earthquake		Maximum Ground Acceleration	Maximum Roof Acceleration	Maximum Roof Acceleration Adjacent Building
		Magnitude	Date			
Foothill Communities Law and Justice Center	San Bernardino County, California	Redlands M = 4.9	Oct 2 1985	0.04g	0.03g	not available
Coal Storage Silo	Takenaka Technical Research Laboratory, Japan	M = 6.1	Oct 4 1985	0.09g	0.05g	0.16g
Okumuro Corp. Research Institute Administration Building	Tsukuba, Japan	M = 5.1	June 30 1987	0.20g	0.02g	not available
Tohoku University	Sendai, Japan	M = 6.5	April 23 1987	0.04g	0.04g	0.27g
Oiles Technical Center	Fujisawa, Japan	Tokyo to Tobu M = 6.0	March 18 1988	0.04g	0.04g	0.08g

1.4.5. Studies on Economical Impact of Seismic Isolation Systems

Seismic isolation systems provide significant contributions to the economy. Wai and Nana analyzed the economical impacts of seismic isolation systems at their research [20]. They emphasized that seismic isolation systems provide significant economical benefits like annual export income of $5m to the economy. Wai and Nana noted that seismic isolation cost is approximately between 2% to 5% of total construction cost. Similarly, it is observed that the isolated design cost less than 6% of total construction cost compared to the conventional design for two-storey building (Fire Department Command and Facility for Los Angeles County in US. [4].

The seismic isolation technology is in a global competition with leading countries such as the US, Japan, the UK, Italy, Canada and New Zealand. Since common technology and isolators are complex, demand high specification and have high cost, New Zealand is researching a less complex and lower cost system to be able to export its products to developing countries like India, Turkey and etc.

In conclusion, seismic isolation systems reduce insurance costs and damages at structures and loss of lives except contributing economy in a monetary level.

CHAPTER 2

TEST SET UP AND TEST METHOD

2.1. Test Set Up

Information about test equipment, data acquisition system, properties of EBs and other materials used in tests are given in this chapter. Full size of two identical BRBs were tested in pairs during tests. Axial compression was applied by vertical hydraulic jack to provide required stress levels. Shear force was applied by horizontal hydraulic jack to the middle plate and its displacement was measured by Linear Variable Differential Transformer (LVDT). Researchers [19,21] suggest that bearing shall be held at constant low temperatures in an environmental chamber. An insulation belt was placed to protect the exposed surface of the frozen bearing from temperature changes during testing. Tests were conducted at laboratory temperatures.

2.1.1. Test Equipment

Test equipment used for seismic isolation systems is located at the Structural Mechanics Laboratory of Civil Engineering Department, METU. Test machine can apply axial loads on bearings at required stress levels combined with cyclic shear force to a pair of EBs at the same time. Testing machine is not attached to ground and is portable. General view of the test equipment is presented in Figure 2.1.

Testing machine has a load capacity of 3000 kN in vertical direction and 500 kN in horizontal direction. Hydraulic cylinders in both directions are capable to resist the pressure of 300 bars. Capacity of reversible load cell placed in horizontal direction is 300 kN LVDT to measure horizontal displacement has a stroke of 300 mm. One other load cell is utilized to measure the vertical load on bearings.

Figure 2.1. General View of the Test Equipment

All of the tests are performed manual control of the machine. The target speed and level of cyclic loads are achieved by adjusting the pressure valve of the machine. A view of the command panel is presented in Figure 2.2.

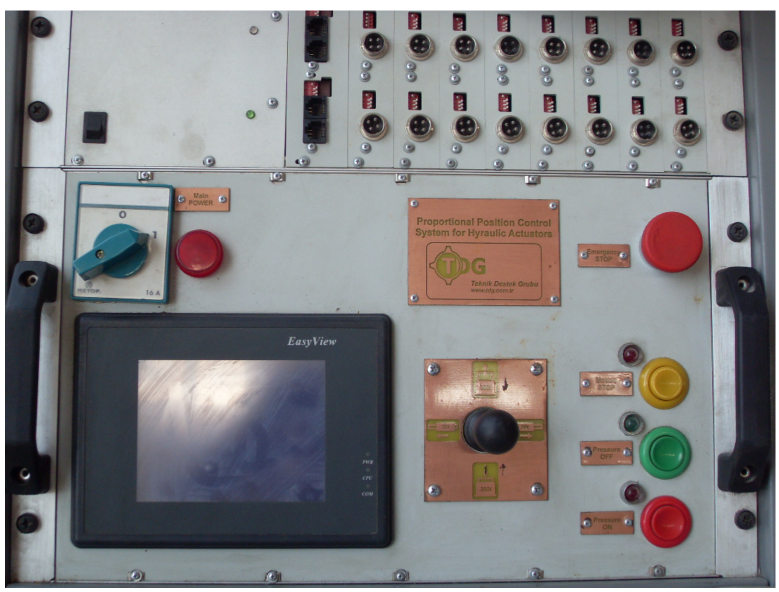

Figure 2.2 View of the Control Panel

Two bearings shall be tested simultaneously since horizontal load is applied to central push-pull plate, and this plate is the only moveable component of testing machine in horizontal direction. Sizes of the fixing steel plates limit the size of the test bearings to a diameter of 360mm.

Schematic layout of the test equipment is presented in Figure 2.3.

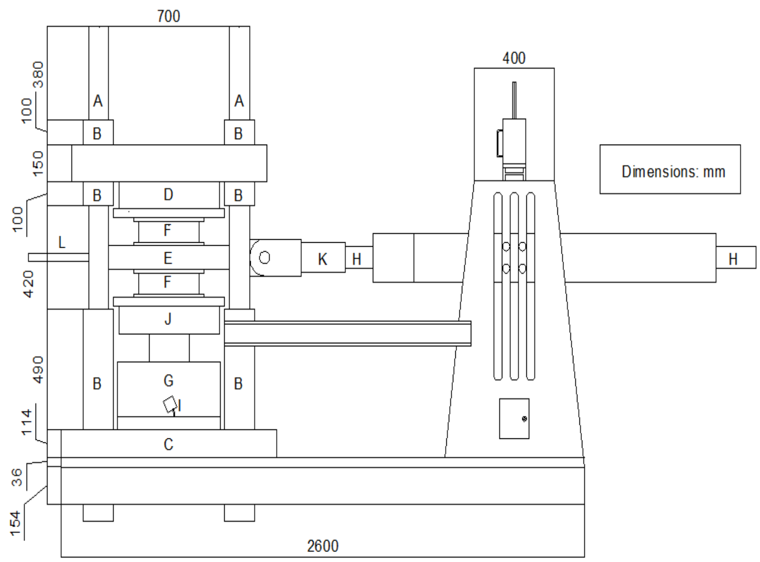

Figure 2.3. Schematic Layout of Test Equipment

In Figure 2.3;

A : four steel rods (Steel Grade St 42)

B : four steel bolts

C : three support plates (Steel Grade St 42)

D : fixed plate

E : push-pull plate

F : bearings to be tested (two bearings are tested simultaneously)

G : hydraulic cylinder (for application of vertical loads)

H : hydraulic cylinder (for application of horizontal loads)

I : load cell in the vertical direction

J : steel plate connected to G

K : load cell in the horizontal direction

L : LVDT

2.1.2. Data Acquisition System

Data acquisition system called System 6000-Model 6100 Scanner that is manufactured by Vishay Micro Measurement was utilized (Gent, 2001). Sample rate for the utilized system is up to 10000 samples per second per channel. System 6000 is operational in between -10^{o}C (14^{o}F) and +50^{o}C (+122^{o}F). Model 6100 scanner accepts up to 20 plug-in input cards. A view of the data acquisition system is presented in Figure 2.4.

Figure 2.4. View of the Data Acquisition System

2.1.3. Insulation Belt and Thermocouples

Polyethylene foam was cut at the required length then it was covered by bubble pack for forming the insulation belt. A view of preparing insulation belt process is presented in Figure 2.5.

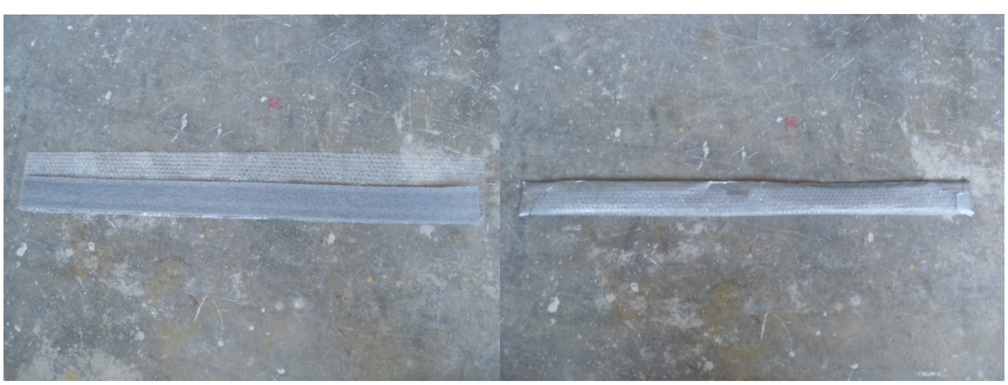

Figure 2.5. View of Preparing Insulation Belt Process

Enda pt100 ep0630 brand, type J thermocouples were utilized for measuring the heat inside the rubber. Type J thermocouples which were utilized in tests have sensitivity of 55μV/C^o and operational at temperatures between -200^{o}C (-328^{o}F) and +1350^{o}C (+2462^{o}F). Rubber part of EB was drilled in three different spots at three different depths. A view of thermocouple inserting process is presented in Figure 2.6.

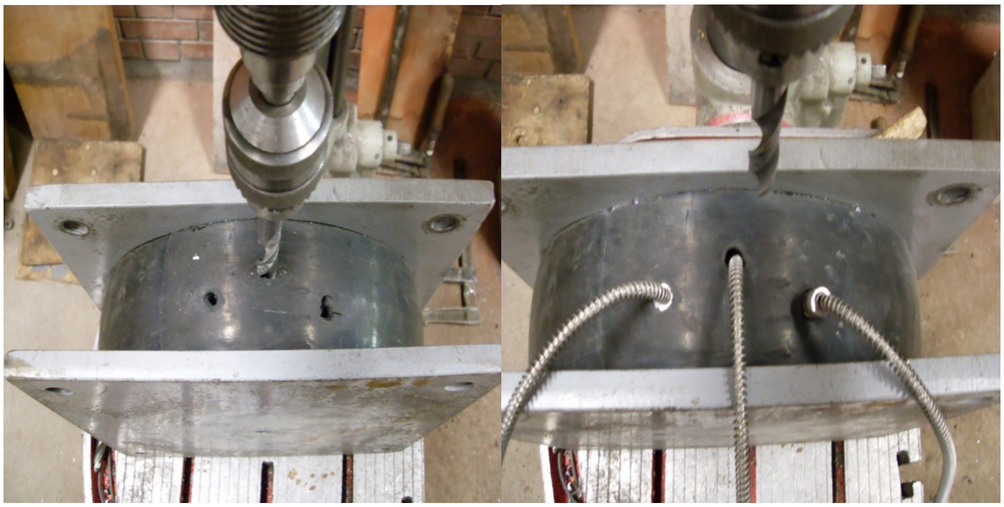

Figure 2.6. View of Thermocouple Inserting Process

Three thermocouples were embedded into rubber at three different depth 85 mm, 55mm and 25 mm respectively. These depths were named as D1 (25mm), D2 (55mm) and D3 (85mm) respectively. D0 was referred as the surface temperature of the bearing. A view of thermocouple layout is presented in Figure 2.7.

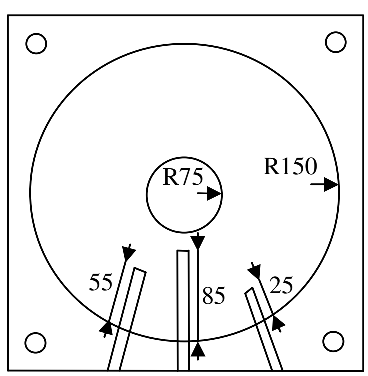

Figure 2.7. Thermocouple Layout

Steel balls with an average diameter of 1.65mm were utilized in the study as granular material to increase the damping characteristics of the EB. Plan view of BRB filled with 1.65mm steel balls are presented in Figure 2.8.

Figure 2.8. Plan View of a BRB

The freezer which was used in this study is able to hold temperatures down to -18^{o}C (-0.4^{o}F) and -36^{o}C (-32.8^{o}F). The view of freezer is presented in Figure 2.9.

Figure 2.9. View of the Freezer

2.2. Test Method

There are five different testing methods; quad-shear, dual lap, inclined-compression, full scale shear test and compression, defining low temperature stiffening tests provided in the National Cooperative Highway Research Program (NCHRP) Report

No 449 [23] for EBs. Test specimens used in this study, EB and BRB, were tested according to full scale shear test method since this method allows us to test the bearings in an open environment up to 30 minutes. However, specified temperatures were controlled by using insulation belt. Tests were conducted on full size elastomeric bearing (EB) and ball rubber bearing (BRB) at different temperatures subjected to compressive and shear forces and for two different loading cases, service state case and earthquake state case.

2.2.1. Bearings Used in the Test

There are two types of bearings used during tests regarding their inner core case either empty (EB) or full (BRB). Two different sizes were used in tests named as Type A and Type B for those two different types of bearings.

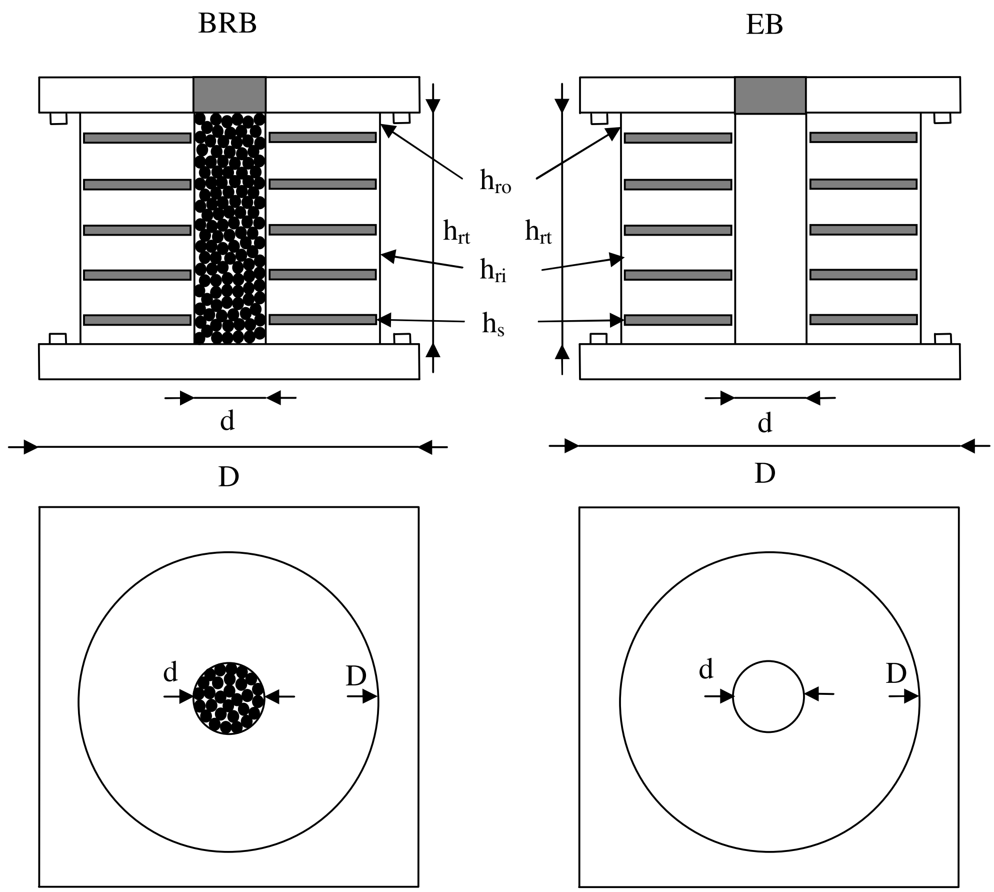

Figure 2.10. Front and Plan View of the Test Bearings

Bearings having the same shape factors but different sizes were tested at different temperature values and stress levels. Sizes of the bearings are given in Table 2.1. EBs are manufactured by vulcanizing thin steel plates and rubber layers under certain pressure and temperature.

Table 2.1 Sizes of the Bearings

Dimensions	Bearing Size	
	A	B
D (mm)	300	210
d (mm)	100	70
h_{ri} (mm)	15	11
h_{ro} (mm)	7.5	5.5
h_s (mm)	2	2
h_{rt} (mm)	85	65

where:

D= diameter of circular bearing

d= diameter of central hole

h_{ri}= thickness of the inner rubber layer

h_{ro}= thickness of the outer rubber layer

h_{rt}= thickness of the total rubber

h_s= inner steel shim thickness

The ratio of D/d was chosen as 3.0 for all bearing types. Front and plan view of the bearings used in this study are presented in Figure 2.10.

2.2.2. Mechanical Properties of Elastomeric Bearings (EBs)

The mechanical properties of EBs will be discussed in this section. Horizontal stiffness of a bearing is expressed by Equation (2.37):

$$K_h = \frac{GA}{h_{rt}} \tag{2.37}$$

where [13]:

A : plan area of EB

G : shear modulus of rubber

h_{rt} : total rubber thickness

K_h : horizontal stiffness of an EB

Shear modulus of the bearing can be calculated as [1]:

$$G = \frac{F_{\gamma=50\%}}{A_{rubber} \times 2 \times 0.5} \tag{2.38}$$

The factor 2 in denominator of Equation (2.38) accounts for simultaneously tested bearings (double shear) while the factor 0.5 accounts for 50% shear strain.

Vertical stiffness of an EB is expressed by following equation:

$$K_v = \frac{E_c A_r}{h_{rt}} \tag{2.39}$$

where:

A_r : area of the overlap between top and bottom bonded areas of the deformed bearing [5]

E_c : instantaneous compression modulus of the rubber-steel composite under the specified level of vertical load [13]

K_v : vertical stiffness of an EB

Compression modulus of a bearing can be expressed in the below equation:

$$E_c = 6GS^2 \tag{2.40}$$

If the shape factor of the bearing is larger than 10, then bulk modulus (K) should be taken into account for the compressibility of the bearing.

Geometrical properties of the bearing is one of the most important factors for determining stability problems of a bearing caused by buckling, failure modes. Therefore, the compression modulus and vertical stiffness of an EB depends on the shape factor. There are two important geometrical unitless factors of an EB named as shape factor (S) and aspect ratio (δ) [17].

$$\delta = \frac{h_{rt}}{W} \tag{2.41}$$

The shape factor for an EB with a hole shall be taken as [3]

$$S = \frac{D^2 - d^2}{4 \times h_{ri} \times (D + d)} \tag{2.42}$$

where:

D : diameter of circular bearing (mm)

d : diameter of central hole (mm)

h_{ri} : thickness of the i^{th} elastomeric layer in EB (mm)

The energy dissipation of isolation systems either utilizes hysteretic energy dissipation or viscous energy dissipation methods. The term viscous refers to dependence of energy dissipation to magnitude of velocity. The term hysteretic refers to the offset between the loading and unloading curves under cyclic loading. The energy dissipation used in this study refers to hysteretic energy dissipation. The idealized force-displacement loop is presented in Figure 2.11.

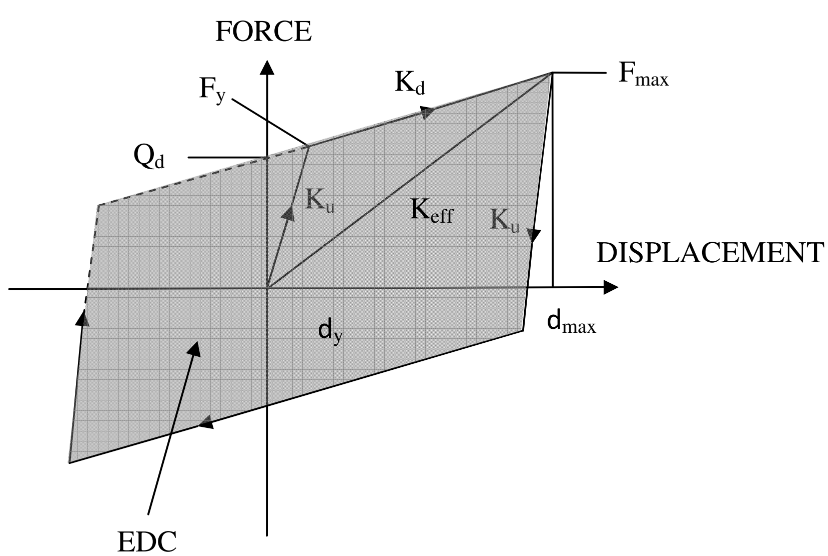

Figure 2.11. Idealized Force Displacement Hysteresis Loop [2]

where:

d_y = Yield displacement

d_{max} = Maximum bearing displacement

EDC = Energy dissipated per cycle = Area of hysteresis loop (shaded)

F_y = Yield force

F_{max} = Maximum force

K_d = Post-elastic stiffness

K_u = Elastic (unloading) stiffness

K_{eff} = Effective stiffness

Q_d = Characteristic strength

Design equations of the EBs in AASHTO specifications [2,3] were used in order to check acceptance of bearings and required calculations are presented in Appendix E.

2.2.3. Temperature Levels

Three different temperature levels were determined and named as T_1, T_2 and T_3. T_1 and T_2 values are representative values for the average maximum and minimum temperatures in the winter season for the provinces located nearby North Anatolian Fault. The recorded extreme temperatures at some provinces in the vicinity of North Anatolian Fault Zone are presented in Table 2.2. The full list of provinces vicinity of North Anatolian Fault Zone and recorded temperature values are presented in Appendix D. According to Roeder and Stanton -35°C (-31°F) is crucial threshold degree for temperature induced stiffening. Instantaneous stiffening is more critical than the crystallization stiffness at temperatures below -35°C (-31°F) [19]. Instantaneous stiffening develops at low temperatures in a short term of period and crystallization stiffness develops in a long-term of period at very low temperatures. T_3 value is mostly representative of a very cold region in Turkey.

T_1: 20°C (68°F) T_2: -18°C (-0.4°F) T_3: -30°C (-22°F)

Table 2.2. Recorded Extreme Temperatures at Provinces in the Vicinity of North Anatolian Fault Zone [9]

Province	Extreme Value (^oC)	December	January	February
		Extreme Temperature Values Occurred in Period Between 1975-2008		
AĞRI	Max.	14.0	7.6	10.2
	Min.	-39.8	-38.0	-42.8
BOLU	Max.	20.1	19.8	20.8
	Min.	-22.6	-18.8	-22.0
ÇANAKKALE	Max.	20.4	18.4	21.2
	Min.	-7.2	-7.2	-11.2
DÜZCE	Max.	26.2	23.4	25.6
	Min.	-16.5	-15.0	-17.3
ERZİNCAN	Max.	16.4	14.0	17.2
	Min.	-25.0	-24.4	-25.2
ERZURUM	Max.	14.0	7.6	9.6
	Min.	-37.2	-36.0	-37.0
İSTANBUL	Max.	21.2	18.3	24.0
	Min.	-3.4	-7.9	-8.0
*	*	*	*	*
*	*	*	*	*
*	*	*	*	*
KOCAELİ	Max.	24.0	22.6	23.7
	Min.	-4.5	-6.0	-8.3
SAKARYA	Max.	26.2	24.2	25.4
	Min.	-6.8	-8.2	-10.0
TUNCELİ	Max.	18.0	14.0	18.1
	Min.	-25.6	-24.0	-26.6
AVERAGE	**Max.**	**20.4**	**17.5**	**20.1**
	Min.	**-18.3**	**-18.9**	**-21.1**

2.2.4. Investigated Compressive Stress Levels

A series of compressive stress levels were investigated on structural response of bearings subjected to cyclic load. At each temperature level; the series of tested compressive stress levels were selected based on the temperature sensitive bearing rigidity. The stresses were computed based on the gross area of the bearing. However, the inner core of BRBs, steel balls, resists about half of the applied axial load and the true stress on the surrounding rubber portion is much less than the indicated values. Therefore the stress values given below are average stresses. In any case the corresponding compressive strain on rubber portion is less than the industry accepted threshold strain value of 0.07. Strains on the bearing are expected to be lesser in real case since the stress values calculated by considering the gross area of the bearing. The investigated stress and strain levels for corresponding temperature levels are presented in Table 2.3. In Table 2.3 "*" symbols denote not tested case due to possible tension tear out of rubber.

Table 2.3. Investigated Stress and Strain Levels for Corresponding Temperature Levels

Temperature Level	Investigated Stress and Strain Levels				
T_1	σ_1: 0.0 MPa	σ_2: 1.5 MPa	σ_3: 3.0 MPa	*	*
	ε_{1A}: 0.00	ε_{2A}: 0.02	ε_{3A}:0.05	*	*
	ε_{1B}: 0.00	ε_{2B}: 0.03	ε_{3B}: 0.05	*	*
T_2	σ_1: 0.0 MPa	σ_2: 1.5 MPa	σ_3: 3.0 MPa	σ_4: 4.5 MPa	*
	ε_{1A}: 0.00	ε_{2A}: 0.02	ε_{3A}: 0.05	ε_{4A}: 0.07	*
	ε_{1B}: 0.00	ε_{2B}: 0.03	ε_{3B}: 0.05	ε_{4B}: 0.08	*
T_3	σ_1: 0.0 MPa	σ_2: 1.5 MPa	σ_3: 3.0 MPa	σ_4: 4.5 MPa	σ_5: 6.0 MPa
	ε_{1A}: 0.00	ε_{2A}: 0.02	ε_{3A}: 0.05	ε_{4A}: 0.07	ε_{5A}: 0.09
	ε_{1B}: 0.00	ε_{2B}: 0.03	ε_{3B}: 0.05	ε_{4B}: 0.08	ε_{5B}: 0.11

2.2.5. Temperature Control

Elastomeric bearing (EB) cold weather temperature conditioning is based on the low temperature full scale test method defined in (NCHRP) Report No 449 [23] since bearings can be exposed to room temperature for up to 30 minutes according to the test requirements. Therefore, the following temperature control method was used in this test program in the lack of an environmental chamber that can accommodate a full scale testing machine inside. Some of the frozen bearings were covered with insulation belts to minimize the temperature drop in the bearing during testing.

Figure 2.12. View of Thermocouple Attached to Insulated and Uninsulated Bearings

The thawing time period both for insulated and uninsulated rubber frozen to -30^{o}C (-22^{o}F) was determined by recording temperature at every minute of warming time through thermocouple readings as depicted in Figure 2.12.

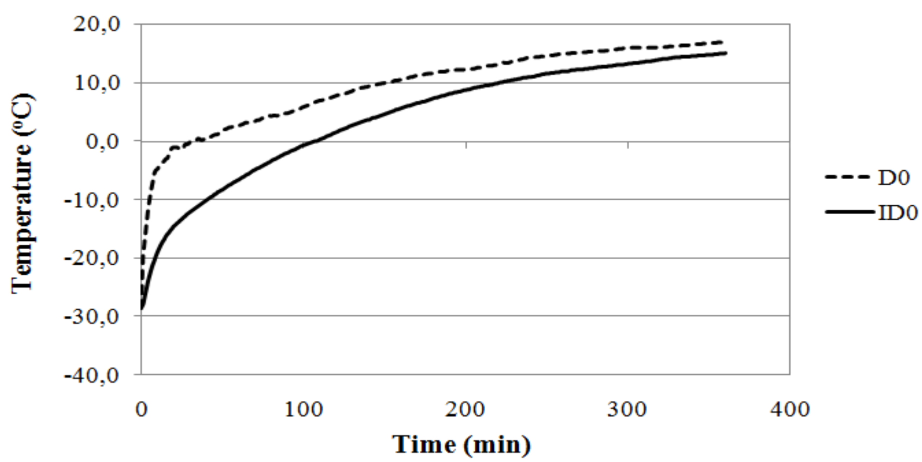

Figure 2.13. Comparison of Surface Temperature Records between Insulated and Uninsulated Bearing

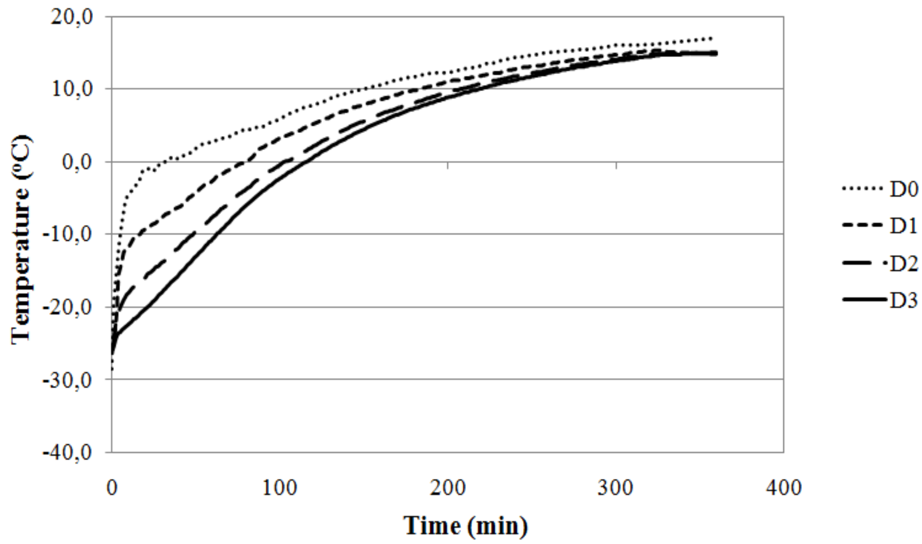

Figure 2.14. Temperature Change at Different Depths of an Uninsulated Bearing

It was observed that an uninsulated bearing kept in freezer for a day at -30°C (-22°F) can thaw in room temperature in 6 hours. The insulated bearing was also tested at the same conditions to observe the efficiency of the insulation belt. As can be observed from Figure 2.13 at the end of an hour the surface temperature of the uninsulated bearing is reached to 2.6°C (36.7°F) whereas the surface temperature of insulated bearing is reached to -6.6°C (20.1°F).

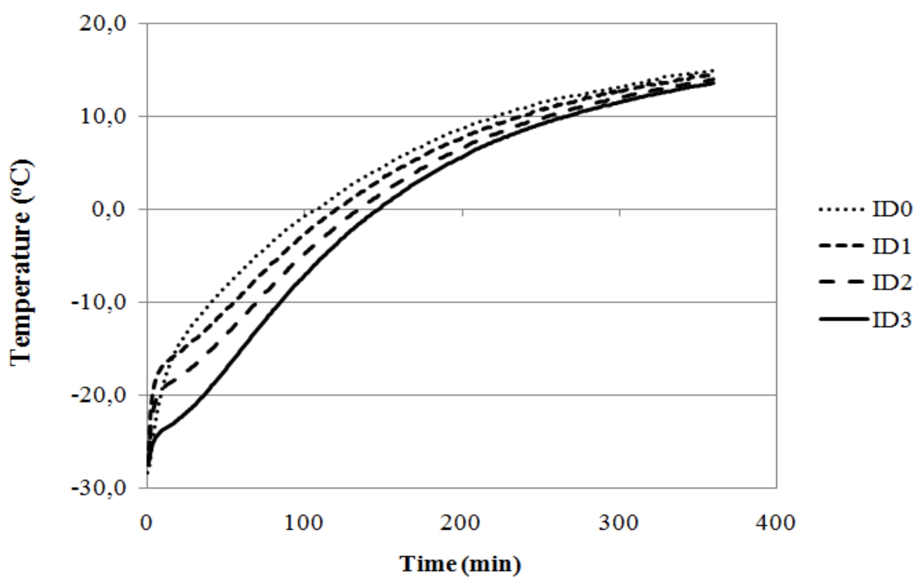

Figure 2.15. Temperature Change at Different Depths of an Insulated Bearing

Temperature readings from outer surface of bearing (D0) may not be accurate since the thermocouple may be reading an average of laboratory temperature and surface temperature. The same bearing was again kept in freezer at -30^{o}C (-22^{o}F) for a day. In the laboratory environment, temperature drop in the bearing for 6 hours were investigated at three different depths measured from outer surface towards to center: 25 mm (D1), 55 mm (D2) and 85mm (D3).

The inner core temperature drop rate is much less than the one recorded for the most outer reading location as shown in Figure 2.14 and 2.15. It shall be noted that insulated bearing has significant advantage to preserve heat compared to uninsulated bearing.

2.2.6. Test Cases

BRBs were tested for two different sizes, Type A and Type B, at two different loading cases as service and earthquake state.

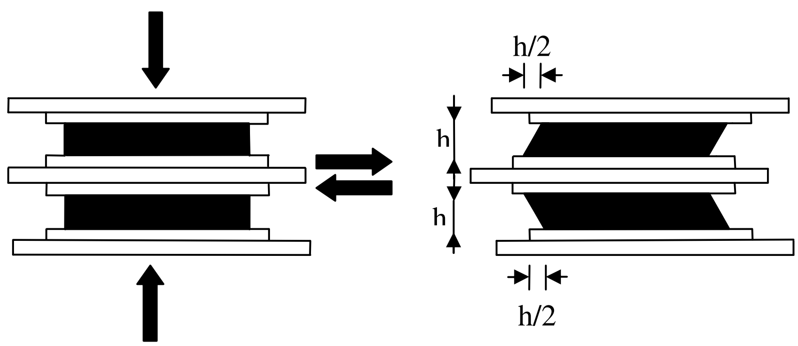

Figure 2.16. View of Bearings at Service State

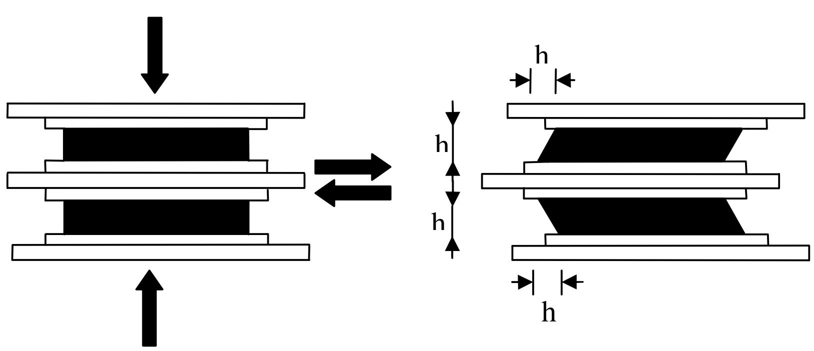

Figure 2.17. View of Bearings at Earthquake State

Views of bearings for service and earthquake states are presented in Figure 2.16 and Figure 2.17 respectively.

Table 2.4. Tests

Test No	**Test Name**	**Test No**	**Test Name**
1	EB_A - T_1 - σ_1	26	BRB_A - T_1 - σ_2
2	EB_A - T_1 - σ_2	27	BRB_A - T_1 - σ_3
3	EB_A - T_1 - σ_3	28	BRB_A - T_2 - σ_1
4	EB_A - T_2 - σ_1	29	BRB_A - T_2 - σ_2
5	EB_A - T_2 - σ_2	30	BRB_A - T_2 - σ_3
6	EB_A - T_2 - σ_3	31	BRB_A - T_2 - σ_4
7	EB_A - T_2 - σ_4	32	BRB_A - T_3 - σ_1
8	EB_A - T_3 - σ_1	33	BRB_A - T_3 - σ_2
9	EB_A - T_3 - σ_2	34	BRB_A - T_3 - σ_3
10	EB_A - T_3 - σ_3	35	BRB_A - T_3 - σ_4
11	EB_A - T_3 - σ_4	36	BRB_A - T_3 - σ_5
12	EB_A - T_3 - σ_5	37	BRB_B - T_1 - σ_1
13	EB_B - T_1 - σ_1	38	BRB_B - T_1 - σ_2
14	EB_B - T_1 - σ_2	39	BRB_B - T_1 - σ_3
15	EB_B -T_1 - σ_3	40	BRB_B - T_2 - σ_1
16	EB_B - T_2 - σ_1	41	BRB_B - T_2 - σ_2
17	EB_B - T_2 - σ_2	42	BRB_B - T_2 - σ_3
18	EB_B - T_2 - σ_3	43	BRB_B - T_2 - σ_4
19	EB_B - T_2 - σ_4	44	BRB_B - T_3 - σ_1
20	EB_B - T_3 - σ_1	45	BRB_B - T_3 - σ_2
21	EB_B - T_3 - σ_2	46	BRB_B - T_3 - σ_3
22	EB_B - T_3 - σ_3	47	BRB_B - T_3 - σ_4
23	EB_B - T_3 - σ_4	48	BRB_B - T_3 - σ_5
24	EB_B - T_3 - σ_5	49	BRB_A - T_3 - $\sigma_{3.5}$
25	BRB_A - T_1 - σ_1	50	BRB_B - T_3 - $\sigma_{3.5}$

Two full size bridge bearings were placed between plates fixed with bolts to test machine framing, and compression load is applied by hydraulic jacks the moveable middle plate was sheared and displacement was measured by LVDT. This type of test is typically referred as full scale shear test [1].

Three fully reverse cyclic shear loads per AASHTO [2] were applied in order to simulate the daily thermal expansion/contraction cycles of bridge bearings. BRBs were subjected to deform 50% of their height at service state tests while deformation level is 100% for earthquake state tests.

Testing speed in service case was kept under average velocity of 0.003 inches/min in order to capture creep behavior at slow speeds [2]. The specimens used in this study, EB and BRB, were tested for service state case at three different temperature levels (T_1, T_2 and T_3) and five different compressive stress levels (σ_1, σ_2, …, σ_5). Earthquake state tests were performed at the 3.50 MPa axial compressive stress level and only for third temperature level, T_3. All test cases are presented in Table 2.4.

2.2.7. Planned Test Schedule

It was aimed to apply same test conditions at all tests. Therefore, bearings were kept in freezer for a day at all tests. The test schedule given in Table 2.5 was organized for using freezer and test machine more efficiently. Tests were conducted on two bearings having different sizes for service state and earthquake state cases, three different temperature levels, axial compressive stresses related to temperature levels for two different inner core cases. Tests were carried out by starting from first temperature level T_1, room temperature, to third temperature level T_3, -30^{o}C, in order to see the effects of temperature on bearings gradually. Moreover, BRBs were tested after EBs so that the contributions of steel balls were observed. Earthquake state tests were performed after service states tests were over for understanding the behavior of BRBs at two different loading cases.

Table 2.5. Test Schedule

Case	Test Type	Freezer	Case	Test Type	Freezer
1	$EB_A - T_1 - \sigma_1$ $EB_A - T_1 - \sigma_2$ $EB_A - T_1 - \sigma_3$		8	$BRB_B - T_1 - \sigma_1$ $BRB_B - T_1 - \sigma_2$ $BRB_B - T_1 - \sigma_3$	$BRB_A - T_2 - \sigma_1$ $BRB_A - T_2 - \sigma_2$ $BRB_A - T_2 - \sigma_3$ $BRB_A - T_2 - \sigma_4$
2	$EB_B - T_1 - \sigma_1$ $EB_B - T_1 - \sigma_2$ $EB_B - T_1 - \sigma_3$	$EB_A - T_2 - \sigma_1$ $EB_A - T_2 - \sigma_2$ $EB_A - T_2 - \sigma_3$ $EB_A - T_2 - \sigma_4$	9	$BRB_A - T_2 - \sigma_1$ $BRB_A - T_2 - \sigma_2$ $BRB_A - T_2 - \sigma_3$ $BRB_A - T_2 - \sigma_4$	$BRB_B - T_2 - \sigma_1$ $BRB_B - T_2 - \sigma_2$ $BRB_B - T_2 - \sigma_3$ $BRB_B - T_2 - \sigma_4$
3	$EB_A - T_2 - \sigma_1$ $EB_A - T_2 - \sigma_2$ $EB_A - T_2 - \sigma_3$ $EB_A - T_2 - \sigma_4$	$EB_B - T_2 - \sigma_1$ $EB_B - T_2 - \sigma_2$ $EB_B - T_2 - \sigma_3$ $EB_B - T_2 - \sigma_4$	10	$BRB_B - T_2 - \sigma_1$ $BRB_B - T_2 - \sigma_2$ $BRB_B - T_2 - \sigma_3$ $BRB_B - T_2 - \sigma_4$	$BRB_A - T_3 - \sigma_1$ $BRB_A - T_3 - \sigma_2$ $BRB_A - T_3 - \sigma_3$ $BRB_A - T_3 - \sigma_4$ $BRB_A - T_3 - \sigma_5$
4	$EB_B - T_2 - \sigma_1$ $EB_B - T_2 - \sigma_2$ $EB_B - T_2 - \sigma_3$ $EB_B - T_2 - \sigma_4$	$EB_A - T_3 - \sigma_1$ $EB_A - T_3 - \sigma_2$ $EB_A - T_3 - \sigma_3$ $EB_A - T_3 - \sigma_4$ $EB_A - T_3 - \sigma_5$	11	$BRB_A - T_3 - \sigma_1$ $BRB_A - T_3 - \sigma_2$ $BRB_A - T_3 - \sigma_3$ $BRB_A - T_3 - \sigma_4$ $BRB_A - T_3 - \sigma_5$	$BRB_B - T_3 - \sigma_1$ $BRB_B - T_3 - \sigma_2$ $BRB_B - T_3 - \sigma_3$ $BRB_B - T_3 - \sigma_4$ $BRB_B - T_3 - \sigma_5$
5	$EB_A - T_3 - \sigma_1$ $EB_A - T_3 - \sigma_2$ $EB_A - T_3 - \sigma_3$ $EB_A - T_3 - \sigma_4$ $EB_A - T_3 - \sigma_5$	$EB_B - T_3 - \sigma_1$ $EB_B - T_3 - \sigma_2$ $EB_B - T_3 - \sigma_3$ $EB_B - T_3 - \sigma_4$ $EB_B - T_3 - \sigma_5$	12	$BRB_B - T_3 - \sigma_1$ $BRB_B - T_3 - \sigma_2$ $BRB_B - T_3 - \sigma_3$ $BRB_B - T_3 - \sigma_4$ $BRB_B - T_3 - \sigma_5$	$BRB_A - T_3 - \sigma_{3.5}$
6	$EB_B - T_3 - \sigma_1$ $EB_B - T_3 - \sigma_2$ $EB_B - T_3 - \sigma_3$ $EB_B - T_3 - \sigma_4$ $EB_B - T_3 - \sigma_5$	$BRB_A - T_1 - \sigma_1$ $BRB_A - T_1 - \sigma_2$ $BRB_A - T_1 - \sigma_3$	13	$BRB_A - T_3 - \sigma_{3.5}$	$BRB_B - T_3 - \sigma_{3.5}$
7	$BRB_A - T_1 - \sigma_1$ $BRB_A - T_1 - \sigma_2$ $BRB_A - T_1 - \sigma_3$	$BRB_B - T_1 - \sigma_1$ $BRB_B - T_1 - \sigma_2$ $BRB_B - T_1 - \sigma_3$	14	$BRB_B - T_3 - \sigma_{3.5}$	

CHAPTER 3

DISCUSSION OF RESULTS

3.1. General

The researches related with the performance of seismic isolators at different temperatures were investigated by the keywords of “seismic isolation” and “temperature” in the known literature and it has been observed that researchers did not publish any material related to this subject. In this regard, BRB low temperature tests are first of its kind except the EB low temperature tests. Therefore, selected parameters of the EB and the BRB were compared to each other. Earlier researches [17,19,21] found out that EB mechanical properties such as shear modulus were effected by temperature changes.

The force deflection characteristics of bilinear hysteresis loops illustrated in Figure 2.11 have two significant parameters which are effected by temperature changes. The key parameters are defined as K_d, the stiffness of the secondary slope of the bilinear hysteresis loop, and the Q_d, the characteristic strength for seismic isolators [2]. The area of the hysteresis loop, EDC, and thus the damping coefficient are effected mainly by Q_d. The effective stiffness K_{eff} and the damping coefficient are effected differently by Q_d and K_d. The effective stiffness of the system K_{eff} and the damping coefficient β_{eq} are two significant variables of isolation systems since they effect the base shear forces (Equation (3.1)), the displacement (Equation (3.2)) and the period (Equation (3.3)).

$$C_S = \frac{K_{eff} \times d}{W} \qquad [2] \qquad (3.1)$$

$$d = \frac{250 \times A \times S_i \times T_{eff}}{B}(mm) \qquad [2] \qquad (3.2)$$

$$T_{eff} = 2\pi \sqrt{\frac{W}{K_{eff} \times g}} \qquad [2] \qquad (3.3)$$

where:

C_s : Elastic seismic response coefficient [2]

K_{eff} : The sum of the effective linear stiffnesses of all bearings and substructures supporting the superstructure segment as calculated [2]

d : Total deck displacement relative to ground ($d_i + d_{sub}$) [2]

A : Acceleration coefficient from section 3 [2]

B : Numerical coefficient related to the effective damping of the isolation system as set forth in table 2 (section 7) [2]

S_i : Numerical coefficient for site soil profile as set forth in table 5-1 for seismically isolated structures [2]

T_{eff} : Period of seismically isolated structure, in seconds, in the direction under consideration [2]

W : Total vertical load of the isolation system ($DL+LL_S$) [2]

3.2. Characteristic Strength (Q_d)

Characteristic strength of a bearing, Q_d, is defined as the ordinate of the hysteresis loop at the zero bearing displacement. Comparison of the normalized characteristic strength, Q_d, values for elastomeric bearings and seismic isolators is given in Table 3.1. It can be observed that characteristic strength increases with decreasing temperature for all specimens since rubber stiffens with low temperature. The specimens used in this study, EBs and BRBs, show similar performance with high damping rubber bearings.

Table 3.1. Comparison of the Normalized Q_d Values at Different Temperatures

Temperature (°C)	Normalized Characteristic Strength (Q_{dC}/Q_{dR})						
	ELASTOMERIC BEARING				SEISMIC ISOLATOR		
	HDRB[a,c,*]	HDRB[b,c,*]	LDRB[b,d,*]	EB	BRB	LRB	FPS
20	1.00	1.00	1.00	1.00	1.00	N/D	N/D
0	1.30	1.30	1.30	N/D	N/D	N/D	N/D
-10	1.40	1.40	1.40	N/D	N/D	N/D	N/D
-18	N/D	N/D	N/D	2.25	1.32	N/D	N/D
-30	2.50	2.00	1.50	2.26	1.74	N/D	N/D

Notes: N/D means no data.

a Large difference between scragged and unscragged properties. A large difference is one in which the unscragged properties are at least 25 percent more than the scragged ones.

b Small difference between scragged and unscragged properties

c HDRB = High Damping Rubber Bearing

d LDRB = Low Damping Rubber Bearing

* AASHTO Specification [2]

3.3. Secondary Stiffness (K_d)

Secondary stiffness of the bearing, K_d, is defined as the second slope of the bilinear hysteresis curve. Steel balls in the central core contribute to the secondary stiffness of the BRB. Contribution of steel balls to secondary stiffness is expressed as percentage of the horizontal stiffness of the elastomeric part (K_h) and given in Equation (3.11). Secondary stiffness of BRBs is effected by shear strain inversely. As maximum shear strain increases secondary stiffness of the bearing decreases. Comparison of the normalized secondary stiffness, K_d, values at different temperatures is given in Table 3.2. It was observed that the normalized secondary stiffness values of BRBs higher than EBs since contribution of steel balls. Moreover, the normalized secondary stiffness values shows significant difference at -30 ^{o}C for HDRBs compared to specimens used in this study since temperature control in this study provided by insulation belt instead of environmental chamber.

Table 3.2. Comparison of the Normalized K_d Values at Different Temperatures

Temperature (^{o}C)	Normalized Secondary Stiffness (K_{dC}/K_{dR})						
	ELASTOMERIC BEARING			SEISMIC ISOLATOR			
	HDRB[a,c,*]	HDRB[b,c,*]	LDRB[b,d,*]	EB	BRB	LRB	FPS
20	1.00	1.00	1.00	1.00	1.00	N/D	N/D
0	1.20	1.10	1.10	N/D	N/D	N/D	N/D
-10	1.40	1.20	1.10	N/D	N/D	N/D	N/D
-18	N/D	N/D	N/D	1.29	1.33	N/D	N/D
-30	2.00	2.00	1.30	1.07	1.23	N/D	N/D

Notes: N/D means no data.

a Large difference between scragged and unscragged properties. A large difference is one in which the unscragged properties are at least 25 percent more than the scragged ones.

b Small difference between scragged and unscragged properties

c HDRB = High Damping Rubber Bearing

d LDRB = Low Damping Rubber Bearing

* AASHTO Specification [2]

3.4. Average Effective Stiffness (K_{eff_avg})

The effective stiffness of the bearing is defined as the value of the maximum lateral force at instance of maximum lateral displacement in the bearing and divided by the maximum lateral displacement. The average effective stiffness term is defined as the average effective stiffness value for the positive and negative sides of the hysteresis loop. Comparison of the average effective stiffness values at different temperatures and compressive stress levels for EB and BRB is given in Table 3.3. It was observed that BRBs for two different types have significantly higher average effective stiffness values compared to the two different types of EBs in all temperature and compressive stress levels since the contribution of steel balls to stiffness. The big size bearings, Type A (geometric component of stiffness term: A/h = 942.48mm), have higher average effective stiffness values compared to small size bearings, Type B (A/h = 629.75 mm), due to pertaining flexible behavior in all temperature and compressive stress levels.

Table 3.3. Comparison of the Average Effective Stiffness Values at Different Temperatures and Compressive Stress Levels for EB and BRB

Temperature (^{o}C)	Compressive Stress (MPa)	K_{eff_avg} (kN/mm)			
		EB		BRB	
		Type A	Type B	Type A	Type B
20	0.0	0.988	0.551	1.197	0.558
	1.5	0.994	0.470	1.540	0.738
	3.0	0.979	0.621	2.000	0.982
-18	0.0	1.048	0.593	1.002	0.723
	1.5	1.063	0.535	1.341	0.794
	3.0	0.978	0.597	1.785	0.953
	4.5	0.947	0.482	3.030	1.517
-30	0.0	0.900	0.510	1.058	0.753
	1.5	0.990	0.620	1.409	0.988
	3.0	0.922	0.567	1.793	1.223
	4.5	0.941	0.505	2.504	1.366
	6.0	0.880	0.425	3.837	1.447

3.5. Equivalent Damping Ratio (β_{eq})

The equivalent damping ratio (β_{eq}) and of test bearings can be computed from the following expression by using the idealized force displacement relationship.

$$\beta_{eq} = \frac{4 \times Q_d \times (d_{\max} - d_y)}{2 \times \pi \times K_{eff} \times d_{\max}^{2}} \tag{3.4}$$

Comparison of the percent equivalent damping ratio (β_{eq} (%)) values at different temperatures and compressive stress levels for EB and BRB is given in Table 3.4. In all these cases, addition of steel balls in central core of the EBs, BRBs, increased the damping capability of the bearing.

Increasing compressive axial load level also results in increase in the damping capacity of the bearing. Similarly, in a previous research [15], it has been documented that BRBs subjected to combined compressive and cyclic lateral loads can provide friction based damping due to the pressurized movements of steel balls at the inner core.

In the temperature drop case for EB, the energy dissipating capability of the bearings increases due to the rigidity gained by the rubber at low temperatures.

It has been known that coefficient of friction increases with temperature rise and decreases with temperature drop [8].

Table 3.4. Comparison of the Percent Equivalent Damping Ratio (β_{eq}) Values at Different Temperatures and Compressive Stress Levels for EB and BRB

Temperature (^{o}C)	Compressive Stress (MPa)	β_{eq} (%)			
		EB		BRB	
		Type A	Type B	Type A	Type B
20	0.0	7.048	3.191	8.786	8.141
	1.5	7.707	8.715	10.266	15.801
	3.0	8.736	10.328	13.697	22.815
-18	0.0	16.812	14.491	9.294	17.365
	1.5	14.098	18.644	14.596	21.672
	3.0	12.824	29.304	18.216	31.751
	4.5	15.360	18.936	25.767	33.949
-30	0.0	12.042	19.202	11.843	17.614
	1.5	14.010	11.567	17.259	21.012
	3.0	10.835	17.662	17.623	25.954
	4.5	13.386	18.430	23.233	29.004
	6.0	15.222	24.223	26.587	29.613

Despite the negative effect of coefficient of friction on energy dissipation performance at low temperatures, the dominant factor resulting in higher damping response is basically due to the increase in rubber rigidity.

Type B bearings about the half scale of Type A bearings in terms of cross-sectional area and volume have a higher damping capability compared to Type A bearing. This type of behavior may be explained by well confinement of steel balls at a small diameter hole than a large diameter hole. Confinement is believed to be a function of space between internal steel shims or thickness of internal rubber layers. The internal steel shim spacing in Type B bearing is about 25% more than the one in Type A bearing and also bulge distance of Type B bearings (Δ_{BB}) is lesser than Type A bearing (Δ_{BA}) as can be seen in Figure 3.1. Well confinement can increase the pressure on steel balls by minimizing the bulging of internal rubber layer that is observed to increase the damping capability of the bearing. This is very similar to reinforcement concrete confinement which is provided by tight spacing of stirrups at the edges of beams or columns.

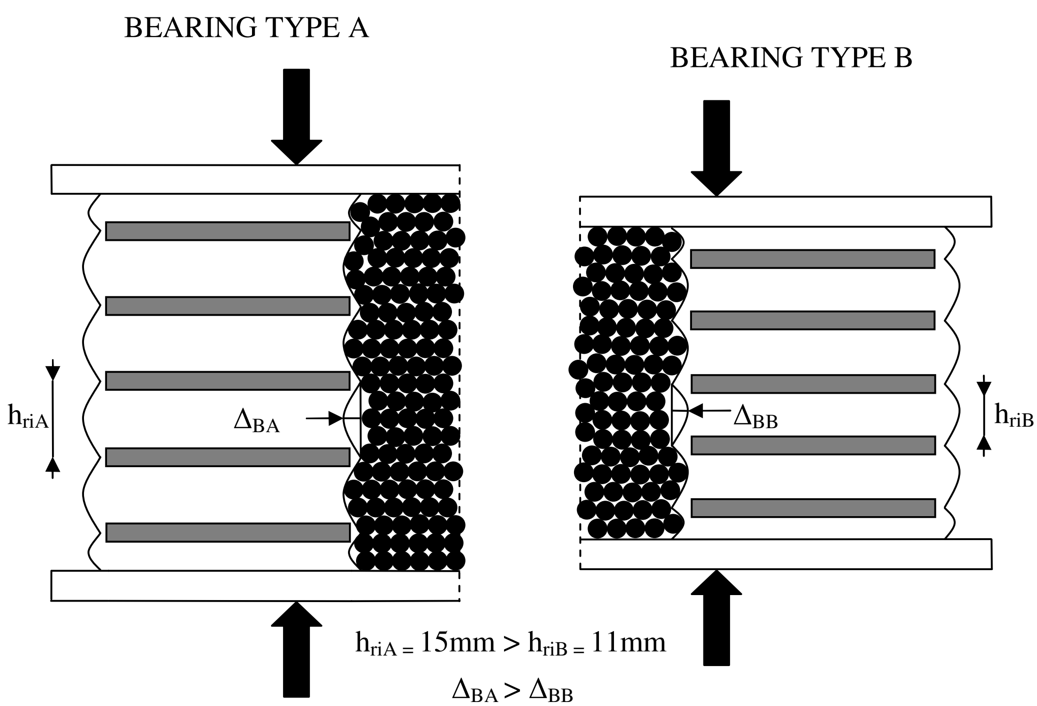

Figure 3.1. Effect of Confinement on the Different Bearing Sizes

3.6. Energy Dissipated per Cycle (EDC)

Energy dissipated per cycle (EDC) is the area of the hysteresis loop which is shown in Figure 2.11 and can be calculated by the following equation written below.

$$EDC = 4 \times Q_d \times (d_{\max} - d_y) \quad (3.5.)$$

Comparison of the energy dissipated per cycle (EDC) values at different temperatures and compressive stress levels for EB and BRB is presented in Table 3.5. Type A bearing, having larger sizes than the Type B bearing, has been observed to have a high EDC as presented in Table 3.5. It has been observed that BRBs have higher EDC compared to EB most of the cases for different temperature and compressive stress levels. The size effect and confinement characteristics of the inner core directly effect the magnitude of EDC.

Table 3.5. Comparison of the Energy Dissipated per Cycle (EDC) Values at Different Temperatures and Compressive Stress Levels for EB and BRB

Temperature (^{o}C)	Compressive Stress (MPa)	EDC (kNmm)			
		EB		BRB	
		Type A	Type B	Type A	Type B
20	0.0	345.045	135.139	674.671	190.275
	1.5	350.088	144.517	576.968	424.460
	3.0	365.238	192.671	634.356	613.265
-18	0.0	1034.701	249.736	802.914	434.998
	1.5	962.794	398.619	933.823	526.920
	3.0	977.085	379.424	1016.721	525.870
	4.5	940.552	328.021	815.130	400.511
-30	0.0	1164.382	424.886	1068.757	477.800
	1.5	1087.725	321.634	1707.409	707.603
	3.0	1081.773	324.971	1460.131	1045.953
	4.5	939.003	473.819	1386.073	1193.664
	6.0	1243.691	444.251	1070.506	1189.677

3.7. Shear Modulus (G)

Shear modulus is one of the most important parameters of elastomeric bearings since it provides flexibility to the bearing. The specimen called as EB used in this study has higher damping values. Therefore, shear modulus values for EB obtained by using the Equation (3.6) for a case where damping effects are minimum, which is $\sigma_1 = 0.0$ MPa case. Computation of shear modulus for no damping case for EB is presented in Figure 3.2. The shear modulus of BRB rubber component can be computed by using the Equation (3.7).

$$G = \frac{F \times h_{rt}}{2\Delta \times A_{bearing}} \tag{3.6}$$

$$G^*_{eq} = \frac{(H_{\max} - \mu \times P_{ver})}{h_{rt} \times A_{bearing} \times d_{\max}} \tag{3.7}$$

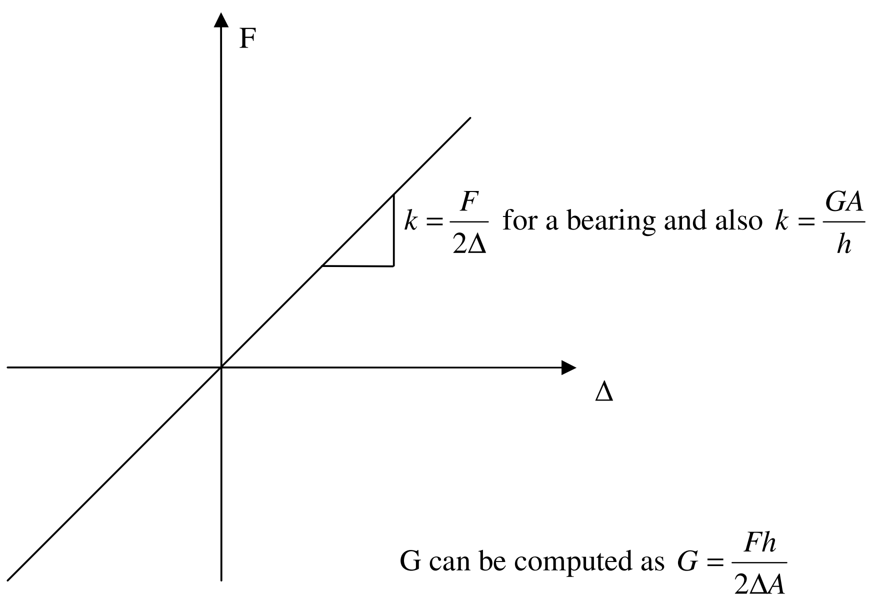

Figure 3.2 Computation of Shear Modulus (G) for No Damping Case for EB

The equation of equivalent shear modulus used for BRB includes steel ball contribution and friction terms. Earlier researches [19, 21] are compared with this study. It was observed that the current AASHTO criterion, G_C/G_R, is satisfied for the specimens used in this study.

Comparison of test results with the earlier research [19] in terms of normalized shear modulus is given in Table 3.6. Normalized shear modulus values of earlier research is measured after 24 hours [19] which is convenient with the values used in this study. The shear modulus at room temperature for EB has similar value with CR55 whereas the BRB has higher room temperature shear modulus then other specimens. It was observed that BRB have higher normalized shear modulus compared to EB since the contribution of steel balls. The maximum increase at stiffness occurred in -18^{o}C for the specimens used in this study since the temperature control in -30^{o}C was not stable at the lack of an environmental chamber.

Table 3.6. Comparison of Test Results with the Earlier Research [19] in Terms of Normalized Shear Modulus

Specimen	Compound	Nominal Hardness Shore A Duro	G_R (MPa)	G_C/G_R			
			Temperature (^{o}C)				
			20	-10	-18	-30	-50
CR50*	Neoprene	51	0.79	1.60	N/D	2.30	74.00
NR50*	Natural Rubber	54	1.07	1.20	N/D	1.30	1.90
CR55*	Neoprene	53	0.97	1.60	N/D	2.00	19.00
NR55*	Natural Rubber	59	1.07	1.20	N/D	1.60	1.80
CR60*	Neoprene	58	1.03	2.30	N/D	2.60	54.00
NR60*	Natural Rubber	63	1.28	1.40	N/D	1.70	2.40
CR65*	Neoprene	64	1.28	1.60	N/D	1.90	18.40
C1*	Neoprene	62	1.24	1.30	N/D	1.70	36.00
C2*	Neoprene	62	1.21	1.30	N/D	2.30	18.00
C3*	Neoprene	62	1.10	1.20	N/D	1.40	N/D
EB_A	Neoprene	60[a]	0.94	N/D	1.15	1.07	N/D
EB_B	Neoprene	60[a]	0.91	N/D	1.05	1.00	N/D
BRB_A	Neoprene	60[a]	1.27	N/D	1.12	1.06	N/D
BRB_B	Neoprene	60[a]	1.44	N/D	1.23	1.22	N/D

Notes: N/D means no data.

a Estimated based on the AASHTO [3] Table 14.7.5.2-1

* The study of Roeder et al. [19]

It was also observed that neoprene compounds significantly stiffen at -50^{o}C. It has been known that neoprene has second order transition between -40^{o}C (-40^{o}F) and -50^{o}C (-58^{o}F) [17,18,19]. According to Murray and Detenber instantaneous thermal stiffness takes places more than 50 times the room temperature stiffness below the second order transition [12].

Comparison of test results with the earlier research [21] in terms of normalized shear modulus is illustrated in Table 3.8. The study of Yakut and Yura [22a] introduce two types of stiffening as instantaneous thermal stiffening and crystallization stiffening, respectively. The instantaneous thermal stiffening values were obtained from the study of Yakut [21] by using Equation (3.8) for convenience with our study.

$$G = Ae^{-BT} \text{ [21]} \tag{3.8}$$

where A and B are statistical constants and T is temperature. Values are presented in Table 3.7.

Table 3.7. Statistical Constants [21]

Material	A	B
NEO150	2.6511	0.0231
NEO100	1.0362	0.0127
NR150	1.3999	0.0135
NR100	0.9483	0.0069

Normalized shear modulus values of earlier research [21] is measured after 24 hours which is convenient with the values used in this study. The specimens used in this study have similar shear modulus values at room temperature. It is shown that neoprene specimens stiffen more than natural rubber as the temperature lowers. The maximum increase at stiffness occurred in -18^{o}C instead of -30^{o}C for the specimens used in this study due to difficulties of keeping temperature precisely at the required temperatures without an environmental chamber.

Table 3.8. Comparison of Test Results with the Earlier Research [21] in Terms of Normalized Shear Modulus

Specimen	Compound	Nominal Hardness Shore A Duro	G_R (MPa)	G_C/G_R	
			Temperature (^oC)		
			20	-18	-30
NEO100*	Neoprene	53	0.80	1.63	1.90
NR100*	Natural Rubber	52	0.83	1.29	1.41
NEO150*	Neoprene	66	1.67	2.41	3.17
NR150*	Natural Rubber	59	1.07	1.66	1.96
EB_A	Neoprene	60[a]	0.94	1.15	1.07
EB_B	Neoprene	60[a]	0.91	1.05	1.00
BRB_A	Neoprene	60[a]	1.27	1.12	1.06
BRB_B	Neoprene	60[a]	1.44	1.23	1.22

Notes:

a Estimated based on the AASHTO [3] Table 14.7.5.2-1

* The study of Yakut, A. [21]

3.8. Design Parameters

This study is complementary study of Özkaya [15]. Therefore, design parameters were analyzed in the light of equations derived by Özkaya [15]. Summary of Design Parameters, O_d, f_L, EDC and damping at an average vertical pressure of 3.00MPa is presented in Table 3.9. The α_r and f_L values are calculated by using Equations of (3.10) and (3.11b). At 50% strain the f_L parameters change from 1.70 to 1.81, that is within 15% tolerance level compared to 1.56 [15]. It was observed that f_L values do not change with temperature.

The α_r parameter used to describe the Q_d design parameter at room temperature case in [15] has a 25% increase in value at cold climate temperature case. In any case, the observed α_r parameters are less than the recommended upper bound limit value determined in [15].

The Q_d values determined in the cold climate tests can be represented by the following equation.

$$Q_d = \alpha_t \times \alpha_r \times P_{ver} < 0.15 \tag{3.9}$$

Where, α_t is the temperature factor suggested as 1.25 for the service case and the earthquake case based on the tests, α_r is the room temperature coefficient ranges from 0.04 to 0.015 [15].

The f_L design term described by Özkaya [15] as contribution of steel balls to secondary stiffness and presented in Equation (3.11b).

Table 3.9. Summary of Design Parameters, O_d, f_L, EDC and Damping at an Average Vertical Pressure of 3.00MPa

Temperature (^oC)	Bearing Type	$\alpha_r = Q_d/P_{ver}$	f_L	EDC (kNmm)	β_{eq} (%)
$T_1 = 20$	BRB_A	0.057	1.81	634.356	13.697
$T_2 = -18$	BRB_A	0.066	1.79	1016.721	18.216
$T_3 = -30$	BRB_A	0.071	1.72	1460.131	17.623
$T_1 = 20$	BRB_B	0.089	1.72	613.265	22.815
$T_2 = -18$	BRB_B	0.087	1.80	525.870	31.751
$T_3 = -30$	BRB_B	0.112	1.70	1045.953	25.954

Characteristic strengths of BRBs can be expressed by using the following equation [15]:

$$Q_d = \alpha_r \times P_{ver,3.4MPa} \tag{3.10}$$

It was observed that the α_r ranges from 0.06 to 0.13 in the tests conducted by Özkaya [15]. Q_d on average can be assumed as 0.095. Contribution of steel balls to secondary stiffness is expressed as percentage of the horizontal stiffness of the elastomeric part (K_h) and formulized as below [15]:

$$K_h\% = \frac{(F_{\max} - Q_{d,BRB})}{d_{\max} \times K_h} \times 100 \qquad (3.11)$$

$$K_d = K2 = f_L \ x \ K_h \qquad (3.11a)$$

For D/d = 3.0, Özkaya [15] proposed that the secondary stiffness parameter f_L can be determined from the equation below.

$$f_L = 1 + 0.01 \ x \ (-0.9035 \ x \ \gamma_{max}\% + 101.95) > 1.20 \qquad (3.11b)$$

BRBs were tested under two different loading cases that are named as service and earthquake state cases. Comparison of significant parameters for the BRBs (Type A and Type B) at service and earthquake cases is illustrated in Table 3.10.

Table 3.10. Comparison of Significant Parameters for the BRBs
(Type A and Type B) at Service and Earthquake Cases

Parameter	Service State Case		Earthquake State Case	
	BRB_A	BRB_B	BRB_A	BRB_B
σ (MPa)	3.000	3.000	3.500	3.500
Q_{d_avg} (kN)	13.311	11.328	37.328	16.547
K_d (kN/mm)	0.706	0.863	1.050	0.263
K_{eff_avg} (kN/mm)	1.682	1.198	1.144	0.588
β_{eq} (%)	17.965	25.838	17.286	24.867
EDC (kNmm)	1488.489	1041.290	9432.811	4157.978

The size effect, magnitude of shear strain and may be confinement is effecting the test results, such as measure of EDC.

CHAPTER 4

CONCLUSIONS AND RECOMMENDATIONS

4.1. Summary

A new seismic isolator named “Ball Rubber Bearing (BRB)” was tested at different temperatures in order to understand the influence of thermal effects on behavior of the bearings. In this scope, size of bearings, temperature cases and compressive stress levels were changed from one test to another one.

Thermal sensitivity tests were performed on efficiency of controlling the temperature inside the bearing by a protective home-made insulation belt. In the experimental stage, a total of 50 reversed cyclic tests in which 48 of the tests were performed for the service state and 2 of the tests were performed for the earthquake state. Test results were compared with earlier researches and the specimens used in this study, EB and BRB, compared with each other.

4.2. Conclusions

Based on the results of this research following conclusions can be drawn regarding the performance of BRB subjected to different temperatures.

- According to international standards, seismic isolation performance of BRBs is determined to be satisfactory. BRBs showed almost double damping percents compared to EBs. Moreover, small size bearings, Type B, have higher damping percentage compared to big size bearings, Type A. The higher damping percentage at the small size bearing is due to the better confinement of the hole. The rubber thickness is about 25% less than the larger size bearing.

- Generally it has been observed that BRBs show better performance at low temperatures in terms of energy dissipation compared to room temperature performance. Similarly, experimental results of the study carried out by Kulak and Hughes [11] show significant increase in the effective damping ratio with lower temperatures.

- It has been observed that the Type A bearings having the same shape factor with Type B, dissipated lower energy at low temperatures and rates. Type A bearings have higher energy dissipation per cycle compared to type B bearings due to the size effect.

- In some types of seismic isolators energy dissipation may arise during high-temperatures. On the contrary, the heat generated at inner core during energy dissipation was not in a high level. Moreover, as a result of temperature measurements heat exchange is not observed in the rubber during cyclic loading.

- The shear modulus of the EB and the BRB increase at lower temperatures as expected but not as significant as observed in the tests done by others.

- It has been observed that increase at compressive stress level results in increase at average effective stiffness (K_{eff_avg}) and equivalent damping ratio (β_{eq}) for BRBs.

- The tested EB shows similar response in terms of characteristic strength and equivalent damping ratio compared to HDRBs.

4.3. Recommendations for Future Researches

In the light of conclusions stated in the previous section, following recommendations are given for future researches and researchers.

- It is suggested to use an environmental chamber for controlling temperature precisely during the tests.

- Testing BRBs having different dimensions can be suggested.

- BRBs having different shape factors may be tested.
- Square and rectangular BRBs may be tested.
- Daily temperature fluctuations may be taken into account for more accurate results.

REFERENCES

[1]. AASHTO M 251-06. (2006). *Standard Specification for Plain and Laminated Elastomeric Bridge Bearings* .

[2]. American Association of State Highway and Transportation Officials (AASHTO). (2001). *"Guide Specification for Seismic Isolation Design"* .

[3]. American Association of State Highway and Transportation Officials (ASSHTO). (2005). *Load Resistant Factor Design (LFRD) Bridge Design Specification, 3rd Edition* .

[4]. Buckle, I. G., & Mayes, R. L. (1990). Seismic Isolation: History, Application and Performance-A World View. *Earthquake Spectra, Vol.6, No.2* , pp. 161-201.

[5]. Buckle, I., Constantinou, M. C., Dicleli, M., & Ghasemi, H. (2006). *"Seismic Isolation of Highway Bridges".* Special Report MCEER-06-SP07.

[6]. Dolce, M., Cardone, D., Marnetto, R., Nigro, D., Palermo, G., "A New Added Damping Rubber Isolator (ADRI): Experimental Tests and Numerical Simulations," 8th World Seminar on Seismic Isolation, Energy Dissipation and Active Vibration Control of Structures, Yerevan, Armenia, 6-10 October 2003.

[7]. Gent, A. N. (2001). *"Engineering with Rubber-How to Design Rubber Components".* Munich: Hanser Publishers.

[8]. htttp://www.labthink.cn/service/show558.htlm, visited September 17, 2010

[9]. http://www.meteor.gov.tr, visited July 09, 2010

[10]. Kelly, T.E., “Base Isolation of Structures,” Holmes Consulting Group Ltd., Revision 0, June 2001, New Zealand.

[11]. Kulak, R. F., & Hughes, T. H. (1993). Frequency and Temperature Dependence of High Damping Elastomers. *SMIRT-12* , 243-248. Argonna National Laboratory, Argonne, USA, IL: Elsevier Science Publishers B.V.

[12]. Murray, R. M., & Detenber, J. D. (1961, April-Jun). "First and second order transitions in neoprene". *Rubber Chemical Tech.* , pp. 668-685.

[13]. Naeim, F., & Kelly, J. M. (1999). *"Design of Seismic Isolated Structures: From Theory to Practice".* John Wiley&Sons.

[14]. Özden, B., & Türer, A. (2005, February 17). "Seismic Isolation with Cheap Scrap Automobile Tires" [In Turkish]. *Workshop on Increase of Seismic Safety of Masonry Structures* . Ankara, Turkey: Middle East Technical University.

[15]. Özkaya, C. (2010, February). Development of a New Seismic Isolator Named "Ball Rubber Bearing". *Unpublished Doctoral Dissertation* . METU.

[16]. Özmen, B., & Nurlu, M. (1999). Deprem Bölgeleri Haritası ile İlgili Bazı Bilgiler. *TMMOB Jeoloji Mühendisleri Odası Haber Bülteni* , 32-35.

[17]. Pınarbaşı, S., & Akyüz, U. (2005). Sismik İzolasyon ve Elastomerik Yastık Deneyleri. *IMO. Teknik Dergi, Yazı 237* , 3581-3598.

[18]. Roeder, C. W., & Stanton, J. F. (1983). Elastomeric Bearings: State of Art. *Journal of Structural Engineering, Vol.109, No: 12* , pp. 2853-2871.

[19]. Roeder, C. W., Stanton, J. F., & Feller, T. (1990). "Low-Temperature Performance of Elastomeric Bearings". *Journal of Cold Regions Engineering, Vol.4, No.3* , pp. 161-201.

[20]. Wai, J. L., & Nana, G. (2004). *Economic Impact of Seismic Isolation Technology.* New Zealand: Ministry of Research and Technology .

[21]. Yakut, A. (2000, May). Performance of Elastomeric Bearings at Low Temperatures. *Ph. D. Disssertation* . The University of Texas at Austin.

[22a]. Yakut, A., & Yura, J. A. (2002). "Parameters Influencing Performance of Elastomeric Bearings at Low Temperatures". *Journal of Structural Engineering, Vol.128, No:8* , pp. 986-994.

[22b.] Yakut, A., & Yura, J. A. (2002). "Evaluation of Low Temperature Test Methods for Elastomeric Bridge Bearings". *Journal of Bridge Engineering, Vol.7, No:1* , pp. 50-56.

[23] Yura, J., Kumar, A., Yakut, A., Topkaya, C., Becker, E., & Collingwood, J. 2001 "Elastomeric Bridge Bearings: Recommended Test Methods" *NCHRP Report 449*, TRB, National Research Council, Washington, D.C. 90pp.

APPENDIX A

TEST RESULTS

In Table A.1 and Table A.2, general information about tests and test results are presented. It should be reminded that presented test results are valid for two simultaneously tested bearings. For one bearing, characteristic strength (Q_d), effective stiffness (K_{eff}) and maximum horizontal force values are 50% of the values in Table A.1 and Table A.2, while equivalent damping ratio is unaltered.

Table A.1. Test Results-1

Test	σ (MPa)	Average Velocity (mm/sec)	Q_{d_avg} (kN)	K_u (kN/mm)	K_d (kN/m)	K_{eff_avg} (kN/mm)
$EB_A - T_1 - \sigma_1$	0.000	12.167	3.835	1.375	0.875	0.913
$EB_A - T_1 - \sigma_2$	1.500	26.445	4.313	1.231	0.688	0.924
$EB_A - T_1 - \sigma_3$	3.000	25.108	4.202	1.276	0.750	0.921
$BRB_A - T_1 - \sigma_1$	0.000	9.670	5.611	1.737	0.738	1.126
$BRB_A - T_1 - \sigma_2$	1.500	6.642	7.176	2.729	1.375	1.479
$BRB_A - T_1 - \sigma_3$	3.000	3.637	8.900	4.050	1.375	1.867
$EB_B - T_1 - \sigma_1$	0.000	8.571	1.587	0.886	0.500	1.107
$EB_B - T_1 - \sigma_2$	1.500	8.907	1.678	0.820	0.500	0.450
$EB_B - T_1 - \sigma_3$	3.000	6.773	2.409	2.373	0.438	0.631
$BRB_B - T_1 - \sigma_1$	0.000	10.792	2.023	1.120	0.588	0.550
$BRB_B - T_1 - \sigma_2$	1.500	9.565	4.546	32.643	0.675	0.779
$BRB_B - T_1 - \sigma_3$	3.000	6.481	7.311	11.342	0.688	0.934
$EB_A - T_2 - \sigma_1$	0.000	7.128	10.040	2.454	0.625	0.991
$EB_A - T_2 - \sigma_2$	1.500	5.912	8.095	1.665	1.063	0.968

Table A.1 (continued)

$EB_A - T_2 - \sigma_3$	3.000	5.948	9.261	1.340	1.000	0.947
$EB_A - T_2 - \sigma_4$	4.500	7.467	8.294	2.193	0.938	0.887
$BRB_A - T_2 - \sigma_1$	0.000	13.038	5.657	1.883	0.888	0.930
$BRB_A - T_2 - \sigma_2$	1.500	8.409	9.258	6.482	1.675	1.440
$BRB_A - T_2 - \sigma_3$	3.000	7.057	12.094	40.826	1.150	1.967
$BRB_A - T_2 - \sigma_4$	4.500	3.616	17.684	41.018	2.300	3.763
$EB_B - T_2 - \sigma_1$	0.000	7.462	3.564	1.565	0.838	0.577
$EB_B - T_2 - \sigma_2$	1.500	9.456	4.447	2.632	0.750	0.557
$EB_B - T_2 - \sigma_3$	3.000	7.792	6.437	1.564	0.625	0.508
$EB_B - T_2 - \sigma_4$	4.500	6.194	3.955	1.048	0.625	0.468
$BRB_B - T_2 - \sigma_1$	0.000	9.238	4.862	0.057	0.925	0.739
$BRB_B - T_2 - \sigma_2$	1.500	4.578	6.546	0.091	0.700	0.885
$BRB_B - T_2 - \sigma_3$	3.000	4.957	8.592	35.807	0.800	1.088
$BRB_B - T_2 - \sigma_4$	4.500	3.417	10.800	872.789	1.225	2.177
$EB_A - T_3 - \sigma_1$	0.000	10.399	8.713	1.707	0.788	0.919
$EB_A - T_3 - \sigma_2$	1.500	9.812	9.558	1.569	0.900	0.910
$EB_A - T_3 - \sigma_3$	3.000	8.608	8.277	1.435	1.000	0.920
$EB_A - T_3 - \sigma_4$	4.500	12.878	9.154	1.390	0.625	0.893
$EB_A - T_3 - \sigma_5$	6.000	15.006	9.929	1.481	0.663	0.845
$BRB_A - T_3 - \sigma_1$	0.000	12.450	7.064	1.962	0.950	0.921
$BRB_A - T_3 - \sigma_2$	1.500	9.752	13.552	3.027	1.500	1.246
$BRB_A - T_3 - \sigma_3$	3.000	12.405	13.311	16.600	0.706	1.682
$BRB_A - T_3 - \sigma_4$	4.500	9.299	17.463	58.279	1.613	2.355
$BRB_A - T_3 - \sigma_5$	6.000	6.276	20.153	91.171	2.275	3.531
$EB_B - T_3 - \sigma_1$	0.000	8.795	5.217	2.401	0.463	0.578
$EB_B - T_3 - \sigma_2$	1.500	9.961	3.477	1.021	0.725	0.563
$EB_B - T_3 - \sigma_3$	3.000	10.393	3.996	1.206	0.588	0.500
$EB_B - T_3 - \sigma_4$	4.500	12.664	4.624	1.167	0.438	0.445
$EB_B - T_3 - \sigma_5$	6.000	13.299	5.034	1.008	0.513	0.389
$BRB_B - T_3 - \sigma_1$	0.000	10.604	5.300	1.555	0.825	0.673
$BRB_B - T_3 - \sigma_2$	1.500	11.734	7.401	7.399	0.663	0.900

Table A.1 (continued)

$BRB_B - T_3 - \sigma_3$	3.000	8.911	11.328	41.790	0.863	1.198
$BRB_B - T_3 - \sigma_4$	4.500	8.418	13.840	65.314	0.750	1.384
$BRB_B - T_3 - \sigma_5$	6.000	8.750	14.420	36.359	0.975	1.453
$BRB_A - T_3 - \sigma_{3.5}$	3.500	19.091	37.328	1.781	1.050	1.144
$BRB_B - T_3 - \sigma_{3.5}$	3.500	26.676	16.547	6.791	0.263	0.588

Table A.2. Test Results-2

Test	Q_{d_avg}/P_{ver}	d_y (mm)	d_{max_avg} (mm)	EDC (kNmm)	β_{eq} (%)
$EB_A - T_1 - \sigma_1$	*	6.954	28.797	335.083	7.048
$EB_A - T_1 - \sigma_2$	0.041	7.914	27.454	337.107	7.707
$EB_A - T_1 - \sigma_3$	0.020	5.389	26.472	354.324	8.736
$BRB_A - T_1 - \sigma_1$	*	14.985	32.918	367.333	5.248
$BRB_A - T_1 - \sigma_2$	0.068	4.975	24.590	563.006	10.017
$BRB_A - T_1 - \sigma_3$	0.042	4.414	19.872	550.276	11.881
$EB_B - T_1 - \sigma_1$	*	5.108	21.947	106.924	3.191
$EB_B - T_1 - \sigma_2$	0.032	2.377	24.604	149.175	8.715
$EB_B - T_1 - \sigma_3$	0.023	2.185	21.090	182.150	10.328
$BRB_B - T_1 - \sigma_1$	*	2.495	26.014	190.280	8.141
$BRB_B - T_1 - \sigma_2$	0.088	0.325	23.430	420.169	13.040
$BRB_B - T_1 - \sigma_3$	0.140	0.650	9.427	510.682	34.484
$EB_A - T_2 - \sigma_1$	*	4.961	32.525	1106.997	16.812
$EB_A - T_2 - \sigma_2$	0.076	4.902	31.993	877.216	14.088
$EB_A - T_2 - \sigma_3$	0.044	10.866	32.104	786.457	12.824
$EB_A - T_2 - \sigma_4$	0.026	4.695	33.271	948.070	15.360
$BRB_A - T_2 - \sigma_1$	*	6.156	38.187	724.825	8.506
$BRB_A - T_2 - \sigma_2$	0.087	2.244	26.590	901.950	14.094
$BRB_A - T_2 - \sigma_3$	0.057	1.048	21.253	977.467	17.512
$BRB_A - T_2 - \sigma_4$	0.056	0.546	11.568	779.659	24.644
$EB_B - T_2 - \sigma_1$	*	2.702	24.073	304.674	14.491
$EB_B - T_2 - \sigma_2$	0.086	1.565	25.615	427.773	18.644
$EB_B - T_2 - \sigma_3$	0.062	3.174	23.895	533.537	29.304
$EB_B - T_2 - \sigma_4$	0.025	4.281	23.128	298.148	18.936
$BRB_B - T_2 - \sigma_1$	*	0.856	23.224	435.009	17.364
$BRB_B - T_2 - \sigma_2$	0.126	0.103	20.906	544.701	22.404
$BRB_B - T_2 - \sigma_3$	0.083	0.118	15.568	530.958	32.058
$BRB_B - T_2 - \sigma_4$	0.069	0.133	9.287	395.437	33.515
$EB_A - T_3 - \sigma_1$	*	9.242	37.884	998.185	12.042

Table A.2 (continued)

$EB_A - T_3 - \sigma_2$	0.090	8.135	37.338	1116.539	14.010
$EB_A - T_3 - \sigma_3$	0.039	10.763	37.796	895.055	10.835
$EB_A - T_3 - \sigma_4$	0.029	8.755	37.323	1046.034	13.386
$EB_A - T_3 - \sigma_5$	0.023	8.740	37.766	1152.824	15.222
$BRB_A - T_3 - \sigma_1$	*	2.156	39.493	1054.973	11.690
$BRB_A - T_3 - \sigma_2$	0.128	2.628	35.544	1784.253	18.035
$BRB_A - T_3 - \sigma_3$	0.063	0.044	28.000	1488.489	17.965
$BRB_A - T_3 - \sigma_4$	0.055	0.477	20.079	1369.279	22.950
$BRB_A - T_3 - \sigma_5$	0.048	0.192	13.472	1070.510	26.587
$EB_B - T_3 - \sigma_1$	*	3.661	26.143	476.708	19.202
$EB_B - T_3 - \sigma_2$	0.067	5.404	27.247	303.772	11.567
$EB_B - T_3 - \sigma_3$	0.038	3.691	24.449	331.813	17.662
$EB_B - T_3 - \sigma_4$	0.030	5.167	29.616	452.253	18.430
$EB_B - T_3 - \sigma_5$	0.024	5.728	26.686	421.975	24.223
$BRB_B - T_3 - \sigma_1$	*	2.790	25.327	477.802	17.614
$BRB_B - T_3 - \sigma_2$	0.142	1.535	24.405	677.040	20.103
$BRB_B - T_3 - \sigma_3$	0.109	0.162	23.142	1041.290	25.838
$BRB_B - T_3 - \sigma_4$	0.089	0.266	21.910	1198.179	28.702
$BRB_B - T_3 - \sigma_5$	0.069	0.723	20.979	1168.396	29.083
$BRB_A - T_3 - \sigma_{3.5}$	0.151	23.950	87.125	9432.811	17.286
$BRB_B - T_3 - \sigma_{3.5}$	0.136	4.440	67.260	4157.978	24.867

Table A.3. Test Results-3

Test	Duration Elapsed in Freezer (min)	Temperature of Bearing at 3 Different Depths (^oC) Before Testing		
		D1 (25mm)	D2 (55mm)	D3 (85mm)
$EB_A - T_1 - \sigma_1$	*	20.0	20.0	20.0
$EB_A - T_1 - \sigma_2$	*	20.0	20.0	20.0
$EB_A - T_1 - \sigma_3$	*	20.0	20.0	20.0
$BRB_A - T_1 - \sigma_1$	*	20.0	20.0	20.0
$BRB_A - T_1 - \sigma_2$	*	20.0	20.0	20.0
$BRB_A - T_1 - \sigma_3$	*	20.0	20.0	20.0
$EB_B - T_1 - \sigma_1$	*	20.0	20.0	20.0
$EB_B - T_1 - \sigma_2$	*	20.0	20.0	20.0
$EB_B - T_1 - \sigma_3$	*	20.0	20.0	20.0
$BRB_B - T_1 - \sigma_1$	*	20.0	20.0	20.0
$BRB_B - T_1 - \sigma_2$	*	20.0	20.0	20.0
$BRB_B - T_1 - \sigma_3$	*	20.0	20.0	20.0
$EB_A - T_2 - \sigma_1$	1162	-19.5	-20.1	-20.0
$EB_A - T_2 - \sigma_2$	1162	-19.5	-20.1	-20.0
$EB_A - T_2 - \sigma_3$	1162	-19.5	-20.1	-20.0
$EB_A - T_2 - \sigma_4$	1162	-19.5	-20.1	-20.0
$BRB_A - T_2 - \sigma_1$	1335	-19.9	-22.1	-22.7
$BRB_A - T_2 - \sigma_2$	1335	-19.9	-22.1	-22.7
$BRB_A - T_2 - \sigma_3$	1335	-19.9	-22.1	-22.7
$BRB_A - T_2 - \sigma_4$	1335	-19.9	-22.1	-22.7
$EB_B - T_2 - \sigma_1$	1267	-23.1	-23.8	-24.4
$EB_B - T_2 - \sigma_2$	1267	-23.1	-23.8	-24.4
$EB_B - T_2 - \sigma_3$	1267	-23.1	-23.8	-24.4
$EB_B - T_2 - \sigma_4$	1267	-23.1	-23.8	-24.4
$BRB_B - T_2 - \sigma_1$	1378	-17.4	-18.1	-18.5
$BRB_B - T_2 - \sigma_2$	1378	-17.4	-18.1	-18.5
$BRB_B - T_2 - \sigma_3$	1378	-17.4	-18.1	-18.5
$BRB_B - T_2 - \sigma_4$	1378	-17.4	-18.1	-18.5

Table A.3 (continued)

$EB_A - T_3 - \sigma_1$	1310	-23.4	-25.7	-25.9
$EB_A - T_3 - \sigma_2$	1310	-23.4	-25.7	-25.9
$EB_A - T_3 - \sigma_3$	1310	-23.4	-25.7	-25.9
$EB_A - T_3 - \sigma_4$	1310	-23.4	-25.7	-25.9
$EB_A - T_3 - \sigma_5$	1310	-23.4	-25.7	-25.9
$BRB_A - T_3 - \sigma_1$	4229	-25.3	-28.3	-28.7
$BRB_A - T_3 - \sigma_2$	4229	-25.3	-28.3	-28.7
$BRB_A - T_3 - \sigma_3$	4229	-25.3	-28.3	-28.7
$BRB_A - T_3 - \sigma_4$	4229	-25.3	-28.3	-28.7
$BRB_A - T_3 - \sigma_5$	4229	-25.3	-28.3	-28.7
$EB_B - T_3 - \sigma_1$	1410	-26.3	-26.7	-27.3
$EB_B - T_3 - \sigma_2$	1410	-26.3	-26.7	-27.3
$EB_B - T_3 - \sigma_3$	1410	-26.3	-26.7	-27.3
$EB_B - T_3 - \sigma_4$	1410	-26.3	-26.7	-27.3
$EB_B - T_3 - \sigma_5$	1410	-26.3	-26.7	-27.3
$BRB_B - T_3 - \sigma_1$	1350	-24.0	-25.8	-26.6
$BRB_B - T_3 - \sigma_2$	1350	-24.0	-25.8	-26.6
$BRB_B - T_3 - \sigma_3$	1350	-24.0	-25.8	-26.6
$BRB_B - T_3 - \sigma_4$	1350	-24.0	-258	-26.6
$BRB_B - T_3 - \sigma_5$	1350	-24.0	-25.8	-26.6
$BRB_A - T_3 - \sigma_{3.5}$	558	-22.3	-25.3	-25.7
$BRB_B - T_3 - \sigma_{3.5}$	1469	-24.1	-24.8	-25.9

Table A.4. Test Results-4

Test	Duration Elapsed in Freezer (min)	Temperature of Bearing at 3 Different Depths (^oC) After Testing		
		D1 (25mm)	D2 (55mm)	D3 (85mm)
$EB_A - T_1 - \sigma_1$	*	20.0	20.0	20.0
$EB_A - T_1 - \sigma_2$	*	20.0	20.0	20.0
$EB_A - T_1 - \sigma_3$	*	20.0	20.0	20.0
$BRB_A - T_1 - \sigma_1$	*	20.0	20.0	20.0
$BRB_A - T_1 - \sigma_2$	*	20.0	20.0	20.0
$BRB_A - T_1 - \sigma_3$	*	20.0	20.0	20.0
$EB_B - T_1 - \sigma_1$	*	20.0	20.0	20.0
$EB_B - T_1 - \sigma_2$	*	20.0	20.0	20.0
$EB_B - T_1 - \sigma_3$	*	20.0	20.0	20.0
$BRB_B - T_1 - \sigma_1$	*	20.0	20.0	20.0
$BRB_B - T_1 - \sigma_2$	*	20.0	20.0	20.0
$BRB_B - T_1 - \sigma_3$	*	20.0	20.0	20.0
$EB_A - T_2 - \sigma_1$	1162	-4.9	-10.4	-14.4
$EB_A - T_2 - \sigma_2$	1162	-4.9	-10.4	-14.4
$EB_A - T_2 - \sigma_3$	1162	-4.9	-10.4	-14.4
$EB_A - T_2 - \sigma_4$	1162	-4.9	-10.4	-14.4
$BRB_A - T_2 - \sigma_1$	1335	-7.9	-12.4	-16.3
$BRB_A - T_2 - \sigma_2$	1335	-7.9	-12.4	-16.3
$BRB_A - T_2 - \sigma_3$	1335	-7.9	-12.4	-16.3
$BRB_A - T_2 - \sigma_4$	1335	-7.9	-12.4	-16.3
$EB_B - T_2 - \sigma_1$	1267	-9.3	-13.1	-17.7
$EB_B - T_2 - \sigma_2$	1267	-9.3	-13.1	-17.7
$EB_B - T_2 - \sigma_3$	1267	-9.3	-13.1	-17.7
$EB_B - T_2 - \sigma_4$	1267	-9.3	-13.1	-17.7
$BRB_B - T_2 - \sigma_1$	1378	-5.0	-8.0	-12.4
$BRB_B - T_2 - \sigma_2$	1378	-5.0	-8.0	-12.4
$BRB_B - T_2 - \sigma_3$	1378	-5.0	-8.0	-12.4
$BRB_B - T_2 - \sigma_4$	1378	-5.0	-8.0	-12.4

Table A.4 (continued)

$EB_A - T_3 - \sigma_1$	1310	-8.0	-13.4	-17.5
$EB_A - T_3 - \sigma_2$	1310	-8.0	-13.4	-17.5
$EB_A - T_3 - \sigma_3$	1310	-8.0	-13.4	-17.5
$EB_A - T_3 - \sigma_4$	1310	-8.0	-13.4	-17.5
$EB_A - T_3 - \sigma_5$	1310	-8.0	-13.4	-17.5
$BRB_A - T_3 - \sigma_1$	4229	-10.1	-12.4	-17.6
$BRB_A - T_3 - \sigma_2$	4229	-10.1	-12.4	-17.6
$BRB_A - T_3 - \sigma_3$	4229	-10.1	-12.4	-17.6
$BRB_A - T_3 - \sigma_4$	4229	-10.1	-12.4	-17.6
$BRB_A - T_3 - \sigma_5$	4229	-10.1	-12.4	-17.6
$EB_B - T_3 - \sigma_1$	1410	-7.4	-14.5	-18.5
$EB_B - T_3 - \sigma_2$	1410	-7.4	-14.5	-18.5
$EB_B - T_3 - \sigma_3$	1410	-7.4	-14.5	-18.5
$EB_B - T_3 - \sigma_4$	1410	-7.4	-14.5	-18.5
$EB_B - T_3 - \sigma_5$	1410	-7.4	-14.5	-18.5
$BRB_B - T_3 - \sigma_1$	1350	-6.1	-13.3	-18.0
$BRB_B - T_3 - \sigma_2$	1350	-6.1	-13.3	-18.0
$BRB_B - T_3 - \sigma_3$	1350	-6.1	-13.3	-18.0
$BRB_B - T_3 - \sigma_4$	1350	-6.1	-13.3	-18.0
$BRB_B - T_3 - \sigma_5$	1350	-6.1	-13.3	-18.0
$BRB_A - T_3 - \sigma_{3.5}$	558	-8.2	-12.4	-17.6
$BRB_B - T_3 - \sigma_{3.5}$	1469	-7.6	-12.8	-17.1

APPENDIX B

EXPERIMENTAL HYSTERESIS LOOPS

In Appendix B, experimental hysteresis loops are presented for 48 tests. Details about tests and test parameters are presented in Appendix A. It should be reminded that presented hysteresis loops are that of two simultaneously tested bearings. Hysteresis loops are original ones. In other words, no correction was performed to original test data.

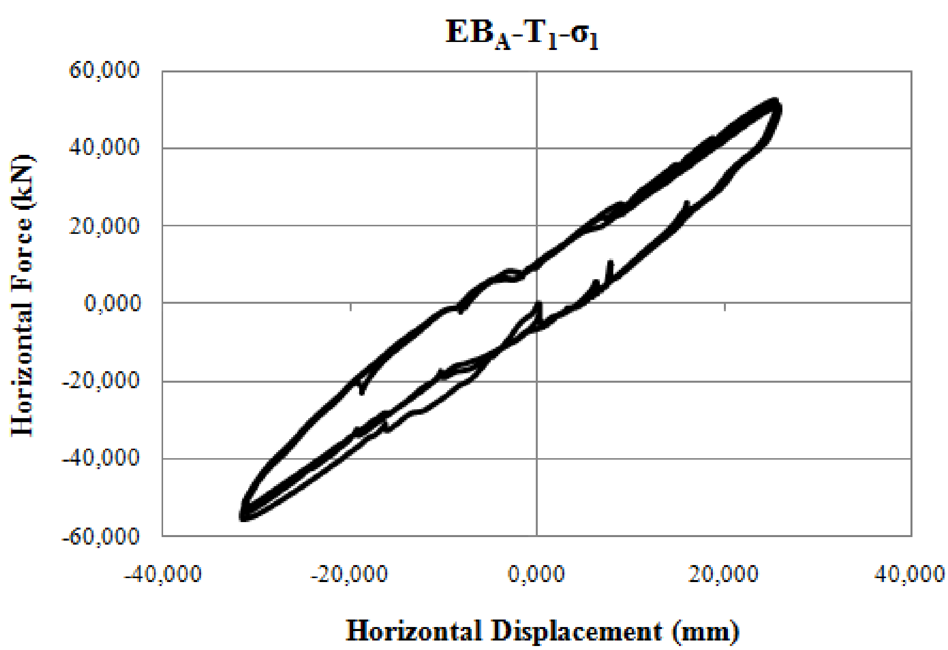

Figure B.1. Hysteresis Loop of Test $EB_A - T_1 - \sigma_1$

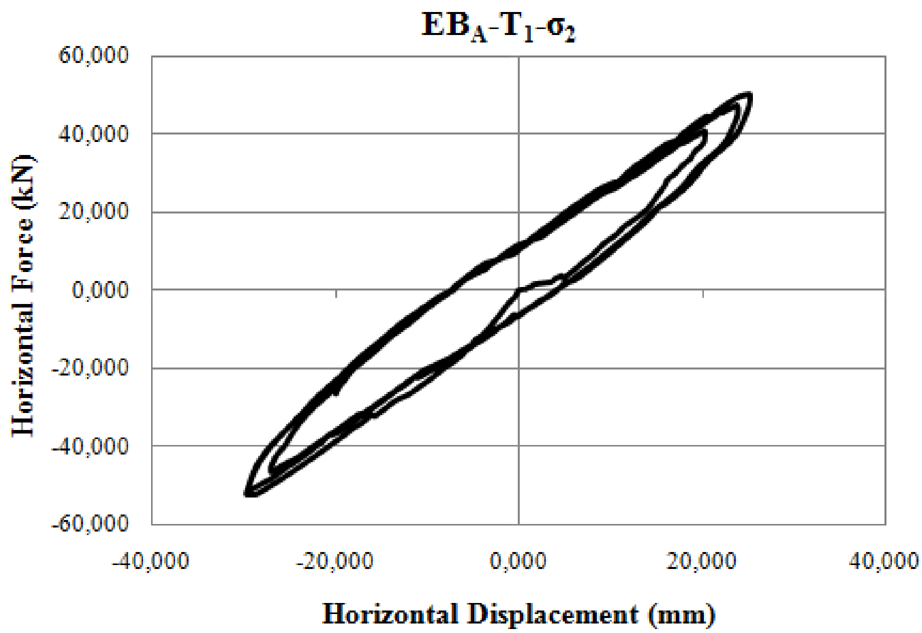

Figure B.2. Hysteresis Loop of Test $EB_A - T_1 - \sigma_2$

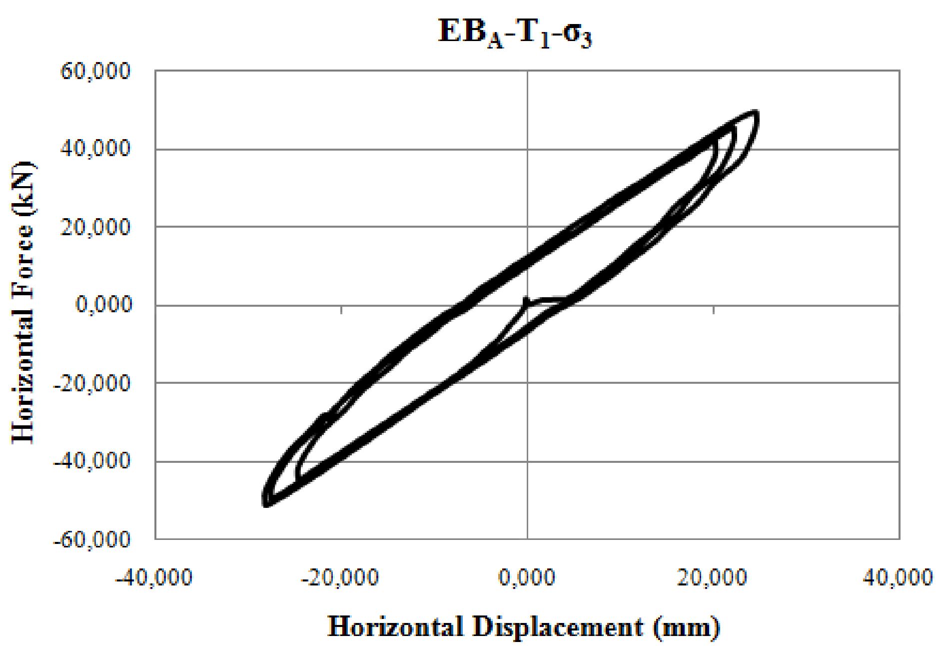

Figure B.3. Hysteresis Loop of Test $EB_A - T_1 - \sigma_3$

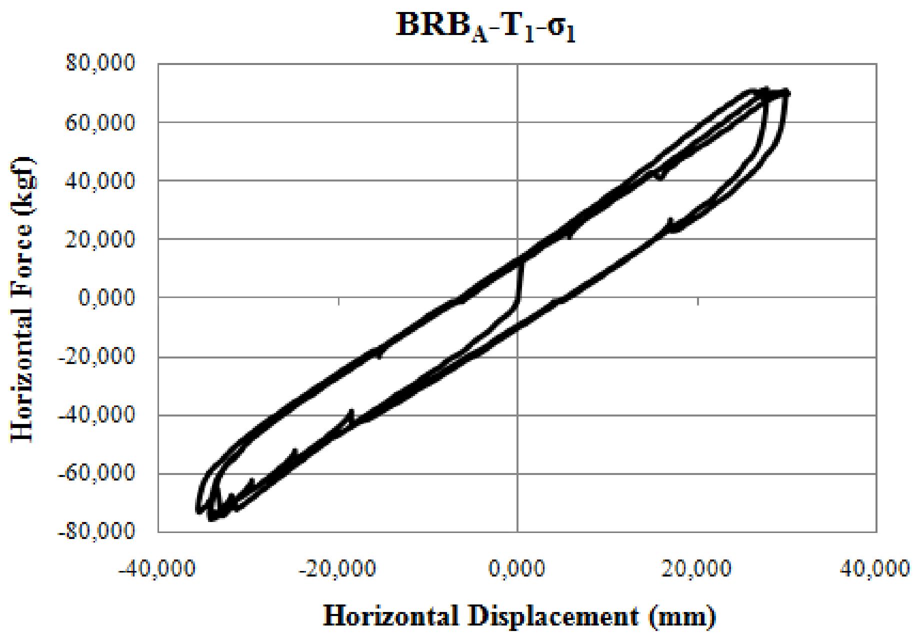

Figure B.4. Hysteresis Loop of Test $BRB_A - T_1 - \sigma_1$

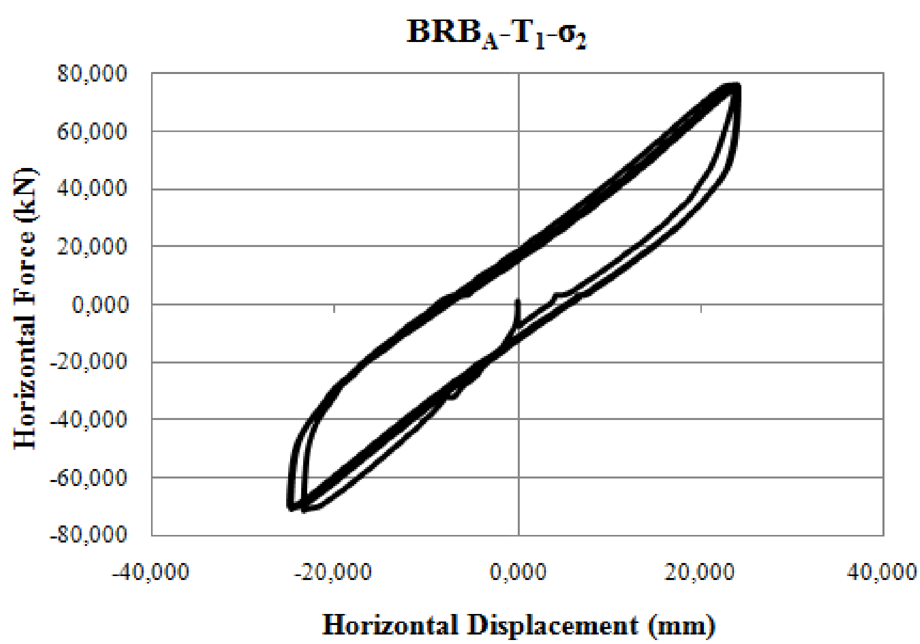

Figure B.5. Hysteresis Loop of Test $BRB_A - T_1 - \sigma_2$

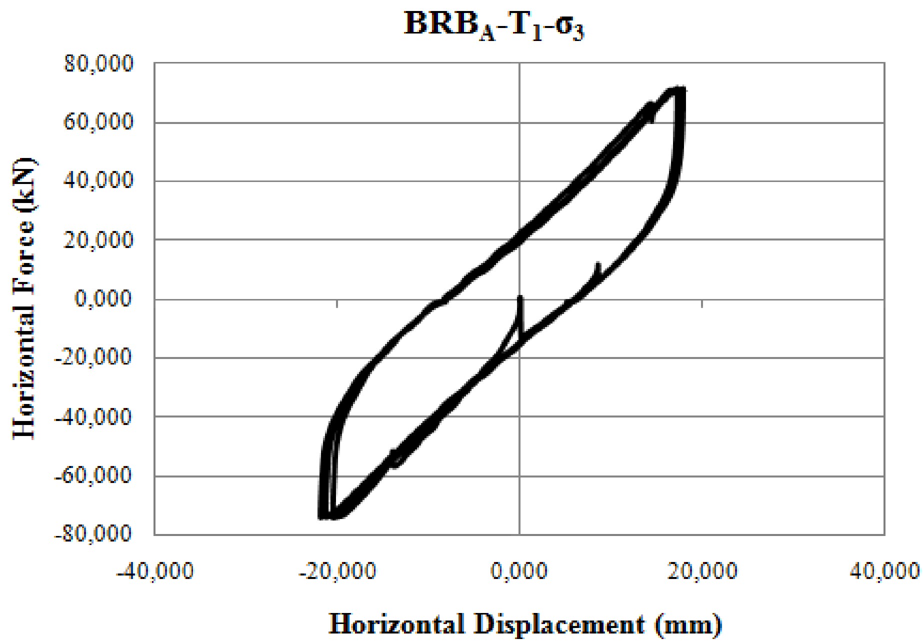

Figure B.6. Hysteresis Loop of Test $BRB_A - T_1 - \sigma_3$

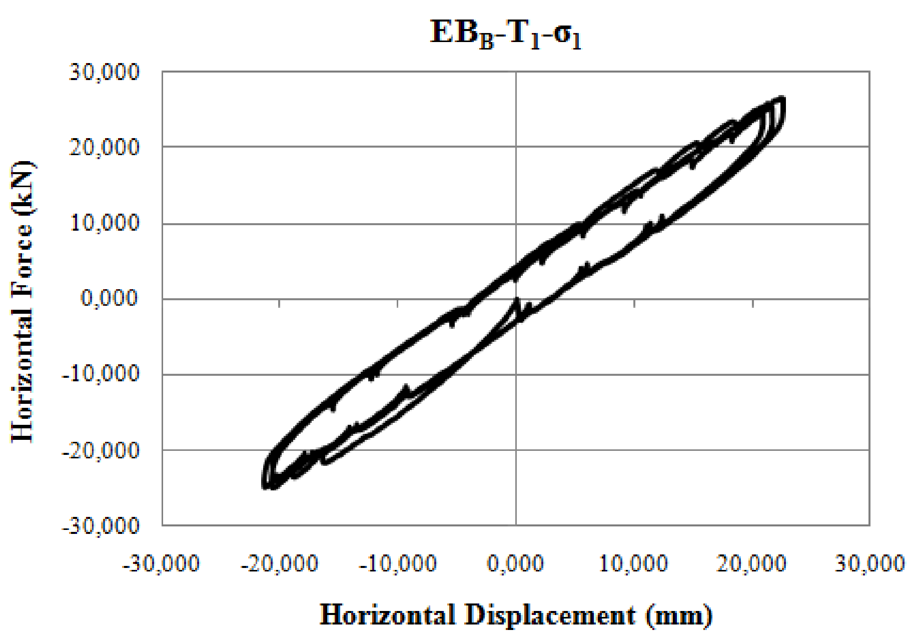

Figure B.7. Hysteresis Loop of Test $EB_B - T_1 - \sigma_1$

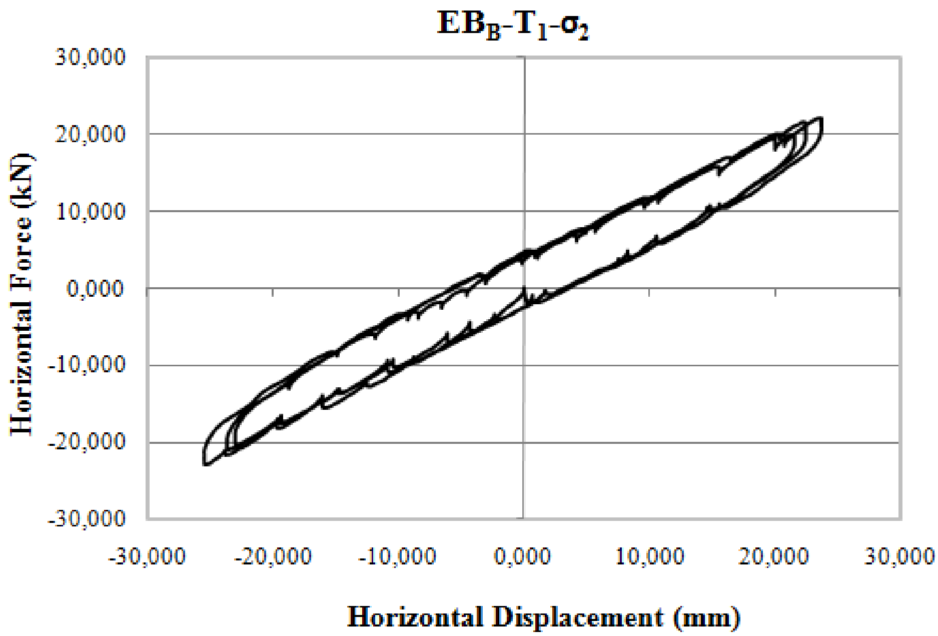

Figure B.8. Hysteresis Loop of Test $EB_B - T_1 - \sigma_2$

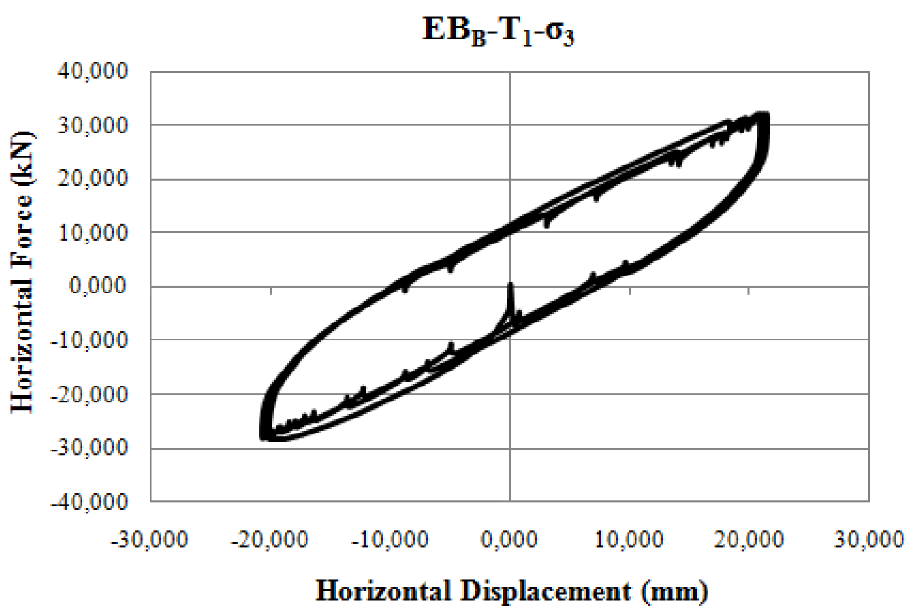

Figure B.9. Hysteresis Loop of Test $EB_B - T_1 - \sigma_3$

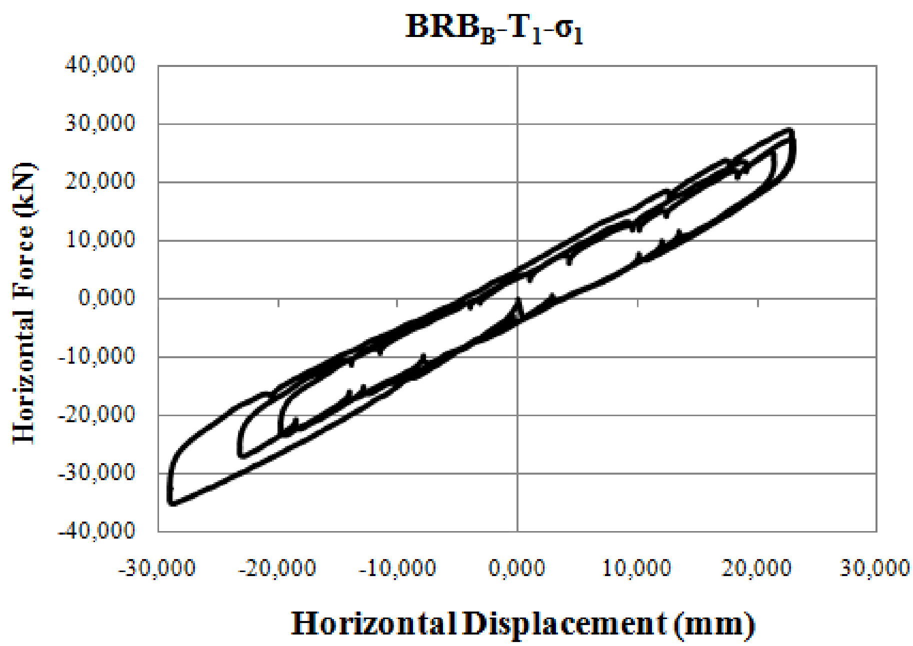

Figure B.10. Hysteresis Loop of Test BRB$_B$ – T$_1$ – σ_1

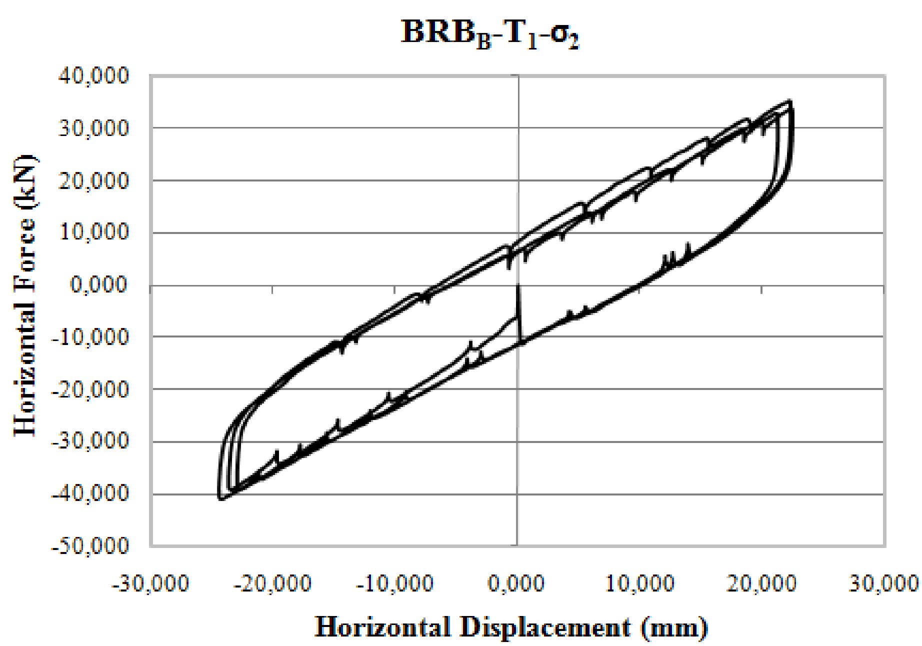

Figure B.11. Hysteresis Loop of Test BRB$_B$ – T$_1$ – σ_2

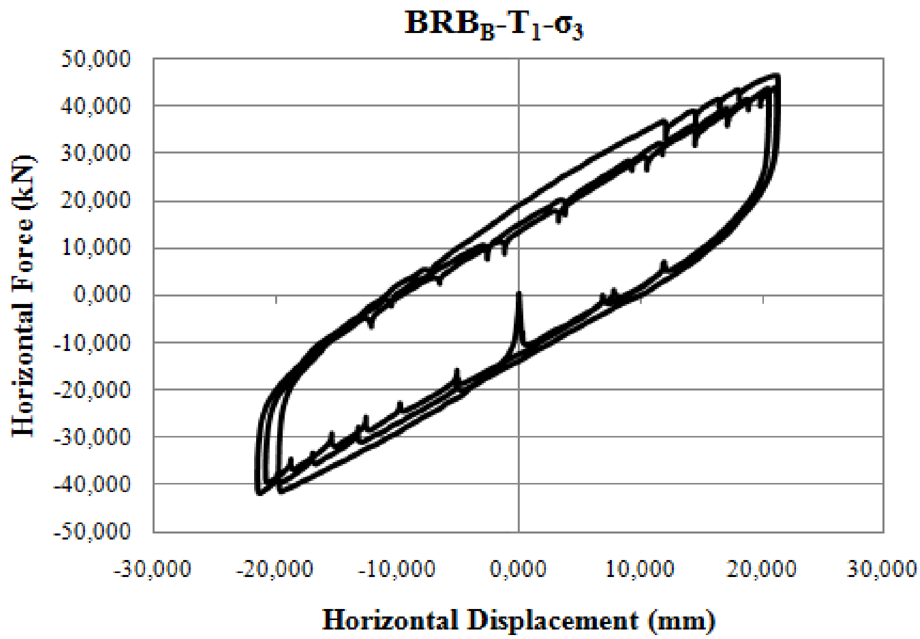

Figure B.12. Hysteresis Loop of Test $BRB_B - T_1 - \sigma_3$

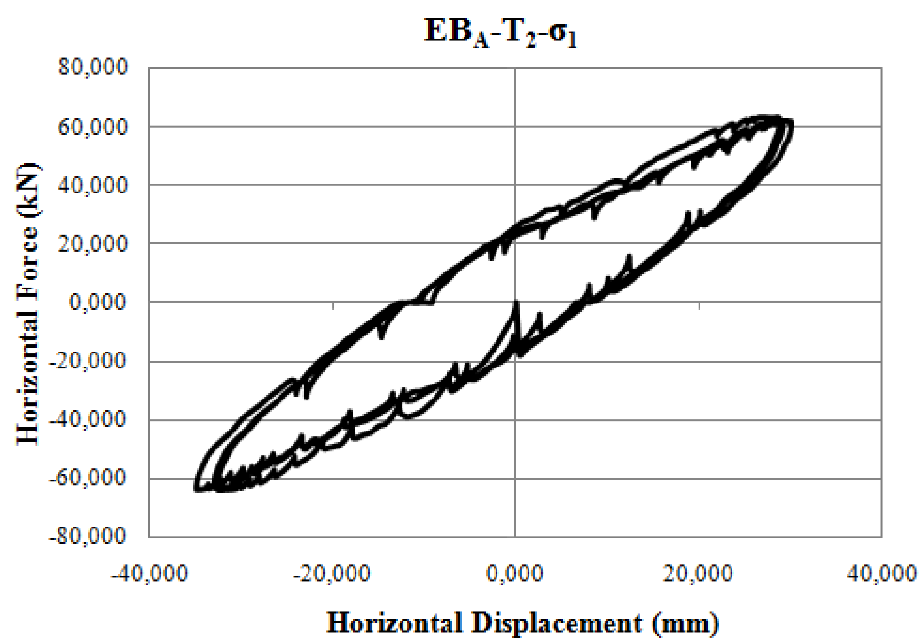

Figure B.13. Hysteresis Loop of Test $EB_A - T_2 - \sigma_1$

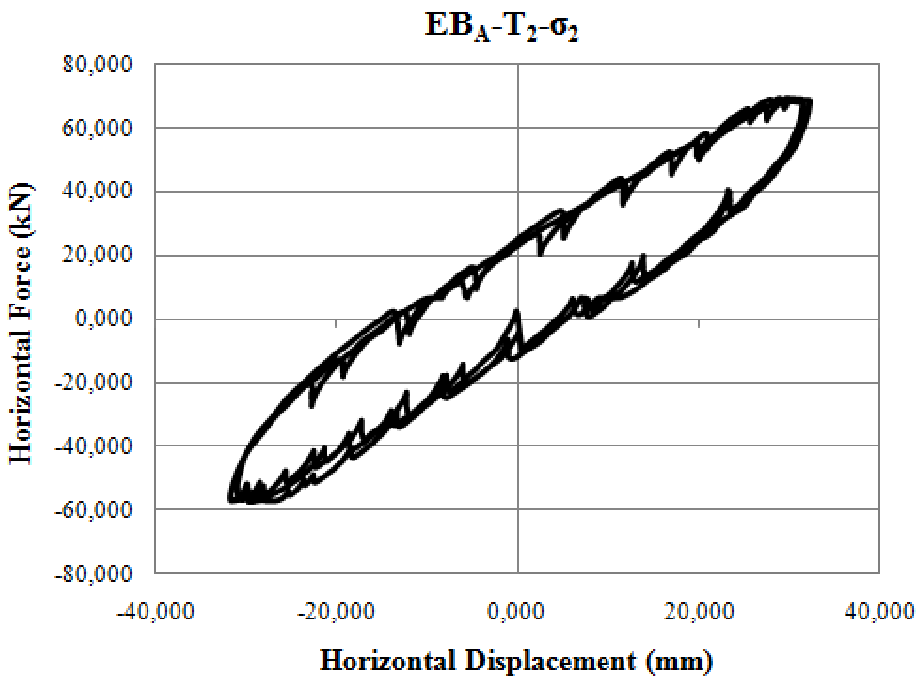

Figure B.14. Hysteresis Loop of Test $EB_A - T_2 - \sigma_2$

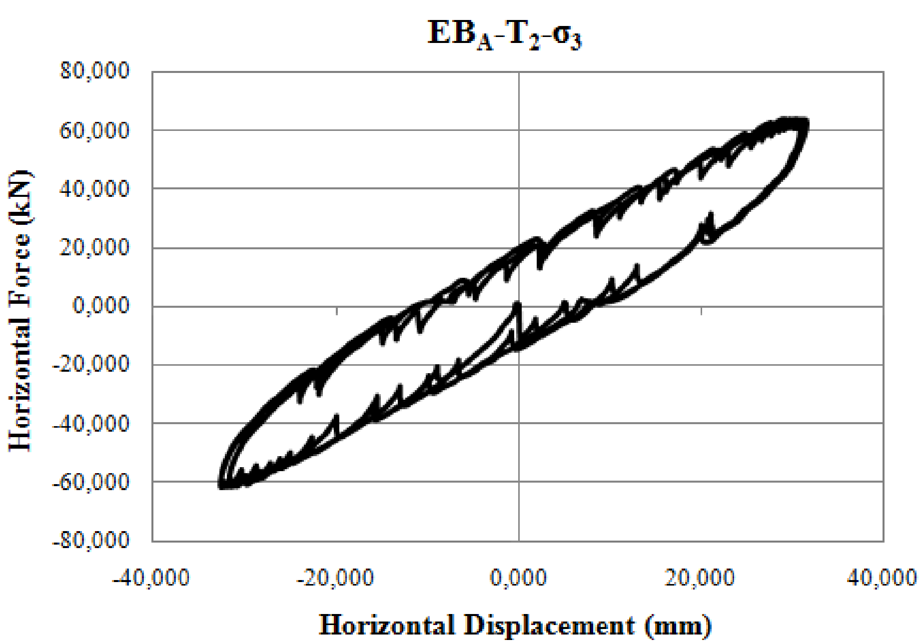

Figure B.15. Hysteresis Loop of Test $EB_A - T_2 - \sigma_3$

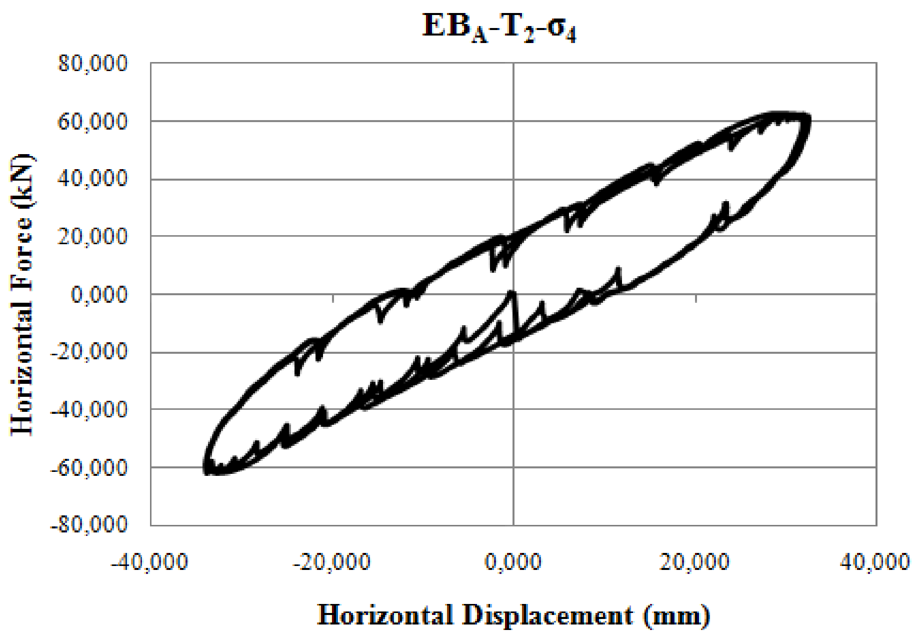

Figure B.16. Hysteresis Loop of Test $EB_A - T_2 - \sigma_4$

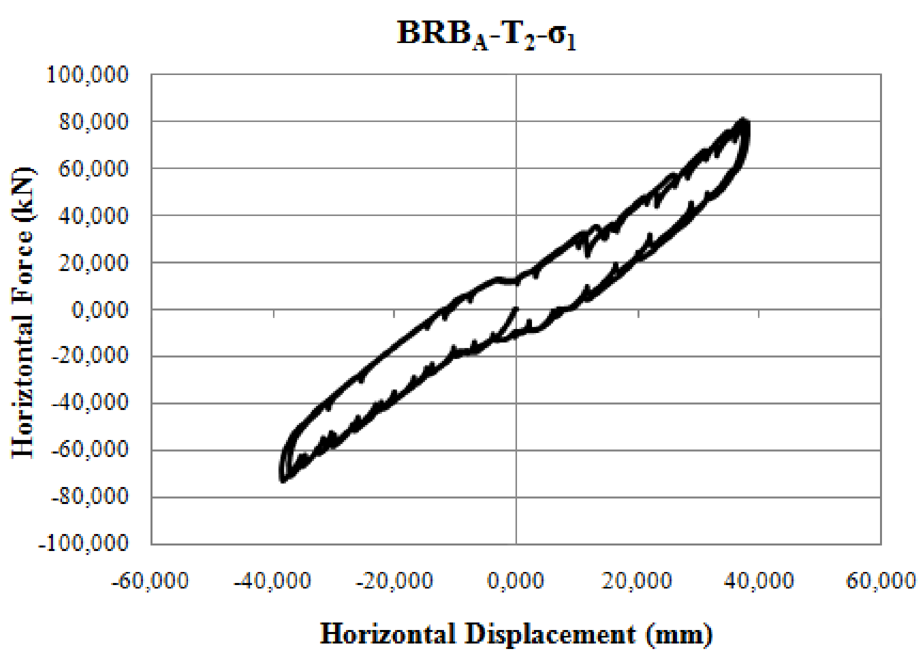

Figure B.17. Hysteresis Loop of Test $BRB_A - T_2 - \sigma_1$

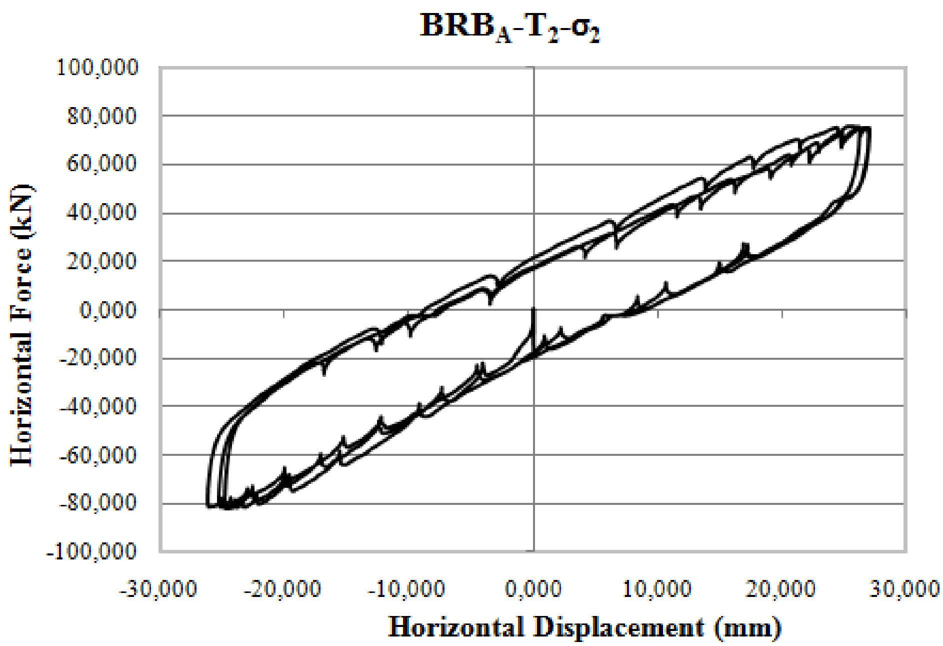

Figure B.18. Hysteresis Loop of Test $BRB_A - T_2 - \sigma_2$

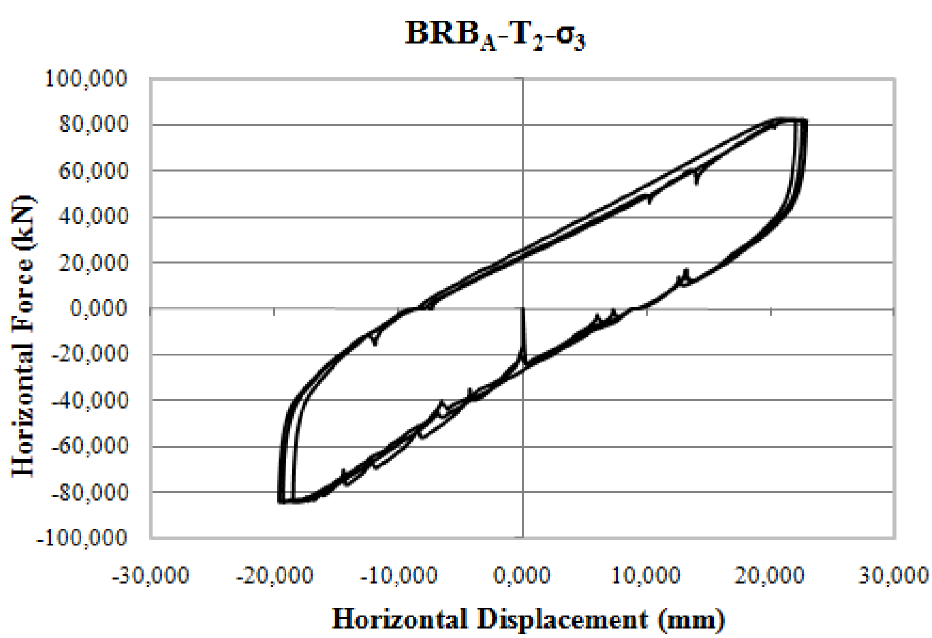

Figure B.19. Hysteresis Loop of Test $BRB_A - T_2 - \sigma_3$

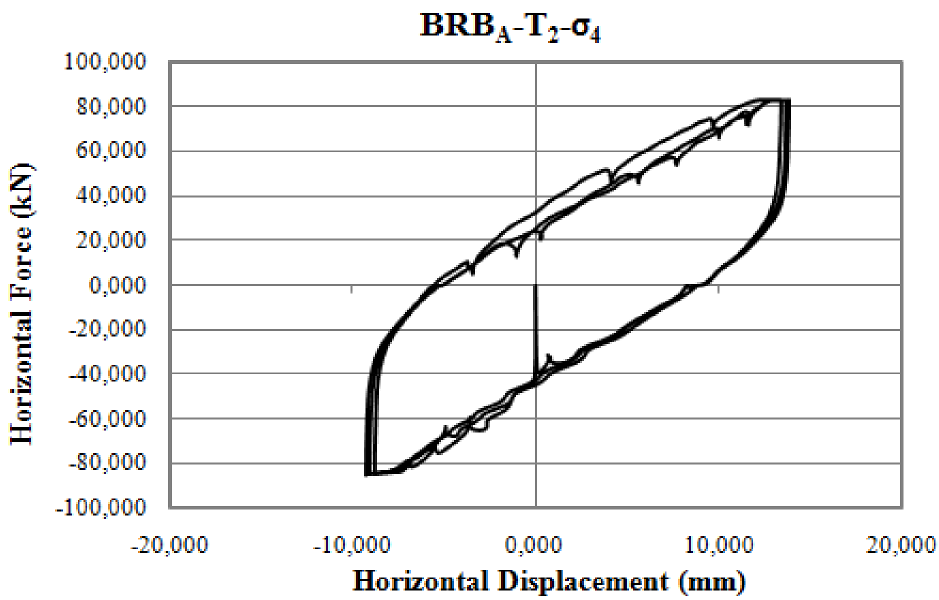

Figure B.20. Hysteresis Loop of Test $BRB_A - T_2 - \sigma_4$

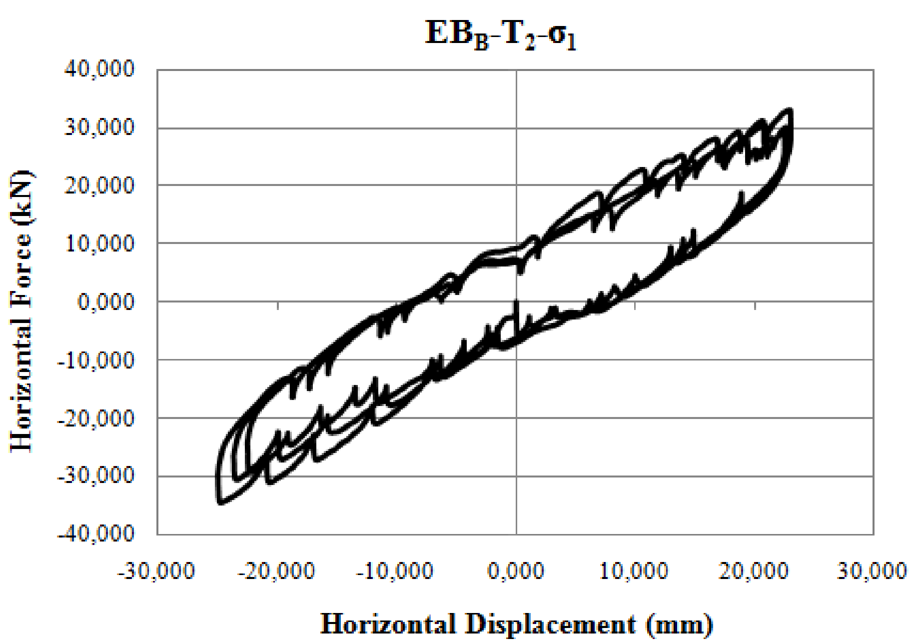

Figure B.21. Hysteresis Loop of Test $EB_B - T_2 - \sigma_1$

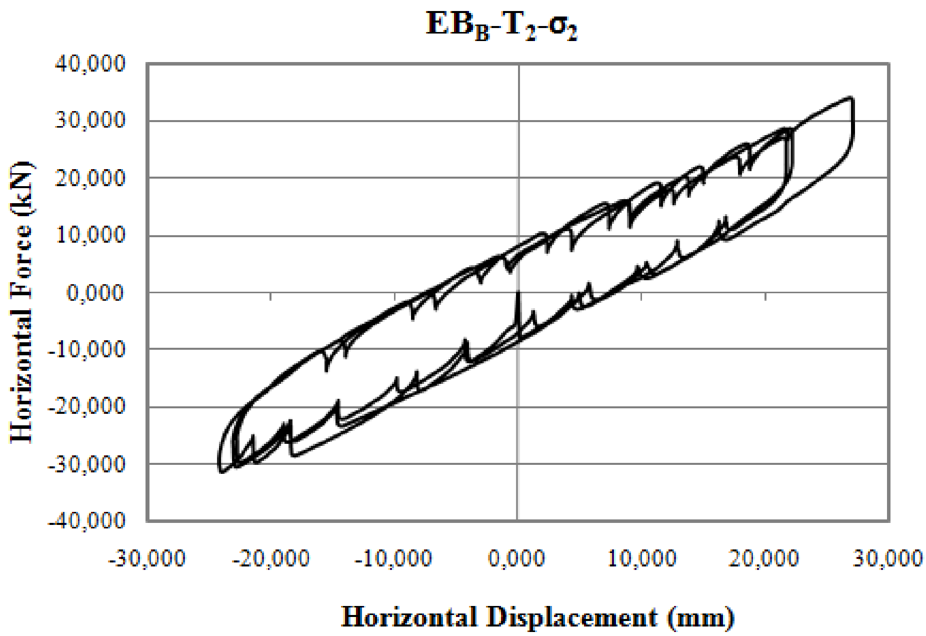

Figure B.22. Hysteresis Loop of Test $EB_B - T_2 - \sigma_2$

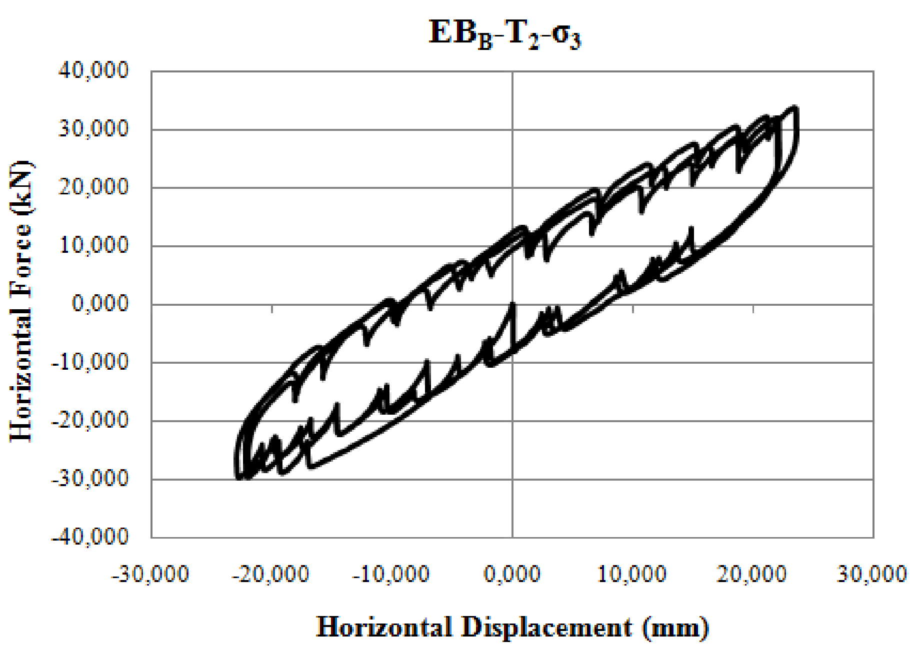

Figure B.23. Hysteresis Loop of Test $EB_B - T_2 - \sigma_3$

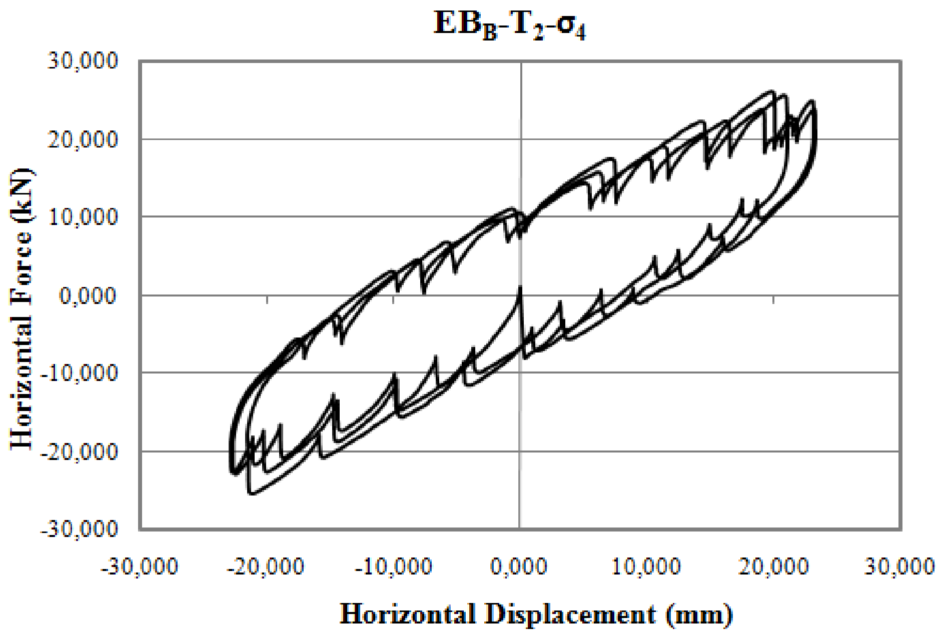

Figure B.24. Hysteresis Loop of Test $EB_B - T_2 - \sigma_4$

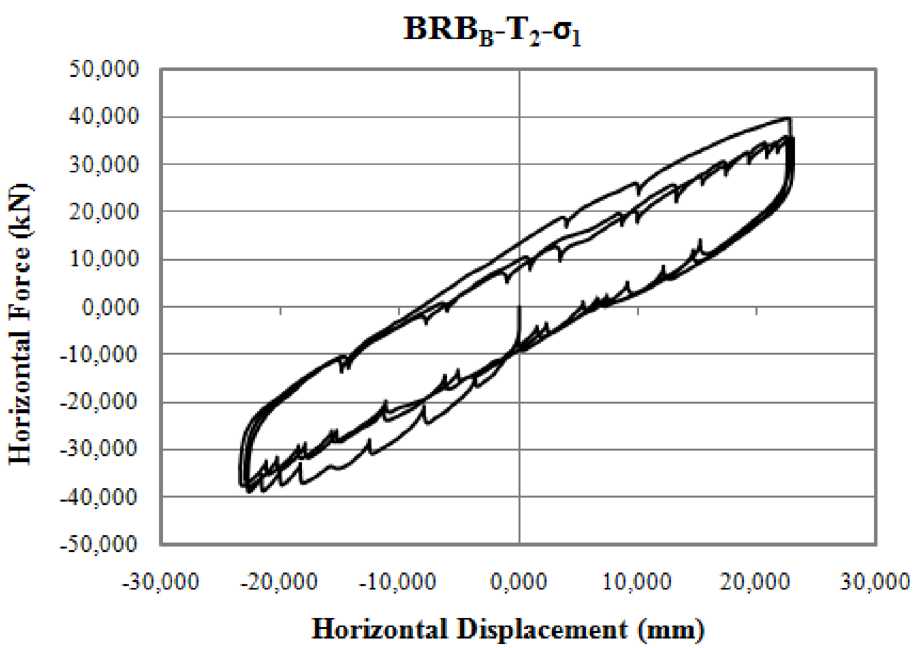

Figure B.25. Hysteresis Loop of Test $BRB_B - T_2 - \sigma_1$

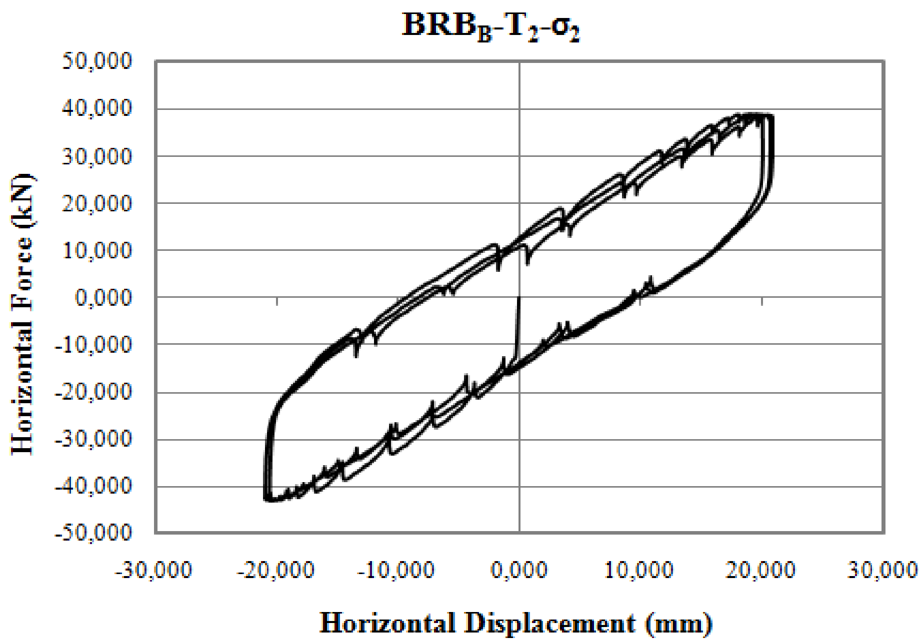

Figure B.26. Hysteresis Loop of Test $BRB_B - T_2 - \sigma_2$

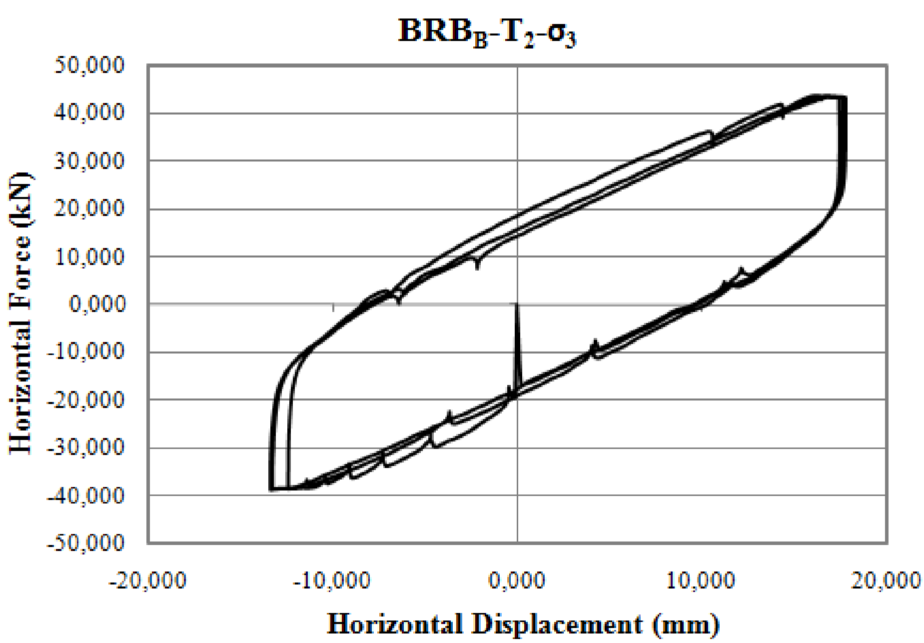

Figure B.27. Hysteresis Loop of Test $BRB_B - T_2 - \sigma_3$

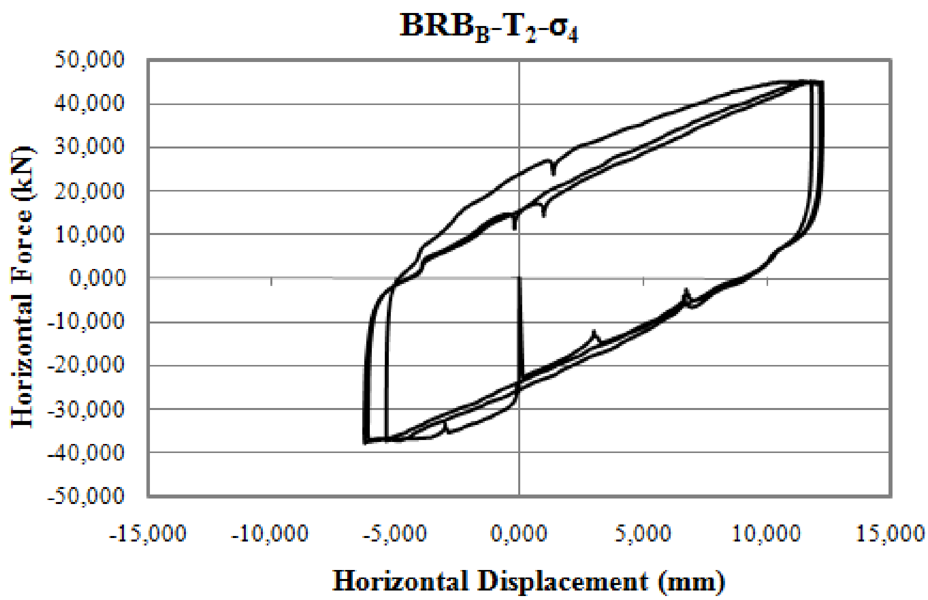

Figure B.28. Hysteresis Loop of Test BRB$_B$ – T_2 – σ_4

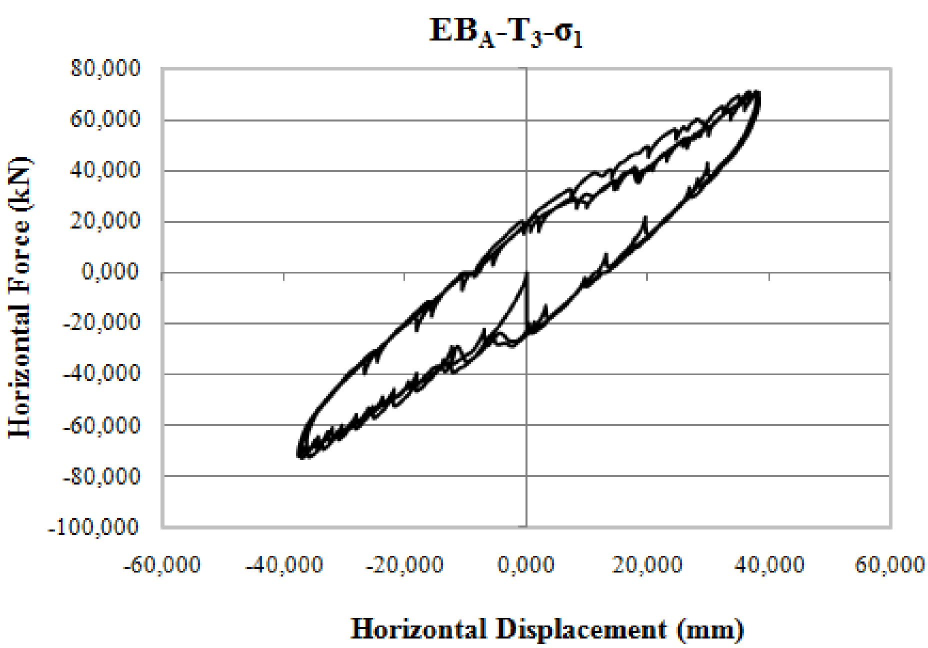

Figure B.29. Hysteresis Loop of Test EB$_A$ – T_3 – σ_1

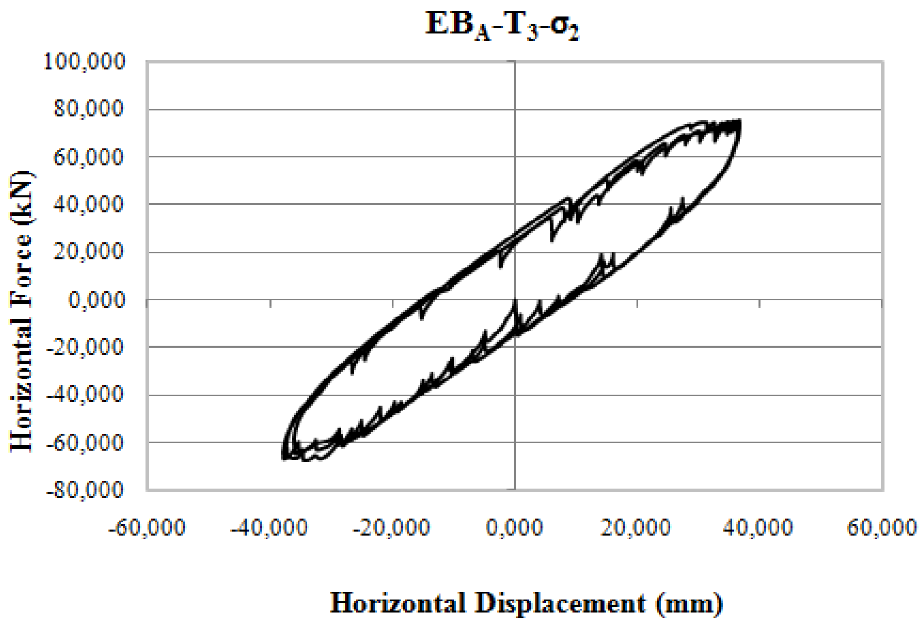

Figure B.30. Hysteresis Loop of Test $EB_A - T_3 - \sigma_2$

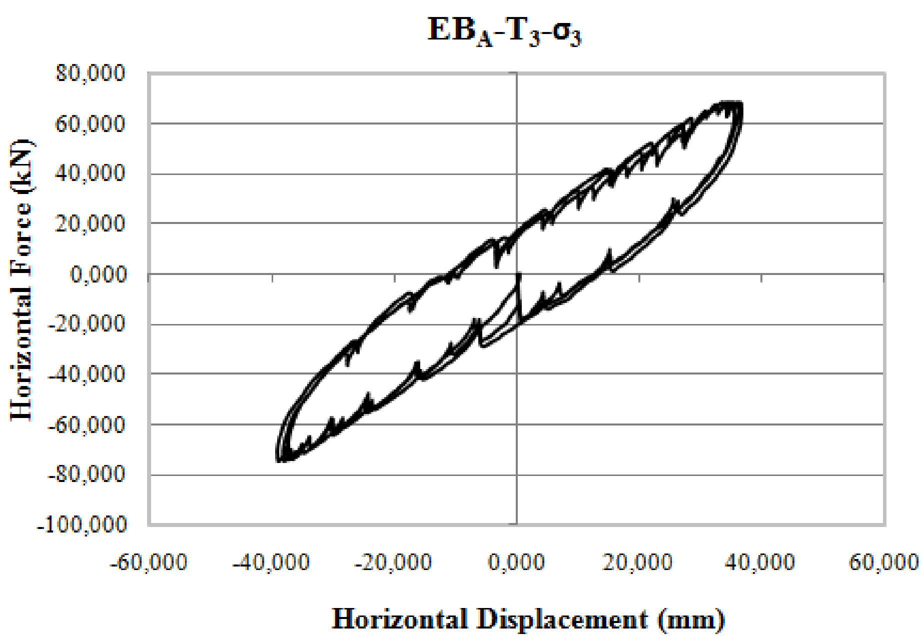

Figure B.31. Hysteresis Loop of Test $EB_A - T_3 - \sigma_3$

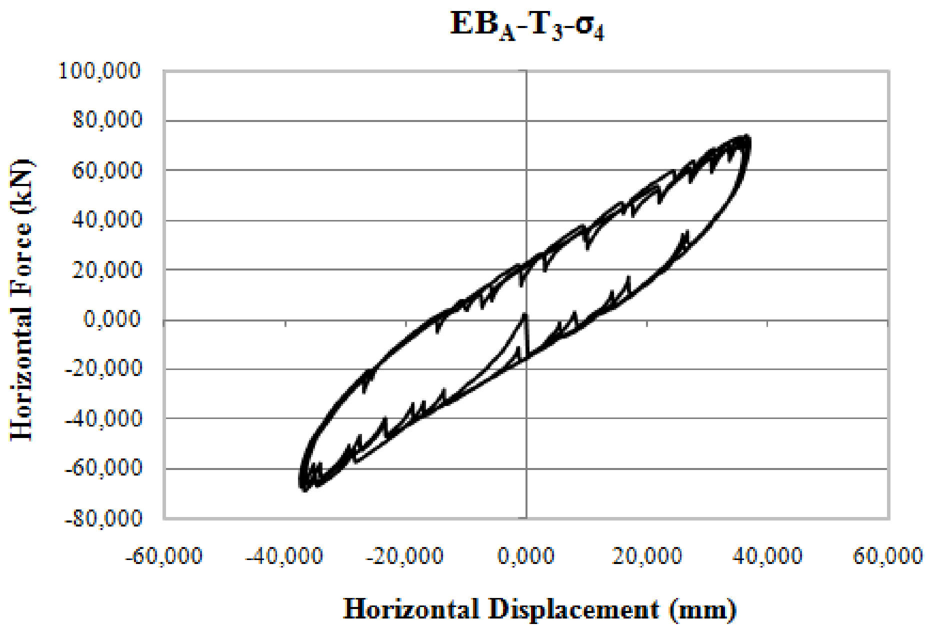

Figure B.32. Hysteresis Loop of Test $EB_A - T_3 - \sigma_4$

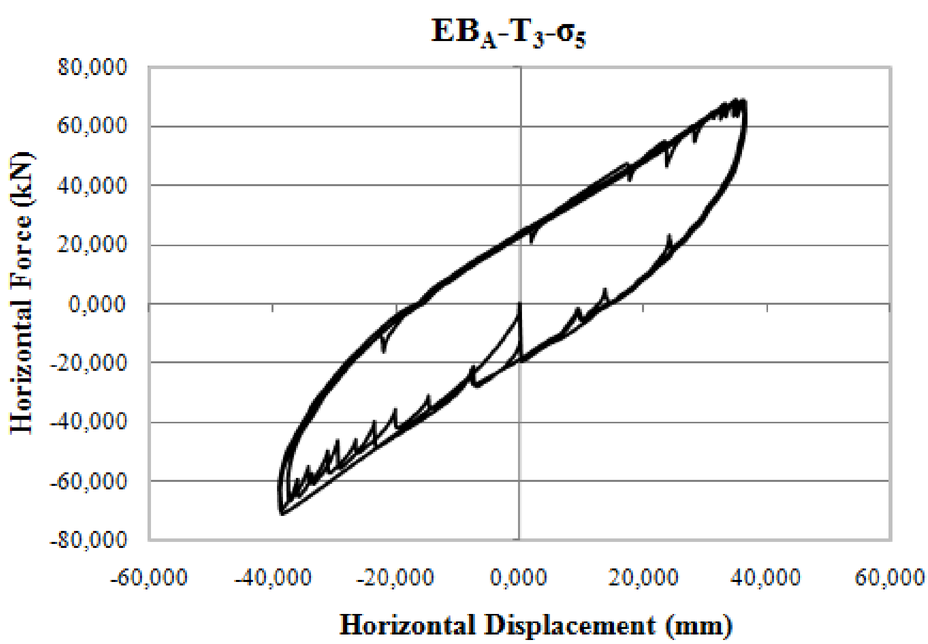

Figure B.33. Hysteresis Loop of Test $EB_A - T_3 - \sigma_5$

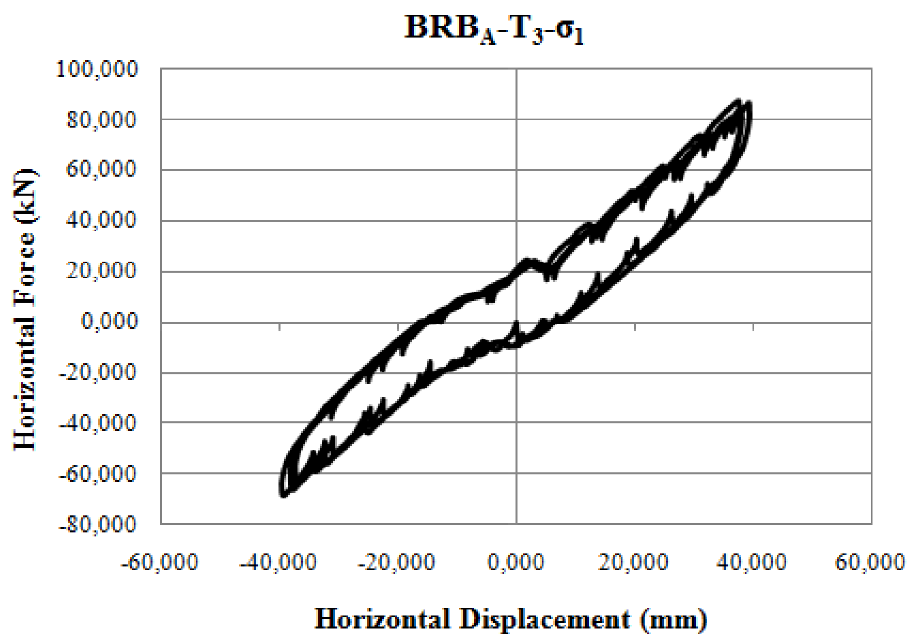

Figure B.34. Hysteresis Loop of Test $BRB_A - T_3 - \sigma_1$

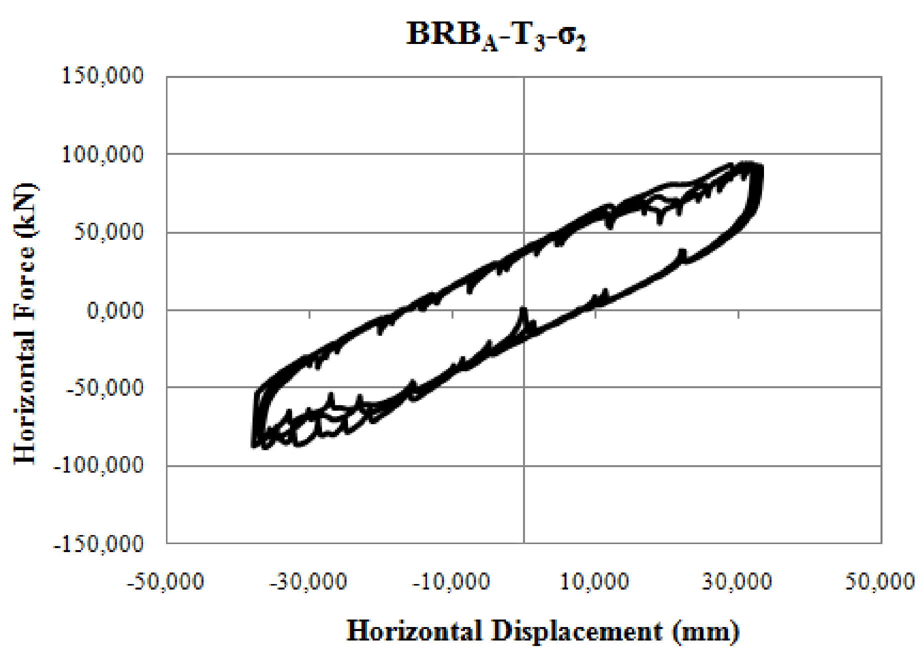

Figure B.35. Hysteresis Loop of Test $BRB_A - T_3 - \sigma_2$

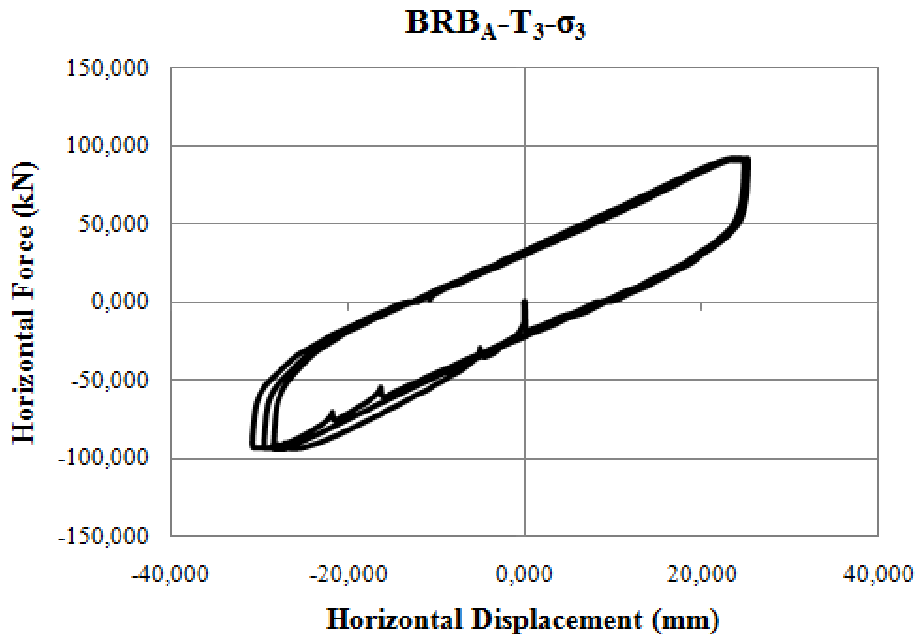

Figure B.36. Hysteresis Loop of Test BRB$_A$ – T$_3$ – σ_3

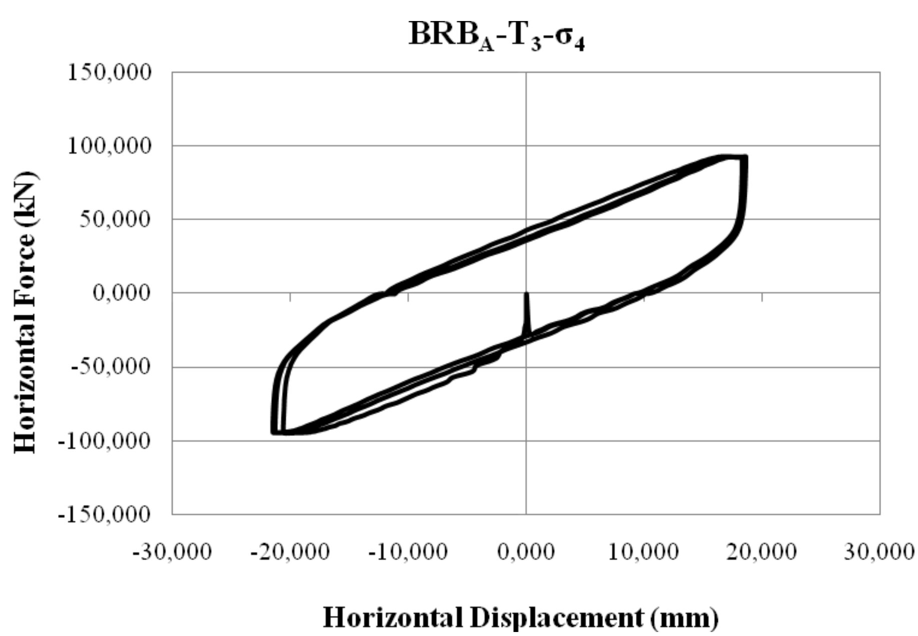

Figure B.37. Hysteresis Loop of Test BRB$_A$ – T$_3$ – σ_4

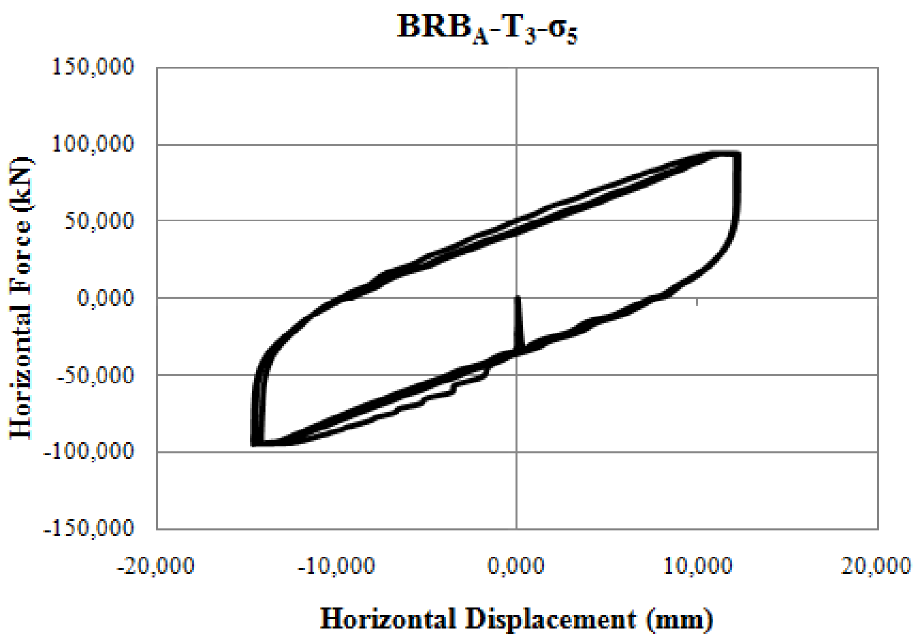

Figure B.38. Hysteresis Loop of Test $BRB_A - T_3 - \sigma_5$

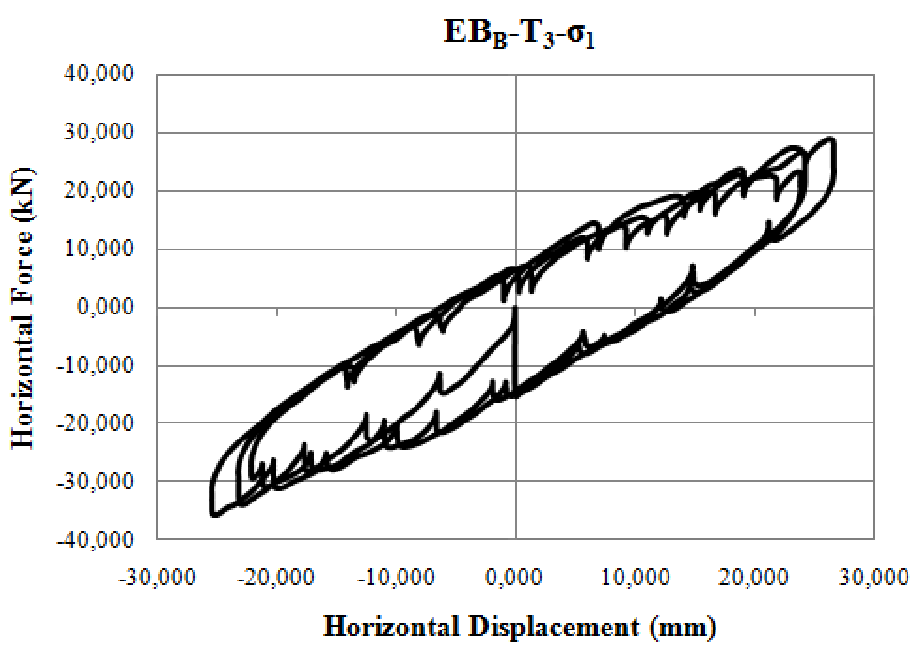

Figure B.39. Hysteresis Loop of Test $EB_B - T_3 - \sigma_1$

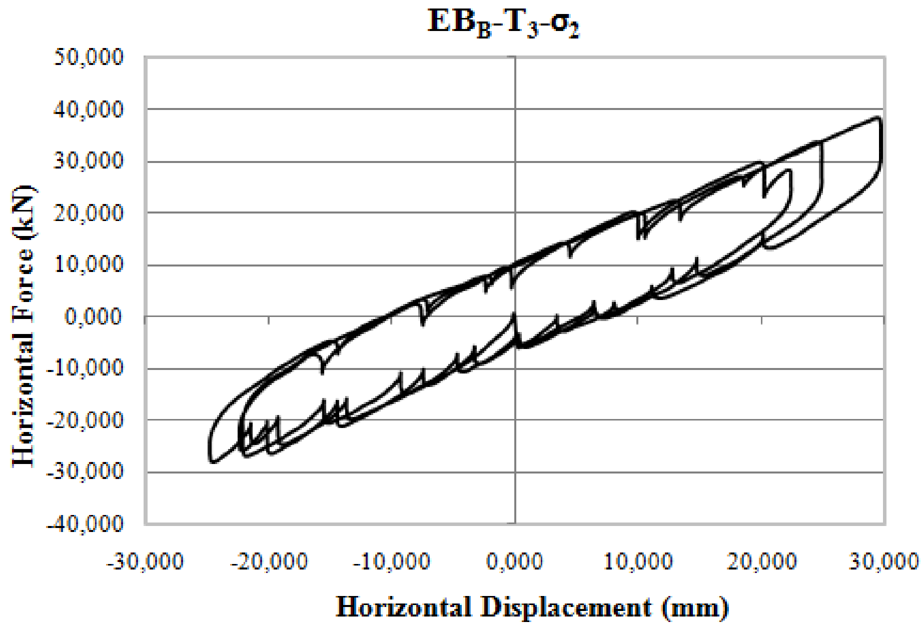

Figure B.40. Hysteresis Loop of Test $EB_B - T_3 - \sigma_2$

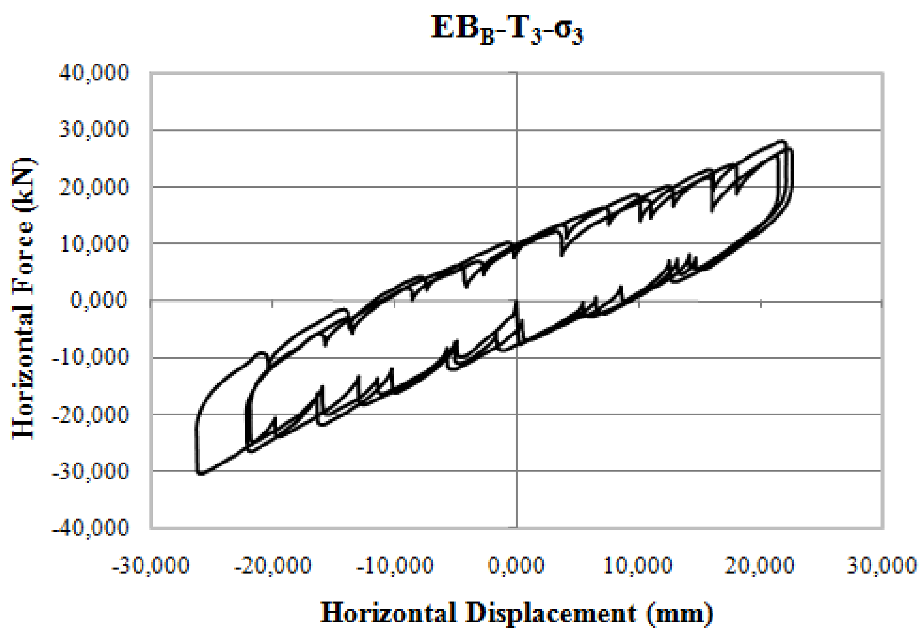

Figure B.41. Hysteresis Loop of Test $EB_B - T_3 - \sigma_3$

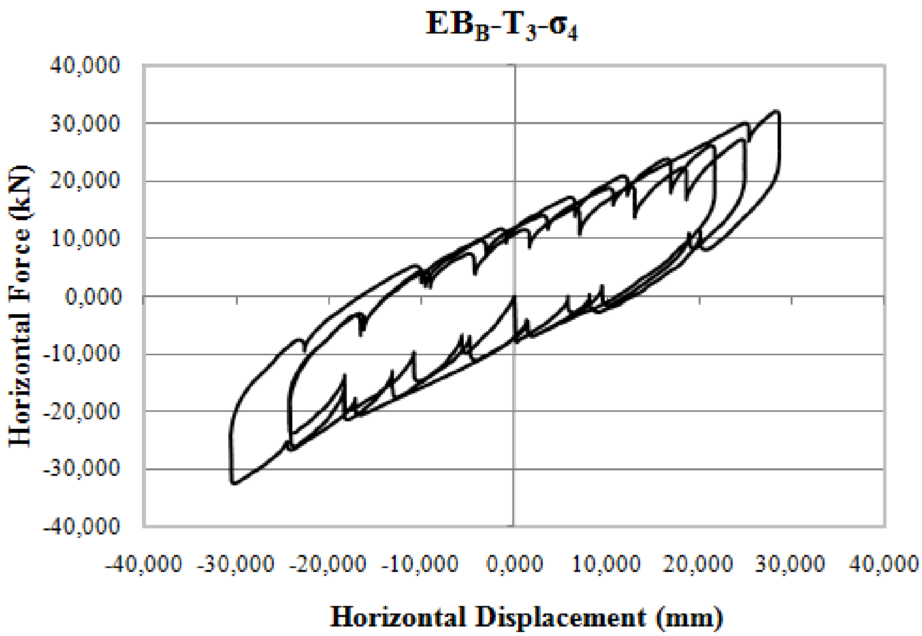

Figure B.42. Hysteresis Loop of Test $EB_B - T_3 - \sigma_4$

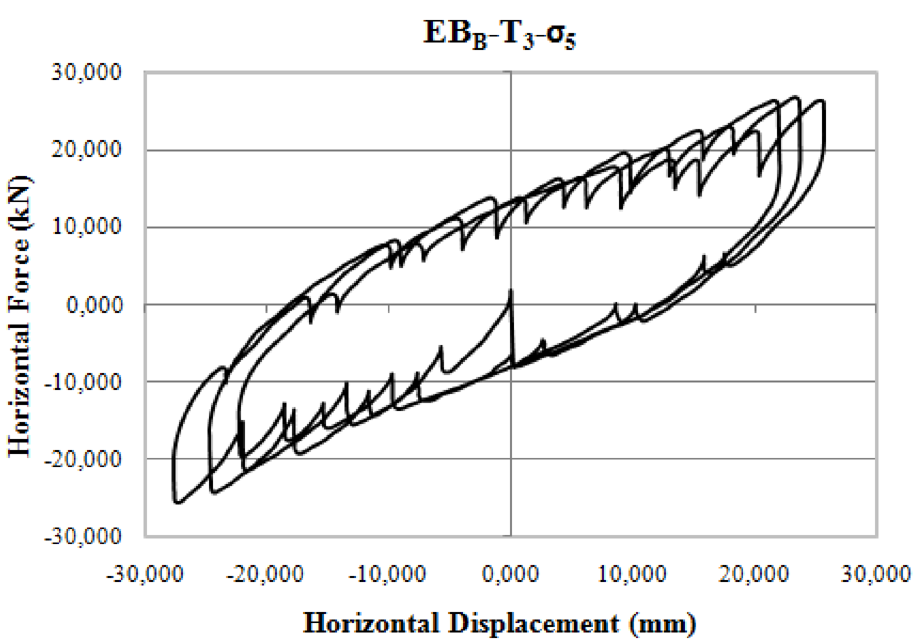

Figure B.43. Hysteresis Loop of Test $EB_B - T_3 - \sigma_5$

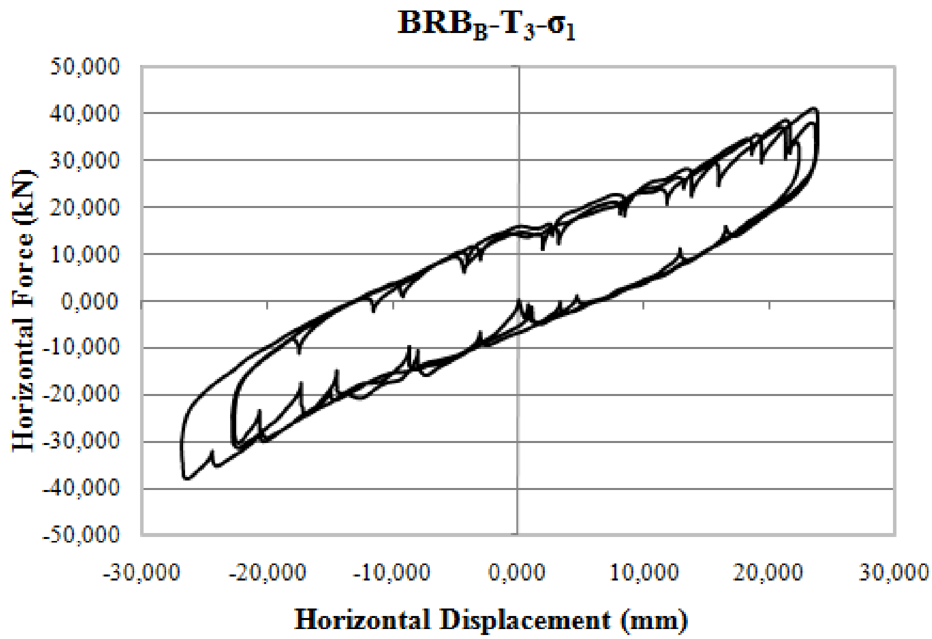

Figure B.44. Hysteresis Loop of Test BRB$_B$ – T_3 – σ_1

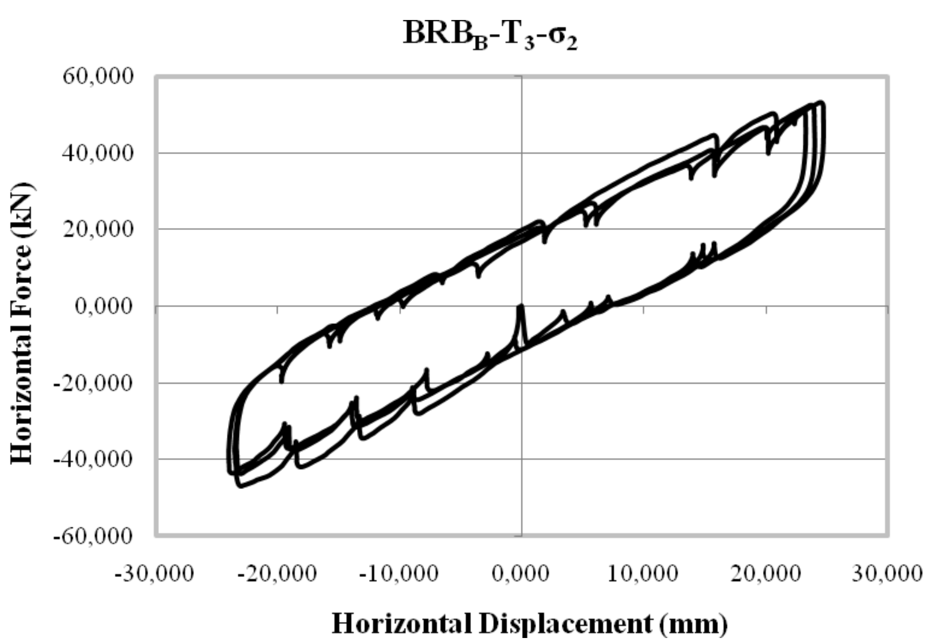

Figure B.45. Hysteresis Loop of Test BRB$_B$ – T_3 – σ_2

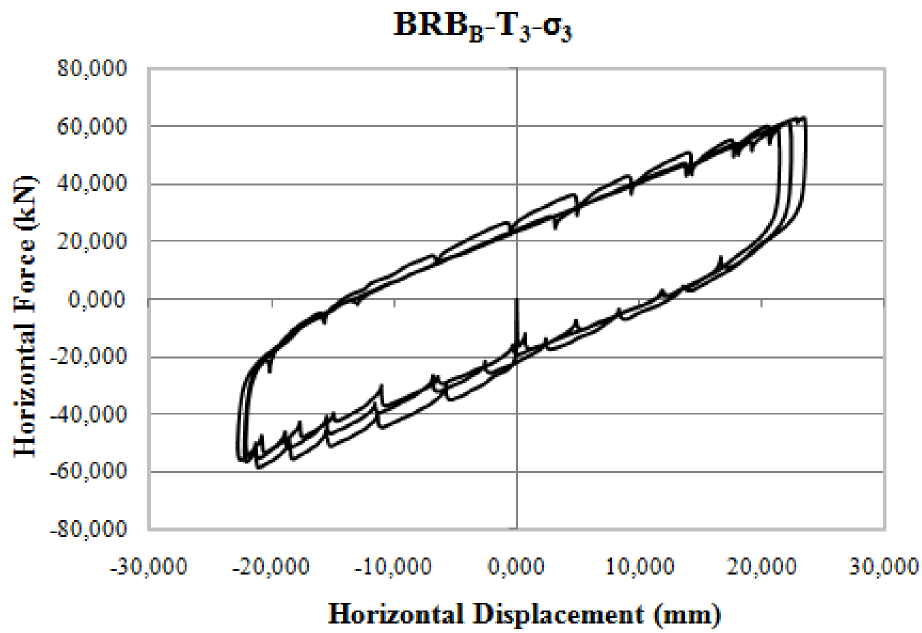

Figure B.46. Hysteresis Loop of Test $BRB_B - T_3 - \sigma_3$

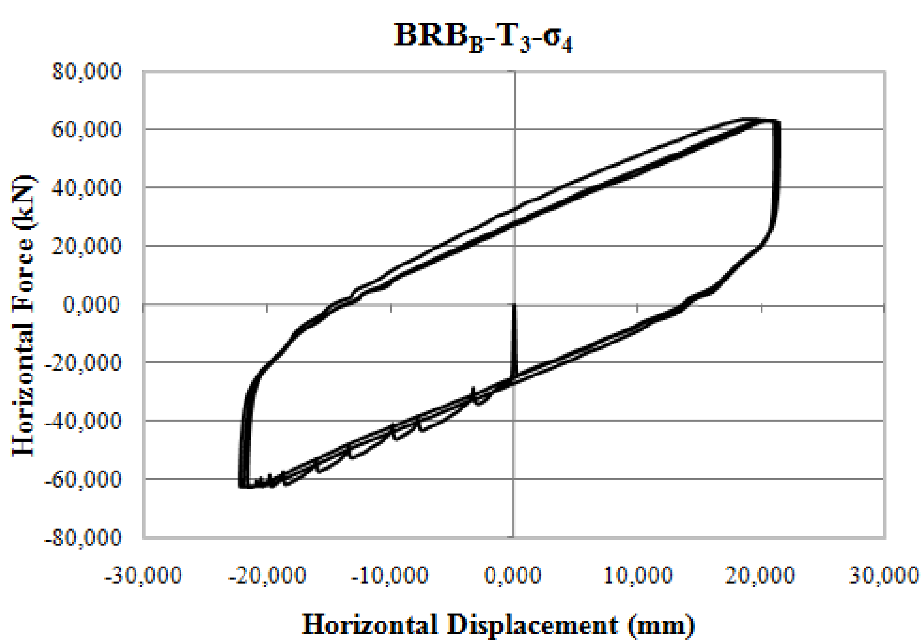

Figure B.47. Hysteresis Loop of Test $BRB_B - T_3 - \sigma_4$

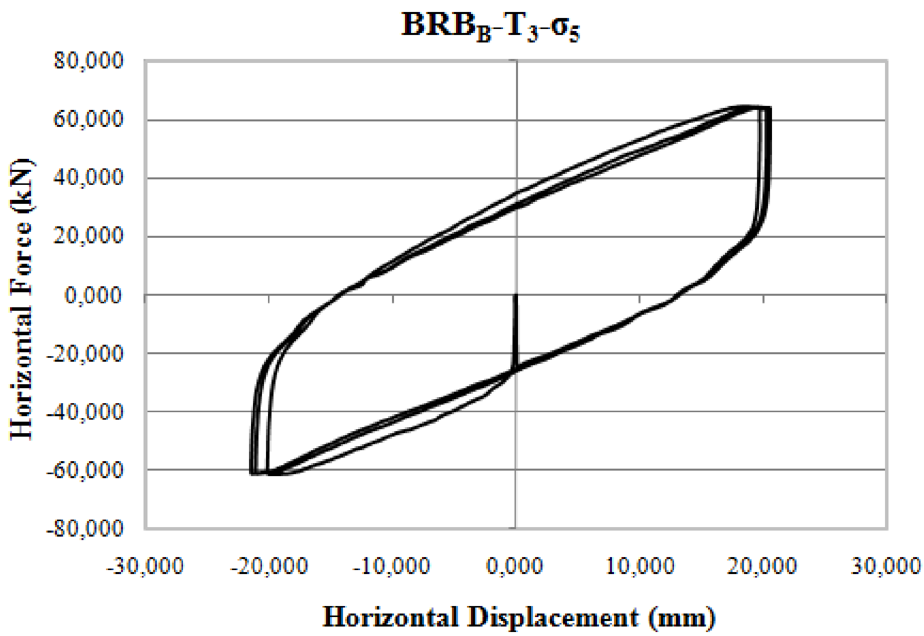

Figure B.48. Hysteresis Loop of Test BRB$_B$ – T$_3$ – σ_5

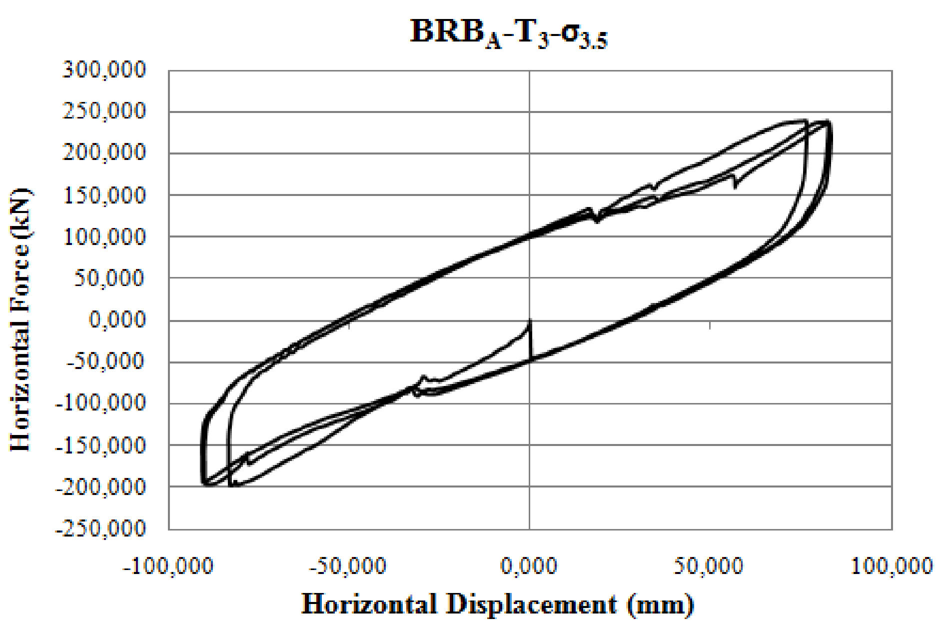

Figure B.49. Hysteresis Loop of Test BRB$_A$ – T$_3$ – $\sigma_{3.5}$

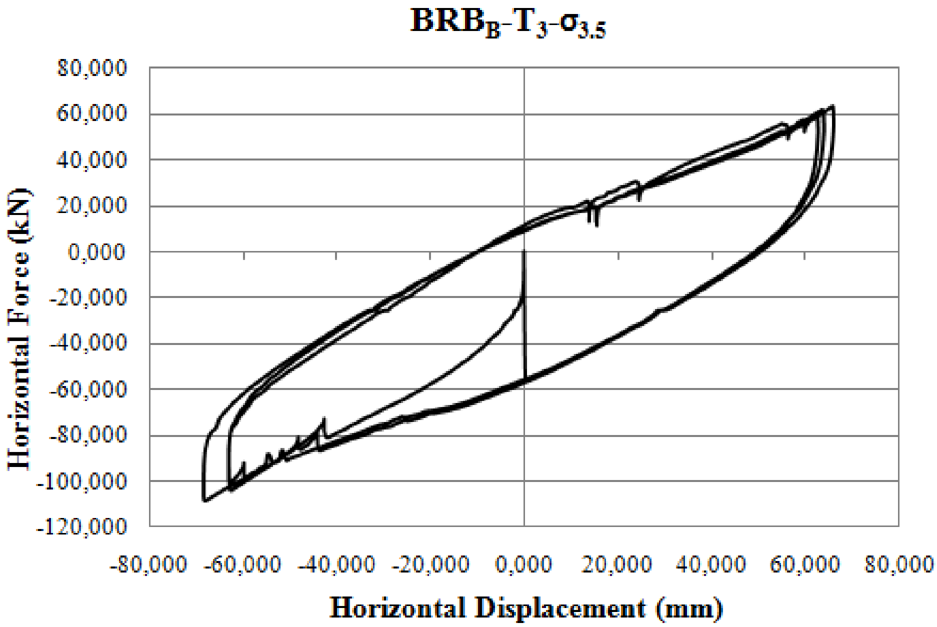

Figure B.50. Hysteresis Loop of Test $BRB_B – T_3 – \sigma_{3.5}$

APPENDIX C

THERMAL TEST DATA

In Appendix C, experimental thermal data recorded for different surfaces of bearing for insulated and uninsulated cases are presented.

Table C.1. Temperature Readings of Insulated and Uninsulated Bearings from Surface of the Bearings for an Hour

Time (min)	D0 (^oC)	ID0 (^oC)	Time (min)	D0 (^oC)	ID0 (^oC)	Time (min)	D0 (^oC)	ID0 (^oC)
0	-28.5	-28.3	25	-1.2	-13.3	50	1.8	-8.3
1	-20.2	-27.9	26	-1.1	-13.0	51	2.0	-8.1
2	-17.2	-26.7	27	-0.5	-12.8	52	2.1	-7.9
3	-14.6	-25.4	28	-0.5	-12.5	53	2.2	-7.7
4	-12.1	-24.1	29	-0.4	-12.3	54	2.4	-7.5
5	-10.1	-23.0	30	-0.1	-12.1	55	2.4	-7.4
6	-8.4	-22.0	31	-0.1	-11.9	56	2.5	-7.2
7	-7.0	-21.1	32	0.0	-11.7	57	2.6	-7.0
8	-5.5	-20.4	33	0.2	-11.5	58	2.6	-6.9
9	-4.9	-19.6	34	0.2	-11.3	59	2.6	-6.7
10	-4.7	-18.9	35	0.5	-11.1	60	2.6	-6.6
11	-4.2	-18.3	36	0.4	-10.9			
12	-4.0	-17.7	37	0.2	-10.7			
13	-3.6	-17.2	38	0.3	-10.5			
14	-3.4	-16.8	39	0.4	-10.3			
15	-3.0	-16.3	40	0.5	-10.1			
16	-2.9	-15.9	41	0.5	-9.9			

Table C.1 (continued)

17	-2.2	-15.6	42	0.8	-9.7
18	-1.5	-15.2	43	0.8	-9.5
19	-1.1	-14.9	44	1.0	-9.4
20	-1.0	-14.5	45	1.1	-9.1
21	-1.0	-14.3	46	1.2	-9.0
22	-1.0	-14.0	47	1.2	-8.7
23	-1.2	-13.8	48	1.5	-8.6
24	-1.4	-13.5	49	1.7	-8.4

Table C.2. Temperature Readings of an Uninsulated Bearing from Surface and at Different Depths for an Hour

Time (min)	D0 (°C)	D1 (°C)	D2 (°C)	D3 (°C)	Time (min)	D0 (°C)	D2 (°C)	D2 (°C)	D3 (°C)
0	-28.5	-26.1	-26.1	-26.1	31	-0.1	-7.4	-13.7	-17.6
1	-20.2	-24.2	-25.0	-25.5	32	0.0	-7.2	-13.5	-17.4
2	-17.2	-23.2	-22.8	-24.6	33	0.2	-7.1	-13.2	-17.1
3	-14.6	-20.3	-21.6	-23.9	34	0.2	-7.0	-12.9	-16.9
4	-12.1	-15.7	-20.7	-23.5	35	0.5	-6.8	-12.8	-16.6
5	-10.1	-14.6	-20.0	-23.4	36	0.4	-6.7	-12.6	-16.4
6	-8.4	-13.7	-19.5	-23.1	37	0.2	-6.6	-12.4	-16.2
7	-7.0	-12.5	-19.0	-22.9	38	0.3	-6.4	-12.1	-16.0
8	-5.5	-12.1	-18.6	-22.7	39	0.4	-6.3	-12.0	-15.8
9	-4.9	-11.9	-18.2	-22.5	40	0.5	-6.2	-11.8	-15.5
10	-4.7	-11.7	-18.0	-22.3	41	0.5	-6.1	-11.5	-15.2
11	-4.2	-11.3	-17.7	-22.1	42	0.8	-5.9	-11.2	-15.0
12	-4.0	-10.9	-17.4	-21.9	43	0.8	-5.7	-11.0	-14.8
13	-3.6	-10.5	-17.2	-21.6	44	1.0	-5.4	-10.9	-14.5
14	-3.4	-10.3	-17.0	-21.5	45	1.1	-5.2	-10.6	-14.2
15	-3.0	-10.1	-16.7	-21.3	46	1.2	-4.9	-10.4	-14.0
16	-2.9	-10.0	-16.4	-21.1	47	1.2	-4.8	-10.2	-13.8
17	-2.2	-9.9	-16.3	-20.8	48	1.5	-4.6	-10.1	-13.5
18	-1.5	-9.5	-16.1	-20.6	49	1.7	-4.5	-9.8	-13.2
19	-1.1	-9.4	-16.0	-20.4	50	1.8	-4.3	-9.6	-13.0
20	-1.0	-9.2	-15.9	-20.2	51	2.0	-4.1	-9.4	-12.8
21	-1.0	-9.1	-15.5	-20.0	52	2.1	-3.8	-9.3	-12.5
22	-1.0	-8.9	-15.3	-19.8	53	2.2	-3.6	-9.0	-12.3
23	-1.2	-8.8	-15.2	-19.6	54	2.4	-3.4	-8.8	-12.1
24	-1.4	-8.6	-15.0	-19.3	55	2.4	-3.2	-8.6	-11.8
25	-1.2	-8.5	-14.8	-19.1	56	2.5	-3.1	-8.5	-11.5
26	-1.1	-8.4	-14.5	-18.9	57	2.6	-3.0	-8.3	-11.3
27	-0.5	-8.2	-14.4	-18.6	58	2.6	-2.9	-8.1	-11.0
28	-0.5	-8.1	-14.3	-18.3	59	2.6	-2.8	-7.8	-10.9

Table C.2 (continued)

29	-0.4	-7.9	-14.0	-18.1	60	2.6	-2.6	-7.6	-10.6
30	-0.1	-7.6	-13.8	-17.9					

Table C.3. Temperature Readings of an Insulated Bearing from Surface and at Different Depths for an Hour

Time (min)	ID0 (°C)	ID1 (°C)	ID2 (°C)	ID3 (°C)	Time (min)	ID0 (°C)	ID1 (°C)	ID2 (°C)	ID3 (°C)
0	-28.3	-27.5	-27.5	-27.5	31	-11.9	-13.9	-16.6	-20.9
1	-27.9	-25.4	-26.3	-27.1	32	-11.7	-13.8	-16.5	-20.7
2	-26.7	-22.0	-23.8	-26.1	33	-11.5	-13.6	-16.3	-20.5
3	-25.4	-20.3	-22.4	-25.4	34	-11.3	-13.5	-16.2	-20.3
4	-24.1	-19.2	-21.4	-25.0	35	-11.1	-13.3	-16.0	-20.2
5	-23.0	-18.5	-20.8	-24.6	36	-10.9	-13.2	-15.8	-20.0
6	-22.0	-18.0	-20.3	-24.4	37	-10.7	-13.0	-15.7	-19.8
7	-21.1	-17.6	-20.0	-24.2	38	-10.5	-12.8	-15.5	-19.6
8	-20.4	-17.3	-19.7	-24.0	39	-10.3	-12.7	-15.3	-19.4
9	-19.6	-17.0	-19.5	-23.8	40	-10.1	-12.5	-15.2	-19.2
10	-18.9	-16.8	-19.3	-23.7	41	-9.9	-12.4	-15.0	-18.9
11	-18.3	-16.6	-19.1	-23.6	42	-9.7	-12.1	-14.9	-18.8
12	-17.7	-16.5	-18.9	-23.5	43	-9.5	-12.1	-14.7	-18.6
13	-17.2	-16.3	-18.8	-23.4	44	-9.4	-11.8	-14.5	-18.4
14	-16.8	-16.2	-18.7	-23.3	45	-9.1	-11.6	-14.3	-18.2
15	-16.3	-16.0	-18.6	-23.2	46	-9.0	-11.5	-14.2	-18.0
16	-15.9	-15.9	-18.5	-23.1	47	-8.7	-11.3	-14.0	-17.8
17	-15.6	-15.8	-18.4	-23.0	48	-8.6	-11.2	-13.8	-17.6
18	-15.2	-15.7	-18.3	-22.8	49	-8.4	-11.0	-13.7	-17.4
19	-14.9	-15.6	-18.2	-22.7	50	-8.3	-10.8	-13.5	-17.2
20	-14.5	-15.4	-18.0	-22.5	51	-8.1	-10.6	-13.3	-16.9
21	-14.3	-15.3	-17.9	-22.4	52	-7.9	-10.5	-13.1	-16.7
22	-14.0	-15.2	-17.8	-22.3	53	-7.7	-10.4	-13.0	-16.5
23	-13.8	-15.0	-17.6	-22.1	54	-7.5	-10.2	-12.8	-16.3
24	-13.5	-14.8	-17.5	-22.0	55	-7.4	-10.1	-12.6	-16.1
25	-13.3	-14.7	-17.4	-21.8	56	-7.2	-9.9	-12.4	-15.9
26	-13.0	-14.5	-17.3	-21.7	57	-7.0	-9.7	-12.2	-15.7
27	-12.8	-14.4	-17.2	-21.5	58	-6.9	-9.5	-12.1	-15.5

Table C.3 (continued)

28	-12.5	-14.3	-17.0	-21.4	59	-6.7	-9.4	-11.9	-15.2
29	-12.3	-14.1	-16.9	-21.2	60	-6.6	-9.1	-11.8	-15.0
30	-12.1	-14.0	-16.8	-21.1					

APPENDIX D

METEOROLOGICAL DATA

The recorded meteorological data belonging to winter season at provinces in the vicinity of North Anatolian Fault Zone are presented in the following tables. These data are obtained from Turkish State Meteorological Service [9].

Table D.1 Meteorological Records of Ağrı for Winter Season [9]

AĞRI	December	January	February
Average Temperature (°C)	-6.1	-10.5	-9.4
Average Max. Temperature (°C)	-1.5	-5.1	-3.4
Average Min. Temperature (°C)	-10.5	-15.9	-15.0
Mean Sunshine Duration (hour)	1.8	2.1	2.9
Mean Number of Rainy Days	11.7	11.6	11.8
Mean Annual Precipitation (kg/m^2)	42.7	38.0	50.6
Maximum Temperature (°C)	14.0	7.6	10.2
Minimum Temperature (°C)	-39.8	-38.0	-42.8

Table D.2. Meteorological Records of Amasya for Winter Season [9]

AMASYA	December	January	February
Average Temperature (°C)	4.4	2.8	4.3
Average Max. Temperature (°C)	8.5	7.0	9.3
Average Min. Temperature (°C)	0.8	-0.9	-0.3
Mean Sunshine Duration (hour)	1.9	2.1	3.1
Mean Number of Rainy Days	12.2	11.8	10.7
Mean Annual Precipitation (kg/m^2)	47.4	46.6	33.7
Maximum Temperature (°C)	22.9	21.3	24.1
Minimum Temperature (°C)	-12.7	-17.2	-20.4

Table D.3. Meteorological Records of Balıkesir for Winter Season [9]

BALIKESİR	December	January	February
Average Temperature (°C)	6.6	5.0	5.6
Average Max. Temperature (°C)	10.2	8.9	10.0
Average Min. Temperature (°C)	3.2	1.4	1.7
Mean Sunshine Duration (hour)	2.3	2.9	3.4
Mean Number of Rainy Days	14.2	13.5	10.9
Mean Annual Precipitation (kg/m^2)	94.0	72.1	50.2
Maximum Temperature (°C)	22.5	20.0	22.8
Minimum Temperature (°C)	-7.0	-9.4	-18.8

Table D.4. Meteorological Records of Bilecik for Winter Season [9]

BİLECİK	December	January	February
Average Temperature (°C)	4.4	2.5	3.4
Average Max. Temperature (°C)	7.6	6.0	7.4
Average Min. Temperature (°C)	1.7	-0.3	0.0
Mean Sunshine Duration (hour)	3.0	3.3	3.9
Average Number of Rainy Days	13.6	13.8	13.1
Mean Annual Precipitation (kg/m^2)	54.6	50.2	37.0
Maximum Temperature (°C)	25.0	18.7	22.2
Minimum Temperature (°C)	-10.0	-13.1	-14.3

Table D.5. Meteorological Records of Bingöl for Winter Season [9]

BİNGÖL	December	January	February
Average Temperature (°C)	0.5	-2.3	-1.4
Average Max. Temperature (°C)	4.6	2.0	3.4
Average Min. Temperature (°C)	-2.7	-5.7	-5.0
Mean Sunshine Duration (hour)	2.7	3.2	4.7
Mean Number of Rainy Days	13.1	12.5	12.5
Mean Annual Precipitation (kg/m^2)	137.4	123.2	142.8
Maximum Temperature (°C)	17.2	13.3	16.0
Minimum Temperature (°C)	-25.1	-23.2	-21.6

Table D.6. Meteorological Records of Bolu for Winter Season [9]

BOLU	December	January	February
Average Temperature (°C)	2.8	1.0	1.9
Average Max. Temperature (°C)	7.2	5.5	7.1
Average Min. Temperature (°C)	-0.9	-2.9	-2.5
Mean Sunshine Duration (hour)	1.9	2.1	2.9
Average Number of Rainy Days	16.0	14.9	14.4
Mean Annual Precipitation (kg/m^2)	60.1	58.3	42.8
Maximum Temperature (°C)	20.1	19.8	20.8
Minimum Temperature (°C)	-22.6	-18.8	-22.0

Table D.7. Meteorological Records of Bursa for Winter Season [9]

BURSA	December	January	February
Average Temperature (°C)	7.2	5.5	5.9
Average Max. Temperature (°C)	11.3	9.7	10.5
Average Min. Temperature (°C)	3.5	1.7	1.8
Mean Sunshine Duration (hour)	2.8	3.1	3.5
Mean Number of Rainy Days	14.3	14.2	12.6
Mean Annual Precipitation (kg/m^2)	96.4	80.3	66.3
Maximum Temperature (°C)	25.8	22.8	25.0
Minimum Temperature (°C)	-8.2	-11.8	-16.4

Table D.8. Meteorological Records of Çanakkale for Winter Season [9]

ÇANAKKALE	December	January	February
Average Temperature (°C)	8.1	6.4	6.4
Average Max. Temperature (°C)	11.2	9.7	9.8
Average Min. Temperature (°C)	5.1	3.3	3.3
Mean Sunshine Duration (hour)	2.9	3.4	4.4
Average Number of Rainy Days	12.4	11.1	10.0
Mean Annual Precipitation (kg/m^2)	100.6	84.9	61.1
Maximum Temperature (°C)	20.4	18.4	21.2
Minimum Temperature (°C)	-7.2	-7.2	-11.2

Table D.9. Meteorological Records of Çankırı for Winter Season [9]

ÇANKIRI	December	January	February
Average Temperature (°C)	1.3	-0.6	1.1
Average Max. Temperature (°C)	5.3	3.5	6.2
Average Min. Temperature (°C)	-2.1	-4.2	-3.4
Mean Sunshine Duration (hour)	1.8	2.1	3.5
Mean Number of Rainy Days	10.6	11.1	9.2
Mean Annual Precipitation (kg/m^2)	42.2	39.9	26.2
Maximum Temperature (°C)	17.6	15.0	19.2
Minimum Temperature (°C)	-18.8	-23.4	-23.9

Table D.10. Meteorological Records of Çorum for Winter Season [9]

ÇORUM	December	January	February
Average Temperature (°C)	1.6	-0.3	0.9
Average Max. Temperature (°C)	6.0	4.2	6.5
Average Min. Temperature (°C)	-2.3	-4.3	-3.8
Mean Sunshine Duration (hour)	2.1	2.5	3.6
Average Number of Rainy Days	12.2	11.9	10.7
Mean Annual Precipitation (kg/m^2)	44.2	37.1	27.4
Maximum Temperature (°C)	19.2	17.5	20.4
Minimum Temperature (°C)	-18.8	-23.3	-27.2

Table D.11. Meteorological Records of Düzce for Winter Season [9]

DÜZCE	December	January	February
Average Temperature (°C)	5.6	3.9	4.8
Average Max. Temperature (°C)	9.8	8.0	9.7
Average Min. Temperature (°C)	2.2	0.5	0.8
Mean Sunshine Duration (hour)	2.0	2.1	3.0
Mean Number of Rainy Days	16.0	15.6	14.1
Mean Annual Precipitation (kg/m^2)	100.2	86.5	69.2
Maximum Temperature (°C)	26.2	23.4	25.6
Minimum Temperature (°C)	-16.5	-15.0	-17.3

Table D.12. Meteorological Records of Erzincan for Winter Season [9]

ERZİNCAN	December	January	February
Average Temperature (°C)	-0.1	-2.7	-1.2
Average Max. Temperature (°C)	4.3	1.9	3.8
Average Min. Temperature (°C)	-3.6	-6.5	-5.3
Mean Sunshine Duration (hour)	2.4	2.8	3.9
Average Number of Rainy Days	10.1	9.4	9.4
Mean Annual Precipitation (kg/m^2)	28.8	25.8	29.3
Maximum Temperature (°C)	16.4	14.0	17.2
Minimum Temperature (°C)	-25.0	-24.4	-25.2

Table D.4. Meteorological Records of Erzurum for Winter Season [9]

ERZURUM	December	January	February
Average Temperature (°C)	-6.4	-9.6	-8.6
Average Max. Temperature (°C)	-1.3	-4.1	-2.7
Average Min. Temperature (°C)	-11.3	-15.0	-14.1
Mean Sunshine Duration (hour)	2.5	2.8	3.8
Mean Number of Rainy Days	12.0	12.1	12.1
Mean Annual Precipitation (kg/m^2)	22.5	19.7	24.4
Maximum Temperature (°C)	14.0	7.6	9.6
Minimum Temperature (°C)	-37.2	-36.0	-37.0

Table D.5. Meteorological Records of Iğdır for Winter Season [9]

IĞDIR	December	January	February
Average Temperature (°C)	-0.2	-2.9	-0.1
Average Max. Temperature (°C)	4.9	2.6	5.6
Average Min. Temperature (°C)	-4.2	-7.3	-4.9
Mean Sunshine Duration (hour)	2.4	2.7	4.1
Average Number of Rainy Days	6.2	5.8	6.5
Mean Annual Precipitation (kg/m^2)	12.0	13.2	16.5
Maximum Temperature (°C)	22.2	18.3	17.6
Minimum Temperature (°C)	-30.2	-23.3	-21.6

Table D.6. Meteorological Records of İstanbul for Winter Season [9]

İSTANBUL	December	January	February
Average Temperature (°C)	8.0	6.1	5.9
Average Max. Temperature (°C)	10.7	9.0	9.2
Average Min. Temperature (°C)	5.4	3.6	3.2
Mean Sunshine Duration (hour)	2.2	2.3	3.1
Mean Number of Rainy Days	16.9	17.3	14.9
Mean Annual Precipitation (kg/m^2)	101.3	83.9	64.9
Maximum Temperature (°C)	21.2	18.3	24.0
Minimum Temperature (°C)	-3.4	-7.9	-8.0

Table D.7. Meteorological Records of Karabük for Winter Season [9]

KARABÜK	December	January	February
Average Temperature (°C)	4.3	3.1	4.5
Average Max. Temperature (°C)	8.8	7.5	10.1
Average Min. Temperature (°C)	0.9	-0.4	0.2
Mean Sunshine Duration (hour)	*	*	*
Average Number of Rainy Days	12.6	12.7	11.0
Mean Annual Precipitation (kg/m^2)	44.0	52.8	29.8
Maximum Temperature (°C)	20.4	22.1	24.8
Minimum Temperature (°C)	-12.0	-13.9	-14.2

Table D.8. Meteorological Records of Kastamonu for Winter Season [9]

KASTAMONU	December	January	February
Average Temperature (°C)	0.6	-0.7	0.6
Average Max. Temperature (°C)	4.3	3.2	5.9
Average Min. Temperature (°C)	-2.4	-4.1	-3.6
Mean Sunshine Duration (hour)	1.8	2.3	3.6
Mean Number of Rainy Days	12.8	13.0	11.2
Mean Annual Precipitation (kg/m^2)	37.6	30.2	24.0
Maximum Temperature (°C)	17.2	17.3	20.2
Minimum Temperature (°C)	-18.2	-18.9	-20.9

Table D.9. Meteorological Records of Kocaeli for Winter Season [9]

KOCAELİ	December	January	February
Average Temperature (°C)	8.1	6.3	6.4
Average Max. Temperature (°C)	11.3	9.7	10.2
Average Min. Temperature (°C)	5.3	3.4	3.3
Mean Sunshine Duration (hour)	2.4	2.4	2.8
Average Number of Rainy Days	16.9	17.2	15.6
Mean Annual Precipitation (kg/m^2)	105.2	93.3	72.2
Maximum Temperature (°C)	24.0	22.6	23.7
Minimum Temperature (°C)	-4.5	-6.0	-8.3

Table D.10. Meteorological Records of Muş for Winter Season [9]

MUŞ	December	January	February
Average Temperature (°C)	-2.8	-7.1	-6.0
Average Max. Temperature (°C)	1.0	-2.9	-1.4
Average Min. Temperature (°C)	-6.1	-11.0	-10.3
Mean Sunshine Duration (hour)	2.2	2.3	3.3
Mean Number of Rainy Days	12.9	13.5	12.3
Mean Annual Precipitation (kg/m^2)	90.2	81.9	106.0
Maximum Temperature (°C)	16.0	10.2	11.6
Minimum Temperature (°C)	-32.0	-32.6	-34.4

Table D.20. Meteorological Records of Sakarya for Winter Season [9]

SAKARYA	December	January	February
Average Temperature (°C)	7.9	6.0	6.2
Average Max. Temperature (°C)	11.3	9.5	10.4
Average Min. Temperature (°C)	4.9	3.0	2.8
Mean Sunshine Duration (hour)	2.4	2.4	3.1
Average Number of Rainy Days	15.8	15.5	13.9
Mean Annual Precipitation (kg/m^2)	103.0	93.0	72.2
Maximum Temperature (°C)	26.2	24.2	25.4
Minimum Temperature (°C)	-6.8	-8.2	-10.0

Table D.21. Meteorological Records of Tokat for Winter Season [9]

TOKAT	December	January	February
Average Temperature (°C)	3.6	2.0	3.2
Average Max. Temperature (°C)	7.6	6.1	8.0
Average Min. Temperature (°C)	0.2	-1.5	-1.0
Mean Sunshine Duration (hour)	2.5	2.8	3.8
Mean Number of Rainy Days	12.4	11.7	11.3
Mean Annual Precipitation (kg/m^2)	42.1	40.8	33.3
Maximum Temperature (°C)	21.8	19.2	22.8
Minimum Temperature (°C)	-21.0	-19.8	-22.1

Table D.22. Meteorological Records of Tunceli for Winter Season [9]

TUNCELİ	December	January	February
Average Temperature (°C)	1.1	-1.6	-0.2
Average Max. Temperature (°C)	5.1	2.5	4.4
Average Min. Temperature (°C)	-2.1	-5.3	-4.3
Mean Sunshine Duration (hour)	2.9	3.5	4.4
Average Number of Rainy Days	12.3	12.1	12.4
Mean Annual Precipitation (kg/m^2)	121.3	107.3	102.3
Maximum Temperature (°C)	18.0	14.0	18.1
Minimum Temperature (°C)	-25.6	-24.0	-26.6

APPENDIX E

DESIGN OF ELASTOMERIC BEARINGS

Bearing design is evaluated per AASHTO LFRD 2005 Section 14 [3]

For bearing Type A:

The unfilled shape factor of the bearing:

$$\mathrm{S} = \frac{300^2 - 100^2}{4 \times 15 \times (300 + 100)} = 3.333$$

The area of the unfilled bearing is computed as:

$$A_{rubber} = (\pi 150^2) - (\pi 50^2) = 62832 \text{ mm}^2$$

The area of filled bearing is computed as:

$$A_{bearing} = \pi 150^2 = 70686 \text{ mm}^2$$

Shear modulus of the bearing is computed by averaging the shear modulus values of all EB_A tests

$$G_{avg} = \frac{\sum_{i=1}^{n} \left(G_i = \frac{K_{eff\_avg} \times h_{rt}}{A_{bearing}} \right)}{n} = 1.050 MPa$$

- In order to limit the shear stresses and strains due to vertical load compressive load, compressive stress in rubber should be checked:

$$\sigma_s \leq 1.66 \times 1.050 \times 3.333 \rightarrow 5.81 MPa \leq 11.00 MPa \tag{E.1}$$

- Check shear deformation:

$$h_{rt} \geq 2\Delta_s \rightarrow 75.000 \langle 78.986 \text{ (within limits – 5\% over)} \tag{E.2}$$

- Check effects of rotation and compression in order to ensure no point in the bearing undergoes net uplift:

$$\sigma_s > 0.75GS\left(\frac{\theta_s}{n}\right)\left(\frac{D}{h_{ri}}\right)^2 \rightarrow \sigma_s > 1.837MPa \tag{E.3}$$

θ = 0.007 rad. (An assumed value)

- Check effects of rotation, compression and shear:

$$\sigma_s < 2.5GS\left[1 - 0.15\left(\frac{\theta_s}{n}\right)\left(\frac{D}{h_{ri}}\right)^2\right] \rightarrow \sigma_s < 7.830MPa \tag{E.4}$$

- Check stability of bearing:

Check if 2A≤B

$$A = \frac{\frac{1.92h_{rt}}{L}}{\sqrt{1 + \frac{2L}{W}}} \tag{E.5}$$

$$B = \frac{2.67}{(S + 2.0) \times \left(1 + \frac{L}{4.0W}\right)} \tag{E.6}$$

for circular bearings W = L = 0.8D:

$$A = \frac{1.92h_{rt}}{(0.80D \times \sqrt{3})} = 0.346 \rightarrow 2\text{A} = 0.692 \tag{E.7}$$

$$B = \frac{2.67}{(S + 2.0) \times 1.25} = 0.401 \tag{E.8}$$

where A and B are parameters used in stability calculations.

Since 2A > B further investigation is required.

In this case:

$$\sigma_s \leq \frac{GS}{(2A - B)} \rightarrow \sigma_s \leq 12.026 MPa \tag{E.9}$$

- Check thickness of steel shims since shims should be able to sustain tensile stresses induced by compression of the bearing:

$$h_s \geq \frac{3h_{\max} \times \sigma_s}{F_y} \rightarrow h_s \geq 0.1875\sigma_s \tag{E.10}$$

where;

h_s : thickness of steel shims

h_{max} : thickness of the thickest rubber layer in the EB

- Check vertical strain under compressive stress:

$$\varepsilon_c = \frac{\sigma_s}{6GS^2} < 0.07 \rightarrow 0.01429\sigma_s < 0.07 \tag{E.11}$$

where;

ε_c : axial strain under compressive stress

σ_s : service average compressive stress due to unfactored total load on elastomer part (in MPa)

n : number of internal rubber layers

Checks according to AASHTO Guide Specification for Seismic Isolation [2];

- Shear strain due to axial compression:

$$\gamma_c = \frac{3SP_{ver}}{1+2kS^2} \approx \frac{P_{ver}}{A_r GS} \qquad \text{(E.12)}$$

where k is elastomer constant.

For d_{max} = 79 mm & D_b = 290 mm area of the overlap between top and bottom bonded areas of the deformed bearing can be calculated as follows [10]:

$$D_b = D - 2 \times c_c \qquad \text{(E.13)}$$

$$\chi = \sqrt{{D_b}^2 - {d_{\max}}^2} = 279mm \qquad \text{(E.14)}$$

$$A_r = 0.5\left(D^2 \sin^{-1}\left(\frac{\chi}{D_b}\right) - d_{\max} \times \chi\right) = 47220mm^2 \qquad \text{(Kelly, T.E., 2001):} \qquad \text{(E.15)}$$

P_{ver} = 247.401 kN at target stress level (σ = 3.500MPa).

Thus shear strain due to vertical compression:

$$\gamma_c = 1.50$$

- Shear strain due to seismic design displacement:

$$\gamma_{s,eq} = \frac{d_{\max}}{h_{rt}} = \frac{79}{75} = 1.05 \qquad \text{(E.16)}$$

- Shear strain due to rotation:

$$\gamma_r = \frac{(D^2\theta)}{(2h_{ri}h_{rt})} = 0.28 \qquad \text{(E.17)}$$

For d_s = ± 15mm, shear strain due to service load displacement:

$$\gamma_{s,s} = \frac{d_s}{h_{rt}} = 0.20 \qquad \text{(E.18)}$$

where

γ_c : shear strain due to vertical compressive load

γ_r : shear strain due to rotation

$\gamma_{s,eq}$: shear strain due to seismic design displacement

$\gamma_{c,c}$: shear strain due to service load displacement

Limits in AASHTO Guide Spec. Section 14.3 [2]

$$\gamma_c = 1.50 \leq 2.5$$

$$\gamma_c + \gamma_{s,s} + \gamma_r = 1.98 \leq 5.0$$

$$\gamma_c + \gamma_{s,eq} + 0.5\gamma_r = 2.69 \leq 5.0$$

Checks according to AASHTO LFRD 2005 Section 14 [3]

For bearing Type B:

The unfilled shape factor of the bearing:

$$S = \frac{210^2 - 70^2}{4 \times 11 \times (210 + 70)} = 3.182$$

The area of the unfilled bearing is computed as:

$$A_{rubber} = (\pi 1052) - (\pi 35^2) = 30788 \text{ mm}^2$$

The area of filled bearing is computed as:

$$A_{bearing} = \pi 105^2 = 34636 \text{ mm}^2$$

Shear modulus of the bearing is computed by averaging the shear modulus values of all EB_B tests

$$G_{avg} = \frac{\sum_{i=1}^{n}\left(G_i = \frac{K_{eff\_avg} \times h_{rt}}{A_{bearing}}\right)}{n} = 0.987 MPa$$

- In order to limit the shear stresses and strains due to vertical load compressive load, compressive stress in rubber should be checked:

$$\sigma_s \leq 1.66 \times 0.987 \times 3.182 \rightarrow 5.21 MPa \leq 11.00 MPa \qquad \text{(E.19)}$$

- Check shear deformation:

$$h_{rt} \geq 2\Delta_s \rightarrow 55.000 \leq 59.232 \text{ (within limits – 5\% over)} \qquad \text{(E.20)}$$

- Check effects of rotation and compression in order to ensure no point in the bearing undergoes net uplift:

$$\sigma_s > 0.75 GS\left(\frac{\theta_s}{n}\right)\left(\frac{D}{h_{ri}}\right)^2 \rightarrow \sigma_s > 1.502 MPa \qquad \text{(E.21)}$$

$\theta_s = 0.007$ rad. (An assumed value)

- Check effects of rotation, compression and shear:

$$\sigma_s < 2.5 GS\left[1 - 0.15\left(\frac{\theta_s}{n}\right)\left(\frac{D}{h_{ri}}\right)^2\right] \rightarrow \sigma_s < 7.100 MPa \qquad \text{(E.22)}$$

- Check stability of bearing:

Check if $2A \leq B$

$$A = \frac{\frac{1.92 h_{rt}}{L}}{\sqrt{1 + \frac{2L}{W}}} \qquad \text{(E.23)}$$

$$B = \frac{2.67}{(S+2.0)\times\left(1+\frac{L}{4.0W}\right)} \tag{E.24}$$

for circular bearings W = L = 0.8D:

$$A = \frac{1.92h_{rt}}{(0.80D\times\sqrt{3})} = 0.363 \rightarrow 2\text{A} = 0.726 \tag{E.25}$$

$$B = \frac{2.67}{(S+2.0)\times 1.25} = 0.412 \tag{E.26}$$

where;

A and B are parameters used in stability calculations.

Since 2A > B further investigation is required.

In this case:

$$\sigma_s \leq \frac{GS}{(2A-B)} \rightarrow \sigma_s \leq 10.002MPa \tag{E.27}$$

- Check thickness of steel shims since shims should be able to sustain tensile stresses induced by compression of the bearing:

$$h_s \geq \frac{3h_{\max}\times\sigma_s}{F_y} \rightarrow h_s \geq 0.1375\sigma_s \tag{E.28}$$

where;

h_s : thickness of steel shims

h_{max} : thickness of the thickest rubber layer in the EB

- Check vertical strain under compressive stress:

$$\varepsilon_c = \frac{\sigma_s}{6GS^2} < 0.07 \rightarrow 0.01668\sigma_s < 0.07 \tag{E.29}$$

where;

ε_c : axial strain under compressive stress

σ_s : service average compressive stress due to unfactored total load on elastomer part (in MPa)

n : number of internal rubber layers

Checks according to AASHTO Guide Specification for Seismic Isolation [2]**;**

- Shear strain due to axial compression:

$$\gamma_c = \frac{3SP_{ver}}{1+2kS^2} \approx \frac{P_{ver}}{A_r GS} \tag{E.30}$$

where k is elastomer constant.

For d_{max} = 59 mm & D_b = 200 mm area of the overlap between top and bottom bonded areas of the deformed bearing can be calculated as follows [10]:

$$D_b = D - 2\times c_c \tag{E.31}$$

$$\chi = \sqrt{D_b{}^2 - d_{\max}{}^2} = 191mm \tag{E.32}$$

$$A_r = 0.5\left(D^2 \sin^{-1}\left(\frac{\chi}{D_b}\right) - d_{\max}\times\chi\right) = 22361mm^2 \text{ [10]:} \tag{E.33}$$

P_{ver} = 121.226 kN at target stress level (σ = 3.500MPa).

Thus shear strain due to vertical compression:

$\gamma_c = 1.73$

- Shear strain due to seismic design displacement:

$$\gamma_{s,eq} = \frac{d_{\max}}{h_{rt}} = \frac{59}{55} = 1.07 \tag{E.34}$$

- Shear strain due to rotation:

$$\gamma_r = \frac{(D^2\theta)}{(2h_{ri}h_{rt})} = 0.26 \tag{E.35}$$

- For $d_s = \pm 15$mm, shear strain due to service load displacement:

$$\gamma_{s,s} = \frac{d_s}{h_{rt}} = 0.27 \tag{E.36}$$

where

γ_c : shear strain due to vertical compressive load

γ_r : shear strain due to rotation

$\gamma_{s,eq}$: shear strain due to seismic design displacement

$\gamma_{c,c}$: shear strain due to service load displacement

Limits in AASHTO Guide Spec. Section 14.3 [2]

$$\gamma_c = 1.73 \le 2.5$$

$$\gamma_c + \gamma_{s,s} + \gamma_r = 2.26 \le 5.0$$

$$\gamma_c + \gamma_{s,eq} + 0.5\gamma_r = 2.93 \le 5.5$$